universal personal communications

Riaz Esmailzadeh
Masao Nakagawa

TEAMFLY

TDD-CDMA

for wireless communications

TDD-CDMA for Wireless Communications

For a listing of recent titles in the *Artech House Universal Personal Communications Series,* turn to the back of this book.

TDD-CDMA for Wireless Communications

Riaz Esmailzadeh
Masao Nakagawa

Artech House
Boston • London
www.artechhouse.com

Library of Congress Cataloging-in-Publication Data
Esmailzadeh, Riaz.
TDD-CDMA for wireless communications/Riaz Esmailzadeh, Masao Nakagawa.
p. cm. — (Artech House universal personal communications series)
Includes bibliographical references and index.
ISBN 1-58053-371-X (alk. paper)
1. Code division multiple access. I. Nakagawa, M. (Masao) II. Title. III. Series.
TK5103.452 .E66 2002
621.3845'6—dc21 2002032680

British Library Cataloguing in Publication Data
Esmailzadeh, Riaz
TDD-CDMA for wireless communications.—
(Artech House universal personal communications series)
1. Time division multiple access 2. Code division multiple access 3. Wireless communication systems
I. Title II. Nakagawa, Masao
621.3'845

ISBN 1-58053-371-X

Cover design by Yekaterina Ratner

Regarding the copyrighted 3GPP figures in Chapter 7, 3GPP TSs and TRs are the property of ARIB, CWTS, ETSI, T1, TTA, and TTC, who jointly own the copyright in them. They are subject to further modifications and are therefore provided to you "as is" for information purposes only. Further use is strictly prohibited.

© 2003 ARTECH HOUSE, INC.
685 Canton Street
Norwood, MA 02062

All rights reserved. Printed and bound in the United States of America. No part of this book may be reproduced or utilized in any form or by any means, electronic or mechanical, including photocopying, recording, or by any information storage and retrieval system, without permission in writing from the publisher.

All terms mentioned in this book that are known to be trademarks or service marks have been appropriately capitalized. Artech House cannot attest to the accuracy of this information. Use of a term in this book should not be regarded as affecting the validity of any trademark or service mark.

International Standard Book Number: ISBN 1-58053-371-X
Library of Congress Catalog Card Number: 2002032680

10 9 8 7 6 5 4 3 2 1

Contents

TEAMFLY

Team-Fly®

Preface

This is a graduate-level book on the *time division duplex* (TDD) mode of *code division multiple access* (CDMA) technology for mobile communications. Its purpose is to familiarize the reader with the specific technologies related to the TDD mode of CDMA communications. In the TDD mode, transmission and reception to and from a user are carried out in the same frequency band, with transmission/reception switching at specific time slots. The TDD mode, as opposed to the more widely known and used frequency division duplex mode, has been used in non-CDMA mobile communications systems such as DECT and PHS. It has now become an integral part of the *wideband CDMA* (WCDMA) standards.

The reader is assumed to have a general knowledge of cellular mobile communications. However, a compact introduction to the subject matter in each chapter is expected to assist the beginner engineer to comprehend the subject matter. A comprehensive list of conference and journal papers in the references has also been provided for the reader who wants to gain a deeper insight into the TDD-CDMA technology.

The motivation for this book has been the lack of specific literature on the TDD-CDMA technology. While much of this material has been available in the form of individual papers, a book dealing specifically with the details of TDD-CDMA has not been available. Many books on CDMA have dedicated a chapter to TDD. However, these have not been comprehensive enough to explain what makes the TDD technology unique and valuable in specific applications. As the TDD mode becomes a major part of third-

generation standards, and as it promises to become even more prominent in fourth-generation standards, it is appropriate to dedicate an entire book to TDD to discuss the specific techniques that are only possible in a TDD mode of operation.

We authors have the distinction of being associated with TDD-CDMA from the very beginning. Our work with TDD-CDMA started when Riaz Esmailzadeh came to Japan in 1990 to start his Ph.D. studies at Nakagawa Laboratory at Keio University. His work performed during 1991 to 1994 was the first to propose TDD-CDMA and was to form the basis for future TDD-CDMA activities and standards. Our collaboration continued long after the studies were completed. Dr. Esmailzadeh became involved with the WCDMA standardization, and a number of students at the Nakagawa Laboratory continued working with the TDD mode. We have seen it become a part of the WCDMA standards, as well as integral technology for some private spread spectrum systems. We have further promoted the technology to see that it is positively considered for the fourth-generation standards. These systems are targeted for implementation in the latter part of this decade.

Acknowledgments

We authors were encouraged to undertake this project by Mr. Kambiz Homayounfar, the CEO of the Genista Corporation, where Dr. Esmailzadeh was previously employed. His constant encouragement and support was an important factor in the accomplishment of this work. We are indebted to Dr. Mario Luoni, Dr. Tadashi Matsumoto, Dr. Essam Sourour, Dr. Anand R. Prasad, Dr. Jun Du, and Dr. Terence Percival, who, along with many others, have encouraged, supported, and assisted us through the many years we have been working on this topic. Our editors at Artech House were exact and helpful. Their skills in project management prevented this book from dragging on and ensured its timely publication. We are further grateful to Matsushita Communication Industrial Co., Ltd. for permitting us to publish in part their paper on their TDD-CDMA system and experimental results. The permission by the IEICE, IEEE, and 3GPP to reproduce some figures from copyrighted material is hereby acknowledged and appreciated.

Most of all, we are grateful to our families who endured our preoccupation with this project over and above other work-related activities. This book is dedicated to them.

1

Introduction

The telecommunications industry was born almost 150 years ago with the establishment of the first Morse transmission line between Washington, D.C., and Baltimore, Maryland, in the United States. Some 32 years later, in 1876, Alexander Graham Bell demonstrated the first voice communication device, which he called a telephone. The telephone was an overnight success; by early 1881 the first American Bell company annual report showed that almost all major North American cities already had telephone exchanges, with a total of 132,692 telephone subscribers [1]. This explosive rate of growth was maintained until almost every home in North America had a telephone.

The first wireless communication was not to take place for another 30 years, and not until the first decade of the twentieth century. However, while wired communication soon became inexpensive and found its way into almost every home, the wireless and mobile means of communication were costly and did not become popular. Instead, they found their applications in broadcasting, intercontinental and satellite communications, and mobile military, police, and emergency communications. Whereas the wired communications explosion was instantaneous, the wireless revolution did not occur until the 1980s.

1.1 Mobile Communications

The mobile communications revolution took place for a number of reasons. Foremost among these was the decrease in the cost of mobile telephony because of the advent of transistors and high-speed signal processing. The cost of mobile devices and services was further reduced because of the economies of scale, as more and more subscribers found the services affordable. The price for a mobile phone has dropped to less than $100 from more than $2,500 since 1983, in large part due to increases in manufacturing volume. Moreover, many operators have subsidized the cost of mobile phones, reducing the initial cost to the user to zero.

As a result, wireless/mobile communications was the fastest growing field in the electronics and telecommunications industry during the 1990s, becoming the largest consumer product industry in history—even bigger than the PC that emerged at the same time. The explosive growth in demand for mobile and cordless voice and data communication services caused significant reductions in system costs that in turn fueled further demand. To keep up with such demand, the technology had to evolve constantly, resulting in the development of numerous systems, some of which are presently in service or in the implementation phase; some have even come into service, had a short life span, and have already been phased out.

The demography of mobile users and their demands have also changed greatly. The initial customers were mostly business users, who for the most part required wide-area connectivity and who were not greatly concerned with the communications quality or size and cost of the mobile units. Nowadays, it is a commodity product used by all people. Users now demand small, light, and inexpensive mobile units with low service charges. Moreover, users now demand other services in addition to the telephony services, such as data and video communications. The growing demand has meant that more efficient bandwidth utilization methods have had to be developed, and that more bandwidth be allocated for mobile communications services.

Research since the early 1990s has been geared toward finding solutions to the challenges mentioned, such as enabling higher transmission rates, better bandwidth usage efficiency, and service provision diversity. Further challenges have been reducing the size and cost of the handheld devices and improving the quality of service.

The third generation of mobile communications systems promises to provide these and a global service such that you can always be reached, wherever you are in the world, using the very same phone [2]. Now that the

technology has delivered the dream, questions are being raised about whether it is possible to avoid being reached.

Mobile systems and services have been classified in a number of different ways. Figure 1.1 shows some of these services to illustrate the emergence of new technologies [3–5]. The figures gives approximates of the time at which they appeared on the market or are expected to appear. Cellular mobile communication systems are broadly divided into the first, second, and third generations of services, based on whether the system is analog or digital, and voice or multimedia, that is, based on the extent to which the services they provide differ. The first generation of mobile systems has already been phased out by and large and the second-generation systems have been in operation now for some 10 years and are expected to be replaced by or evolve into the third-generation systems, which are presently being rolled out.

A general trend can be observed in the utilized multiple-access schemes: from *frequency-division multiple access* (FDMA) to *time-division multiple access* (TDMA) and *code-division multiple access* (CDMA). TDMA and CDMA developments were generally made in response to the above-mentioned challenges, particularly better frequency utilization efficiency and service provision flexibility as compared with FDMA [6, 7]. They were also capable of accommodating multirate services, one of the main requirements of future multimedia mobile communications.

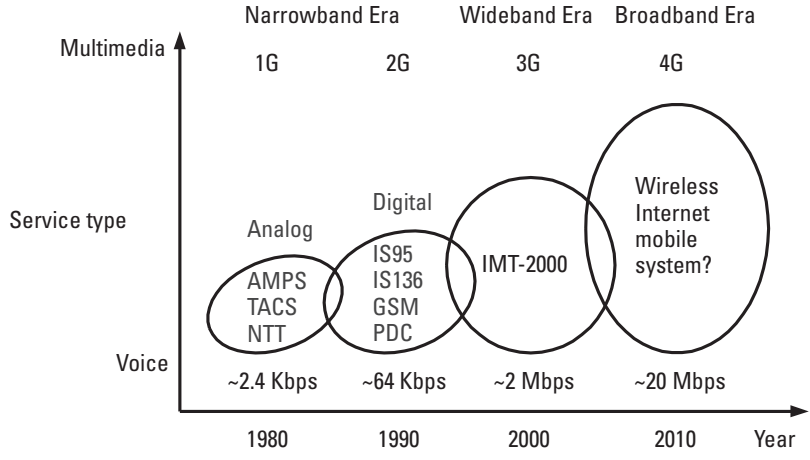

Figure 1.1 Generations of mobile communications. (*Source:* [5], © 2001 IEICE.)

Figure 1.2 illustrates the difference between these three access techniques. In FDMA systems, a user is assigned a portion of a frequency band over which it transmits its information and which it keeps for the duration of the connection. In TDMA systems, a frequency band is shared between several users, who in turn use the channel for transmission (or reception) of information at clearly defined time intervals. In a CDMA system, many users use the same frequency band, all the time, and are distinguished at the receiver by a unique spreading code.

1.2 TDD Systems

An emerging trend can also be detected in the duplex mode of operation of mobile services. *The time-division duplex* (TDD) schemes seem to be gradually gaining favor, at the expense of the more broadly used *frequency-division duplex* (FDD) mode. The TDD systems are appearing in the low-power end of the domain, where simplicity and low cost are major concerns.

As shown in Figure 1.3 most of the lower power, small-area cellular systems (usually provided in microcells, with little round-trip propagation delays on the order of a few microseconds) of the second generation used TDD as their duplex mode. In Europe the Digital European Cordless Telephone (DECT) standard is based on TDD-TDMA [8], in Japan also, the *Personal Handyphone System* (PHS) is based on TDD-TDMA [3]. For the third-generation systems, two TDD-CDMA standards have already been adopted: *time-division/code-division multiple access* (TD-CDMA) as part of the 3GPP standards, and *time-division/synchronous code-division multiple access* (TD- SCDMA) in China. These systems are expected to be rolled out in the 2002–2003 time frame. Furthermore, TDD-CDMA is increasingly the focus of research and is being experimented with in combination with multicarrier CDMA for fourth-generation devices [9].

The main difference between the two modes, as shown in Figure 1.4, is that duplex transmission is carried in alternate time slots for the TDD mode in the same frequency channel, whereas FDD uses two separate channels for continuous duplex transmission. In fact, all half-duplex systems, such as amateur radio, are TDD systems. The communications parties alternately talk and listen or send and receive information, using a manual switch. In "modern" TDD systems, the switching between the uplink and downlink is standardized and automatic.

One of the advantages of using TDD over FDD is its design simplicity. This is because only one set of electronics (filters, oscillators, and so forth) is

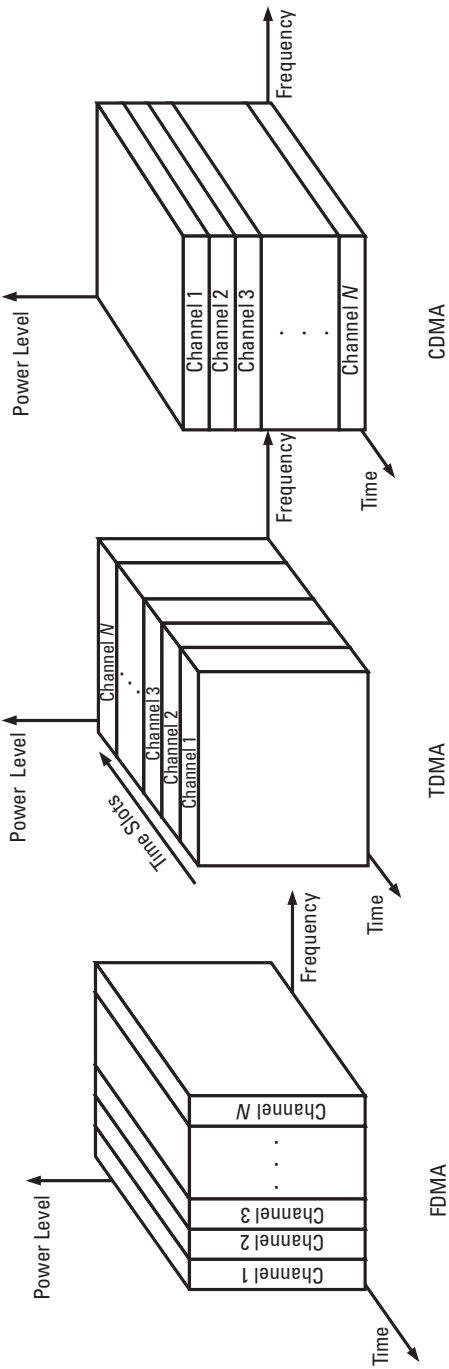

Figure 1.2 FDMA versus TDMA versus CDMA.

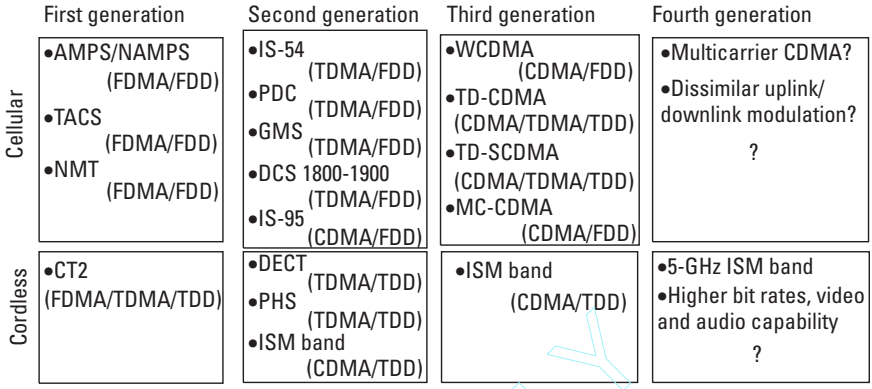

Figure 1.3 Mobile communication device generations.

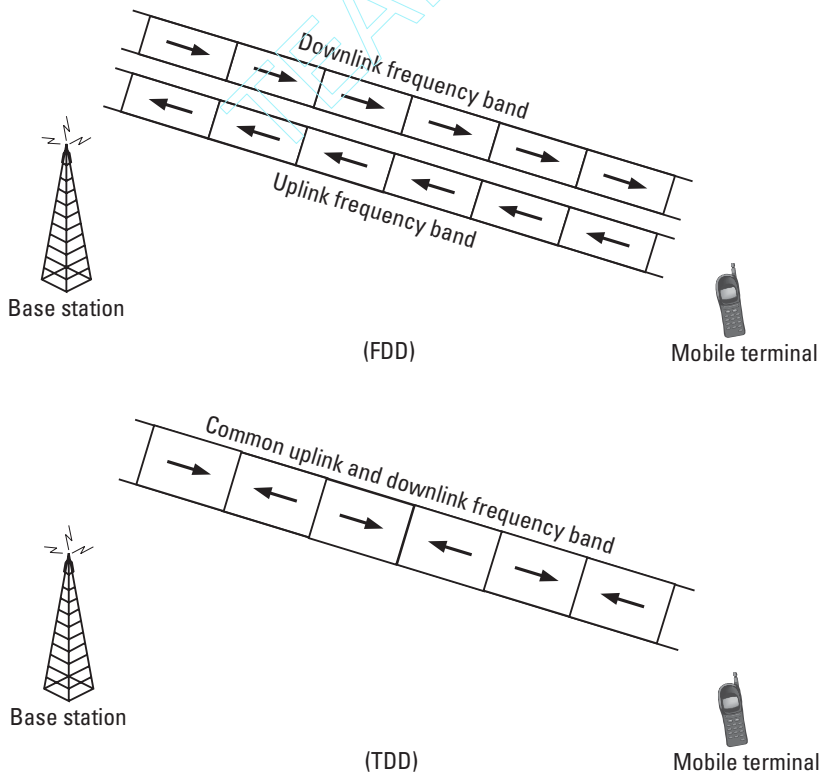

Figure 1.4 TDD and FDD.

Team-Fly®

required at both mobile and base stations for both forward and reverse link transmissions. This is significant in the low-power, low-size end of the mobile communications market. Separation of the duplex operation in time also eliminates cross-talk between the transmitter and the receiver and further enables simple device implementation.

However, the most important advantage of TDD over FDD is that since the same frequency channel is used in both directions, the channel characteristics are reciprocal for the two links. This fact can be used to implement a number of important functions in an open-loop fashion including power control, signal preemphasis and shaping, and transmission diversity to respond to unfriendly urban mobile channel conditions. All of these functions will help further reduce the case and complexity of the portable mobile unit, resulting in less costly devices.

Some requirements of TDD systems, such as synchronous network designs and limited cell size, have delayed the wider acceptance of these systems, preventing them from becoming a more widely utilized standard. The question remains regarding the degree of acceptance they will receive in future generations of mobile telecommunications standards.

1.3 Spread Spectrum Communications

One mobile communications access scheme, which found popularity in the 1990s, is the spread spectrum–based CDMA technique. As mentioned above, in CDMA, all users transmit in the same frequency band and access the transmission medium at the same time. Every user's signal is modulated by a unique deterministic code sequence, a duplicate of which can be generated at the receiver. By correlating the received signal with the same sequence, the desired signal can be demodulated. All unwanted signals will not be demodulated and will remain effectively as noise.

R. C. Dixon in [10] defines the following two criteria for a spread spectrum system: (1) The transmission bandwidth is much greater than the bandwidth or rate of the information being sent, and (2) some function other than the information being sent is employed to determine the resulting modulated RF bandwidth. Based on this definition, spread spectrum systems have existed in one form or another for a long time. In essence, the art of spread spectrum is seen in the way it spreads the signal energy onto a very wide bandwidth; transmits the expanded signal; and then, at the receiver, reconcentrates the energy back into the original bandwidth. As a result of this process, the signal can be transmitted at very low power levels with a

minimum probability of detection and interception, and it can be very resistant to jamming and interference.

The concept of spreading a signal with a noise-like source was first tried by M. Rogoff, an engineer at the U.S. Federal Telecommunications Laboratory. He conceived the idea of multiplying a signal by a pure random noise source, and constructed a noise wheel, which could modulate a digital information source by means of optical switches. The noise wheel was constructed from 1,440 random numbers, taken out of a Manhattan telephone directory and printed on a sheet of film with constant transmissivity. One wheel was used at the transmitter and another wheel at the receiver to spread and despread the information signal. The wheels, rotating synchronously at 900 rpm, modulated and demodulated a 1-bps information signal. The noise wheel was used in a transcontinental experiment and was shown to operate soundly under conditions where conventional systems would fail [11].

The Rogoff system demonstrated the practicality of a class of spread spectrum systems, namely, *direct sequence* (DS). Another class, known as *frequency hopping* (FH), also used a very wide frequency band to transmit and receive a relatively narrowband signal by rapidly changing the carrier frequency over the entire band. These systems had obvious applications in military communications due to their excellent antijamming capability and inherent privacy. Because of these and their high cost, the spread spectrum systems remained exclusively within the military for many decades.

The cost of the spread spectrum modulators remained high until cheaper and faster digital signal processors were produced. Only then did it become possible to use these systems for nonmilitary applications. The most logical of these applications is in the area of mobile communications [12]. The mobile channels suffer from multipath fading, which can cause variation in the received power level of up to 40 dB to 60 dB. In addition, communication must be carried out under interference from a number of other users, which act similarly to jammers. The military spread spectrum systems were developed to operate under similar conditions.

This book discusses the combination of the TDD mode of transmission with spread spectrum–based CDMA systems. It explains the factors that distinguish the TDD mode of operation from the FDD mode. We then discuss how these are used to provide mobile communications with special features. First we give a general technical background. Chapter 3 then discusses the special features of the TDD mode. In Chapters 4, 5, and 6 we discuss how these features are utilized in actual systems to improve different aspects of wireless communications performance. Chapters 7 and 8 discuss the basis of two public mobile communication standards, and several private wireless

communications systems, which are based on TDD spread spectrum. Finally, Chapter 9 provides a viewpoint of how TDD and spread spectrum combination can be used in future, fourth-generation communication systems.

References

[1] Lynch, R. J., "PCN: Son of Cellular? The Challenges of Providing PCN Services," *IEEE Communications Magazine,* February 1991, pp. 56–57.

[2] Grubb, J. L., "The Traveller's Dream Come True," *IEEE Communications Magazine,* November 1991, pp. 48–51.

[3] Balston, D. M., and R. C. V. Macario, *Cellular Radio Systems,* Norwood, MA: Artech House, 1993.

[4] Cox, D. C., "Wireless Network Access for Personal Communications," *IEEE Communications Magazine,* December 1992, pp. 96–115.

[5] Adachi, F., "Wireless Past and Future—Evolving Mobile Communications Systems," *Trans. IEICE on Fundamentals Elec. Commun.,* Vol. E84-A, No. 1, January 2001, pp. 55–60.

[6] Skold, J., B. Gudmundson, and J. Farjh, "Performance and Characteristics of GSM-Based PCS," *Proc. IEEE Vehicular Technology Conference,* 1995, pp. 743–748.

[7] Gilhousen, K. S., et al., "On the Capacity of a Cellular CDMA System," *IEEE Trans. on Vehicular Technology,* May 1991, pp. 303–312.

[8] Goodman, D. J., "Trends in Cellular and Cordless Communications," *IEEE Communications Magazine,* June 1991, pp. 31–40.

[9] Takahashi, H., and M. Nakagawa, *Antenna and Multi-Carrier Pre-Diversity System Using Time Division Duplex in Selective Fading Channel*, IEICE Technical Report RCS9545, July 1995.

[10] Dixon, R. C., *Spread Spectrum Systems,* New York: Wiley Interscience, 1976.

[11] Simon, M. K., et al., *Spread Spectrum Communications,* Rockville, MD: Computer Science Press, 1985.

[12] Schneiderman, R., "Spread Spectrum Gains Wireless Approval," *Microwave and RF Magazine,* May 1992, pp. 31–42.

2

Mobile Radio Communications

This chapter provides an introduction to the principles, concepts, and techniques of public wireless and mobile communications systems. We first define the areas of the technology that this book addresses. These include the characteristics of the transmission channel in the bands of interest; in particular, signal fading effects and how these effects can be mitigated by power control, and diversity techniques, such as exploiting multipath signal arrival and antenna diversity. We then describe in more detail spread spectrum modulation techniques and CDMA. This chapter is intended to be a short reference for the concepts later introduced in this book.

2.1 Radio Communication System

A block diagram of a digital radio communication system using a spread spectrum technique is shown in Figure 2.1. Such a system is designed to deliver information over a radio channel. The information source may be voice, video, or audio, for which a source encoder converts analog information into a digital stream. A source encoder usually uses compression techniques to reduce the size of the data stream to be transmitted. The data source may also be a data stream, such as a TCP/IP source. *Forward error correction* (FEC) is used to reduce the probability of erroneous detection due to factors such as noise or fading. This is also referred to as *channel coding*.

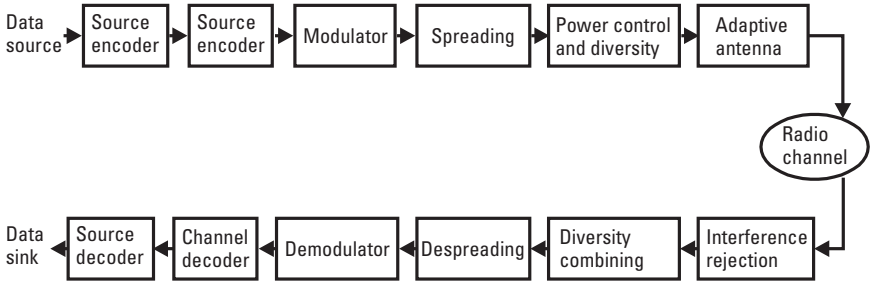

Figure 2.1 A radio communication system.

The resulting output is then modulated, and the resulting signal bandwidth is spread over a large frequency spectrum by one of two spread spectrum techniques: direct sequence or frequency hopping. Functions such as power control and transmission diversity are necessary in order to compensate the effects of channel fading. The signal is then transmitted over the air. The transmission (and reception) may be carried over adaptive array antennas. The signal is then carried over the radio channel, received at an (adaptive array) antenna, diversity combined, despread, demodulated, the channel and source decoded, and delivered to the receiver of the information.

The TDD mode of spread spectrum transmission affects in particular the power control, diversity transmission and reception, and adaptive antennas functions. It also affects functions related to interference reduction in a CDMA system.

This chapter presents a technical background for the TDD-CDMA-specific technologies used in a radio communication system, such as the one illustrated in Figure 2.1. The source and channel encoding functions are beyond the scope of this book and the reader is referred to [1–3].

Because the length of a transmission is generally indefinite, organizing data into finite lengths, called frames or packets, facilitates the transmission of information over communication media, and functions such as FEC and error detection. The input stream is therefore broken into a fixed length over one or more steps, and the resulting symbol stream transmitted over fixed intervals. Figure 2.2 illustrates how this process is carried out for voice communication over the downlink of the *wideband CDMA* (WCDMA) system. The voice signal is source encoded using an *adaptive multirate* (AMR) vocoder [2]. The vocoder outputs voice frames have 20-ms lengths. The encoded bits are FEC convolutional encoded, and the resulting frame is processed by a *cyclic redundancy checksum* (CRC) algorithm, which calculates

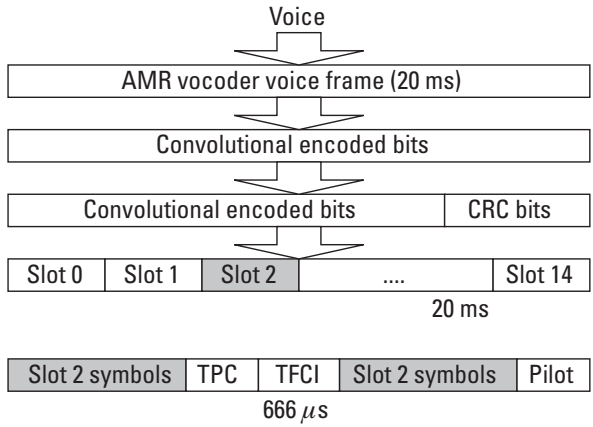

Figure 2.2 Frame and slots in the WCDMA downlink.

a number of CRC bits and adds them to the end of the frame. The frame is then broken down to equal portions of fixed lengths of $\tau_s = 666\ \mu$s, which are referred to as *slots*. Each slot is then transmitted with added control information such as pilot and power control bits [4, 5].

The symbols thus generated are then modulated. The system used throughout this book employs *biphase shift keying* (BPSK) modulation. We start by describing the characteristics of a radio communication system and factors that contribute to the losses a signal experiences as it propagates through a radio channel, such as propagation loss and shadowing. We then describe power control and diversity combining techniques, which are useful in reducing the effects of channel fading. We discuss two diversity combining techniques used in CDMA communications: selection combining and maximal ratio combining. We then continue with a summary on spread spectrum communications, and present mathematical descriptions of frequency-hopping and direct sequence modes of spread spectrum communication. Based on these, we introduce system configurations for public and private communication systems that use a combination of spread spectrum and the TDD mode of transmission.

2.2 Mobile Channel Characteristics

Mobile communication channels are characterized by multipath signal arrival and fading. The received signal is the sum of many reflections of the

transmitted signal from buildings, cars, and the ground, as illustrated in Figure 2.3. Reflected signals, arriving through different paths, have different propagation delay times, amplitudes, and phases. At each point, these signals may add up constructively or destructively. An *in-phase and quadrature* (IQ) vector representation of rays arriving at the antenna of a receiver is illustrated in Figure 2.4. The signal level, measured and drawn in the communication area, consists of hills and troughs, where the hills represent the places where multipath signals add constructively, and the troughs, where they add destructively.

A receiver moving in this environment experiences periods of good reception and bad reception. The rate of reception level variation is known as the fading rate or the Doppler rate, f_d, and depends on the velocity of movement V and carrier wavelength λ. It can be expressed as:

$$f_d \approx \frac{V}{\lambda} \tag{2.1}$$

For modulated signals, the changes in signal level differ for the upper and lower frequencies of the signal spectrum. The concept of the coherence bandwidth of a signal is defined as the maximum frequency bandwidth over which the fading changes are correlated for all frequencies of the band. It is denoted as B_c and is approximated from:

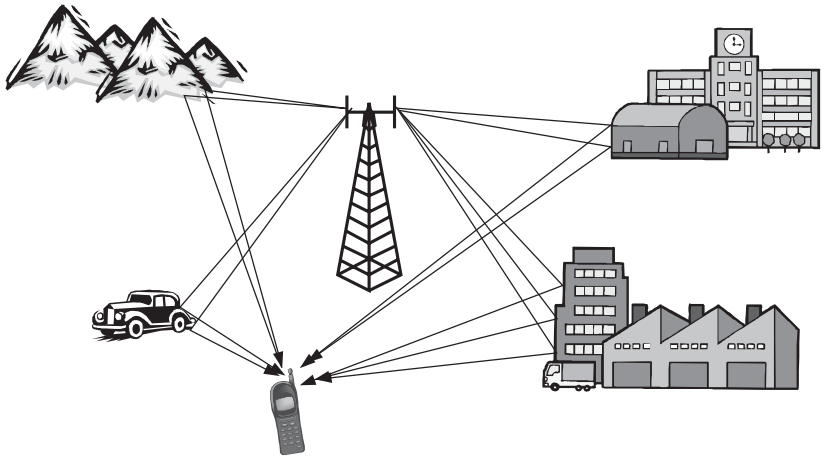

Figure 2.3 Fading due to multipath.

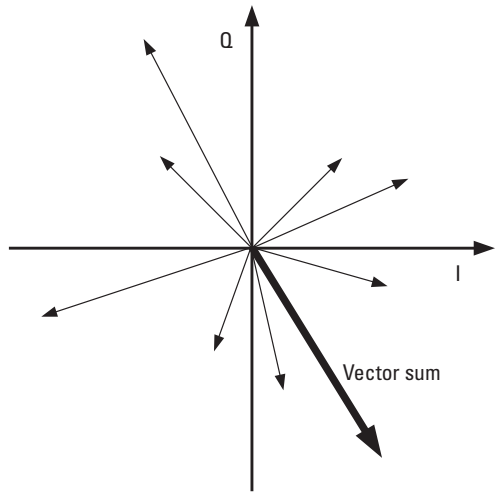

Figure 2.4 Sum of signal rays.

$$B_c \approx \frac{1}{\Delta_m} \tag{2.2}$$

where Δ_m is the maximum significant delay spread of the received signal. Depending on the propagation environment, a channel delay profile, as illustrated in Figure 2.5, may be drawn.

If the receiver bandwidth is large enough, these paths can be separately detected. Based on (2.2), two types of fading channels can be defined. One is a flat fading channel, in which the signal bandwidth is narrower than the coherence bandwidth. In other words, the maximum delay spread is smaller than the inverse of signal bandwidth. In such systems all frequency components of the signal fade coherently. Such signal fading is closely modeled by a Rayleigh random variable. The other is a frequency selective fading channel, where the signal bandwidth is wider than B_c. Here fading is not uniform for different frequency components [6]. As an example, the channel behavior for a narrowband indoor CDMA system, operating with a 1.25-MHz bandwidth (such as the IS-95-based cdmaOne systems) can be closely modeled as flat fading because Δ_m is usually smaller than the inverse of the spreading bandwidth. WCDMA systems operating with a 3.84-MHz bandwidth in outdoor channels, however, are affected by frequency selective fading, since Δ_m can usually be several times larger than the inverse of the T_c. These two types of channels are illustrated in Figure 2.6.

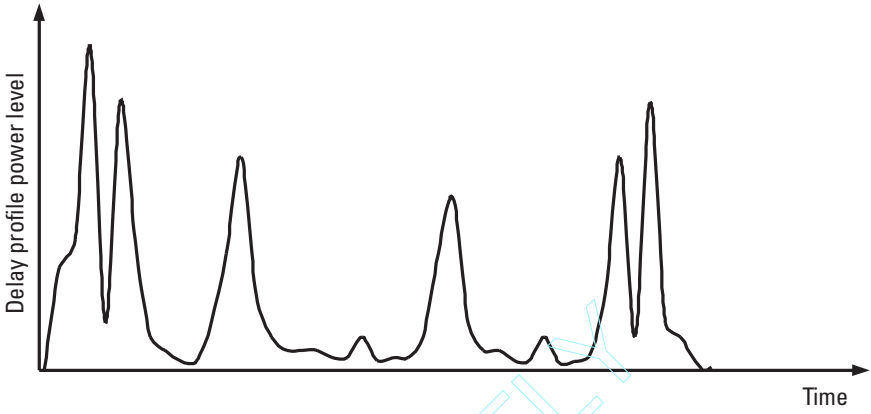

Figure 2.5 A typical channel delay profile.

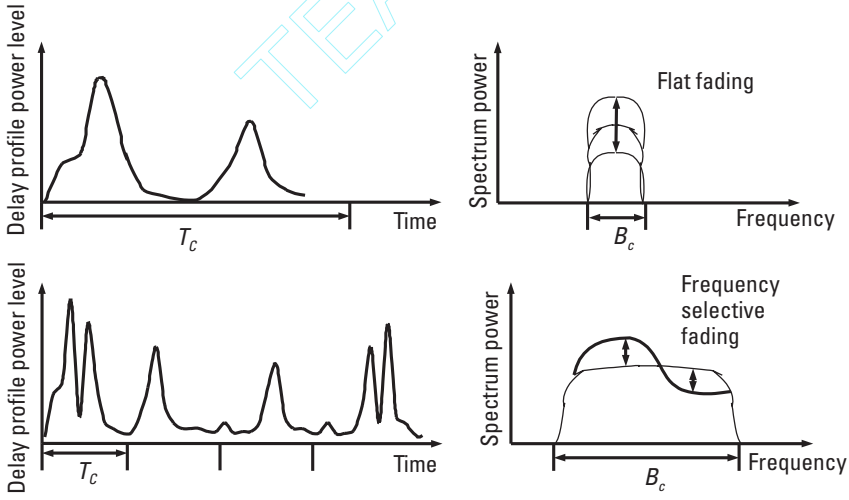

Figure 2.6 Flat and frequency selective fading channels.

The discrete channel impulse response for a fading channel can be represented as [7]:

$$h(t) = \sum_{l=0}^{L-1} \beta_l \exp(J\theta_l)\delta(t - lT_c) \tag{2.3}$$

TEAMFLY

Team-Fly®

where $\delta(t)$ is the propagation delay, β_l is an *identically independently distributed* (i.i.d.) Rayleigh random variable for all paths l, and the angles θ_l are uniformly i.i.d. in $[0,2\pi)$. The propagation delay difference of all independent paths is assumed to be an integer multiple of the chip period T_c. It follows that for a flat fading channel, $L = 1$, and for a frequency selective fading channel, $L > 1$.

Figure 2.7 illustrates the variation of power level in a flat fading channel as a receiver moves in the channel. The pick-to-trough ratio may at times exceed 50 dB.

Transmission of signals over a fading channel requires much larger signal power levels than a nonfading (static) channel for a similar level of performance in terms of, for example, *bit error rate* (BER). To illustrate, BPSK BER for information transmitted over a fading channel using BPSK modulation is calculated from the following equation [8],

$$P_e = \frac{1}{2}\left[1 - \sqrt{\frac{\gamma_b}{1+\gamma_b}}\right] \tag{2.4}$$

where γ_b is the ratio of energy per bit and normalized noise (and interference) power. In comparison, the BER for the same system power over a static channel is as follows:

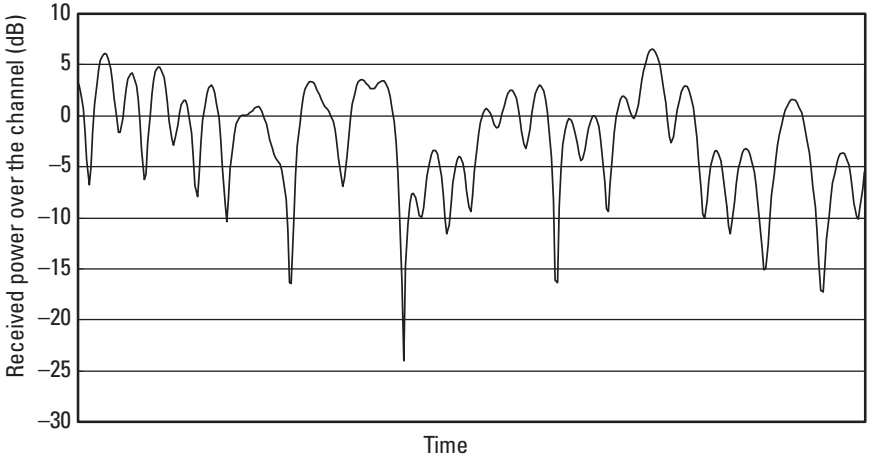

Figure 2.7 The variation of a received signal level over time as a result of the fading process.

$$P_e = \frac{1}{2}\text{erfc}\left(\sqrt{\gamma_b}\right) \tag{2.5}$$

To illustrate, the results of (2.4) and (2.5) are illustrated in Figure 2.8, where we can see that in fading channels, an extra 18 dB of power must be provided to achieve a similar BER of 10^{-3}.

Two techniques to combat the effects of fading channels are power control and diversity combining. Theoretically, extra transmission power can compensate for a shortfall of power during a period of fading and therefore deliver a constant level of power at the receiver antenna. However, considering the range and the speed of the received signal level variations, power control may not be effective in many cases, because the transmitter may not have the power control range to deliver the required power. Diversity combining takes advantage of the fact that different transmission paths go through independent fading patterns, and therefore a signal combined from two independent paths will fade less severely. These two techniques are discussed further in the following sections.

2.2.1 Power Control

Power control is a major aspect of any communication system. It is especially important in mobile communications, where the received power varies greatly as a mobile unit moves around the transmission channel. Mobile units have a limited power supply and cannot transmit with excessive power, but transmitting with inadequate power results in bad quality and an unacceptable BER.

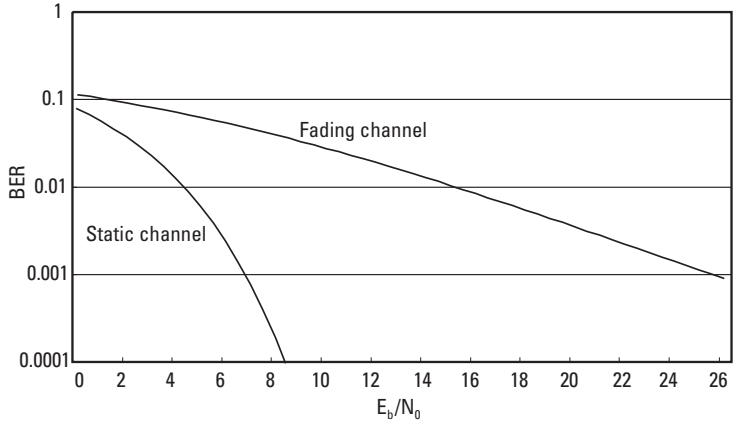

Figure 2.8 BER curves for Rayleigh fading and static channels.

For CDMA systems, power control has added importance. Because all CDMA users appear as interference to other users, any excessive transmission power will increase the overall interference, which results in reduced capacity for the system as a whole. We further discuss the issue of capacity in Chapter 6. It is well known that the user capacity of the CDMA systems can be largely reduced without an effective power control system [9–11].

The power level experienced by a receiver is the transmitted power multiplied by the channel gain (attenuation). The transmission channel gain can be represented as follows:

$$H(t) = h(t)\xi(t)\rho^{-r} \tag{2.6}$$

where $h(t)$ is the Rayleigh fading factor from (2.3); $\xi(t)$ is a shadowing factor and usually modeled as a log-normal variable; ρ is the distance between transmitter and receiver; and r is a factor depending on the environment that is usually between 2 and 4. The power control process acts to compensate for the channel attenuation.

In cellular mobile communications, transmission power must be controlled in both the uplink and downlink. Uplink power control is required for combating the near–far problem. In a cellular environment, the transmission path from a user closer to the cell site is likely to have a much smaller attenuation factor than users farther away. If all users transmit at the same power level, the received power at the base station from a near user can overwhelm the signals from more distant users and may result in disabling their communication with the base station. Thus both near and far users must adjust their transmission power in a way such that their signals arrive at the base station with equal received power levels. Downlink power control is required to increase the user capacity of the base station. Each base station has a limited transmission power budget that must be used to deliver signals to all the mobiles it serves. The lower the transmission power to each user can be kept, the more users that can be served. Furthermore, the amount of interference to the mobile users of other cells needs to be kept as small as possible.

TDD systems can provide CDMA communications with very efficient power control. The topic of power control is further discussed in Chapter 4.

2.2.2 Diversity Combining Techniques

The effect of fading can be reduced if the signal is received from two or more independently faded paths. When these received signals are combined, the fading in one path can be compensated by the received signal from another

path. Figure 2.9 shows how a selected path with the higher signal level from two independent Rayleigh fading paths yields significantly fewer fading periods.

A number of methods are possible for achieving independent diversity. The most commonly used of these methods is space or antenna diversity, where multiple antennas are used to transmit and receive signals. This is illustrated in Figure 2.10 where the base station receives signals from a mobile via two antennas. The antennas need to be sufficiently separated if the fading patterns of signals arriving at the antennas are to be uncorrelated. Generally a separation of 0.5λ is sufficient for this to be true. Alternatively, transmission to a receiver may be carried out via multiple antennas. This is referred to as transmission diversity. The reason is that the receiver may not be large enough to accommodate two antennas with sufficient separation to take advantage of diversity reception. Other diversity methods, aside from this spatial form, include angle-of-arrival diversity, polarization diversity, and time (signal repetition) diversity.

A diversity technique that is of particular importance to CDMA communication is multipath diversity. As discussed above, in frequency selective channels where the propagation delay spread is larger than the reciprocal of the receiver bandwidth (being the spread bandwidth here, with its reciprocal being T_c, the chip period), the signals of any two paths with a

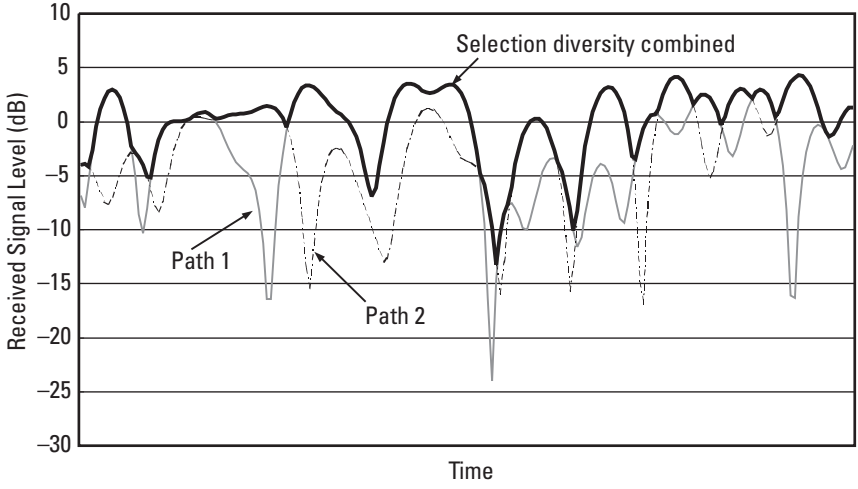

Figure 2.9 Selection diversity combining of two independent fading patterns.

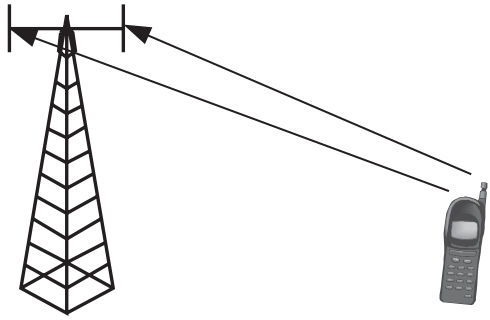

Figure 2.10 Antenna diversity reception.

propagation delay difference of more than T_c can be separated and independently detected [7, 12]. These signals also have independent fading patterns.

2.2.3 Diversity Combining Methods

Several diversity combining methods exist for selecting and combining more credible signals. The combiner usually estimates the signal strength of each path and sets its combining factors based on these estimates. Let us assume that in Figure 2.3, L independent paths carry the information transmitted from a base station to a mobile. A diversity combiner is shown in Figure 2.11. The parameters a_l are set according to the diversity combining method. We define two diversity combining methods:

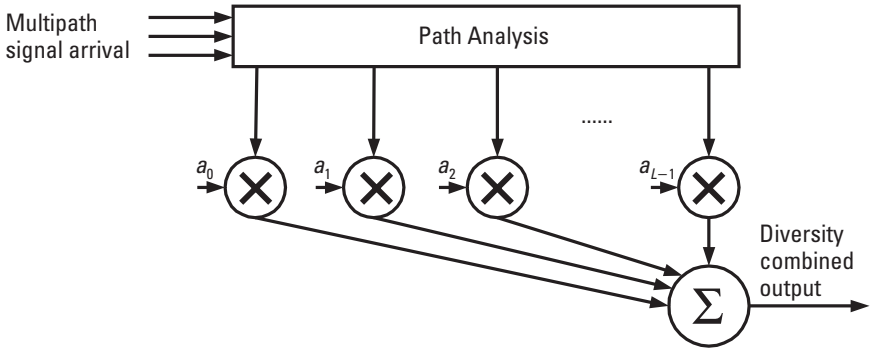

Figure 2.11 A diversity combining receiver.

- *Selection combining.* In this method, the signal from the path with the highest power is selected and the remaining signals are discarded. For example, if path i has the highest received power, the weighing factor a_i is set to one (or generally to a constant), and all other a's are set to zero. If all paths have the same average *signal power-to-noise ratio* (SNR) Γ_0, the probability distribution of the received SNR γ is expressed by

$$p(\gamma) = \frac{M}{\Gamma_0} \exp\left(-\frac{\gamma}{\Gamma_0}\right)\left[1 - \exp\left(-\frac{\gamma}{\Gamma_0}\right)\right]^{M-1} \tag{2.7}$$

  where M is the number of independent fading paths.

- *Maximum ratio combining.* In this method, the phase-locked signals from each path are added in such a way that the more powerful signals are emphasized and the less reliable ones are suppressed. It has been shown in [8] that the optimal ratio for maximizing the SNR is to set $a_l \propto \beta_l$. The probability distribution of the received SNR, γ, when all paths have the same average SNR Γ_0 is found from:

$$p(\gamma) = \frac{1}{M!} \frac{\gamma^{M-1}}{\Gamma_0^M} \exp\left(-\frac{\gamma}{\Gamma_0}\right) \tag{2.8}$$

Equations (2.7) and (2.8) are drawn for M = 1, 2, and 4 paths in Figure 2.12. Note that the one path case has a flat fading case, with an exponential distribution. It is demonstrated that the probability that the received power is large increases as the number of independent paths increases.

The probability of error results for a BPSK modulated system is found from

$$P_e = \frac{1}{2}\int_0^\infty \operatorname{erfc}\sqrt{\gamma}\; p(\gamma)\, d\gamma \tag{2.9}$$

Substituting for the probability distribution from (2.7) and (2.8), the probability error results are found for these diversity combining methods. The results are shown in Figure 2.13. For comparison, results of Figure 2.8 are also included. The improvement in system performance is clearly demonstrated.

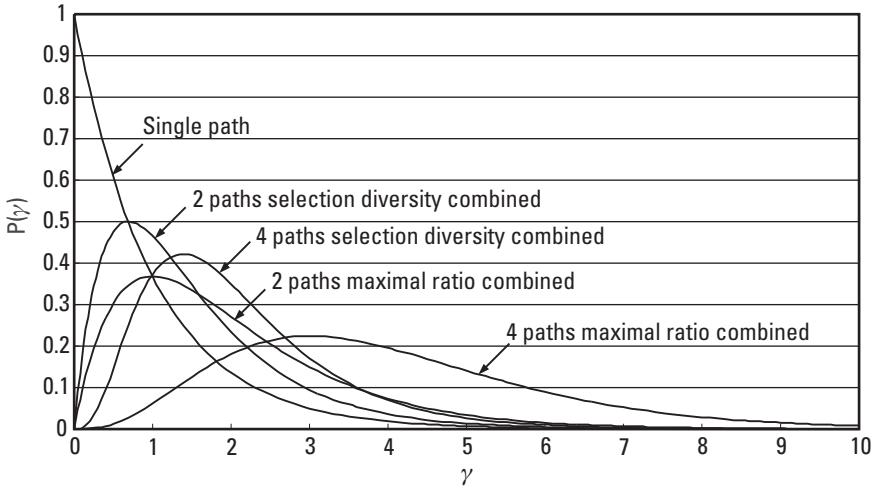

Figure 2.12 The probability of received SNR for diversity combining systems.

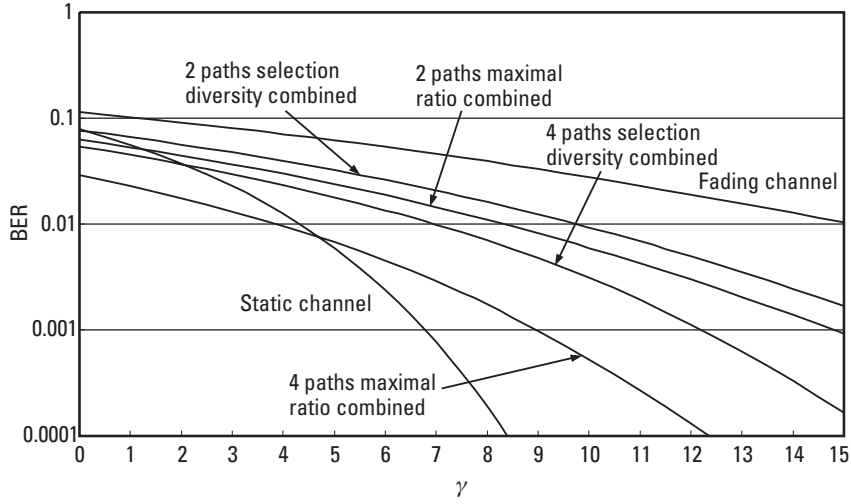

Figure 2.13 BER for diversity combined methods versus γ.

In a CDMA receiver, a multipath combining system, known as rake combiner, analyzes all received signals from independent paths, and optimally combines them in order to increase the signal-to-interference ratio. In

TDD-CDMA systems, the rake operation can be done at the transmitter side. This method, known as *pre-rake* is discussed in Chapter 5.

2.3 Spread Spectrum Communications

A large number of users communicate with each other via the public mobile communication system provided by a number of operators. The number of simultaneous users is generally limited by the bandwidth each operator is assigned and by the multiple-access technology used. Each operator is usually allocated a certain bandwidth, which it uses to serve as large a number of simultaneous users as possible. Several multiple-access techniques have been used in mobile communications. The first-generation systems such as AMPS were based on the FDMA technology. The second-generation systems, such as GSM, were based on the TDMA technology. And the third-generation systems are based primarily on the CDMA technology.

This section gives a general overview of spread spectrum modulation techniques. Based on this a basic introduction is made to the CDMA systems.

The spread spectrum communications technique is characterized by its use of the frequency spectrum in that the spectrum of the transmitted signal is spread over a very wide bandwidth—a bandwidth exceeding that normally required to accommodate the information to be transmitted. This is categorized by two of the most widely used methods of *direct sequence spread spectrum* (DS-SS) and *frequency-hopping spread spectrum* (FH-SS). In both of these methods, a pseudorandom code sequence is utilized to spread or map the signal information over a wide bandwidth. Most TDD-CDMA systems use the latter, although the former is used in a number of communication systems such as GSM. Here we deal with FH-SS technology only briefly, and instead concentrate on the DS-SS mode, which forms the basis for UMTS standards.

The principle behind the spreading of a signal is explained by the Shannon channel capacity formula:

$$C = B_w \log_2\left(1 + \frac{S}{N}\right) \tag{2.10}$$

where C is the capacity of a communication channel in bits per hertz, B_w is the bandwidth in hertz, S is the signal power, and N is the noise power. Equation (2.10) can be rewritten as

$$\frac{C}{B_w} = 1.44 \ln\left(1 + \frac{S}{N}\right) \tag{2.11}$$

which at small SNRs can be approximated as follows:

$$\frac{C}{B_w} = 1.44 \frac{S}{N} \tag{2.12}$$

or

$$B_w \approx \frac{NC}{S} \tag{2.13}$$

From (2.13) the necessary bandwidth for error-free transmission information at very low SNR can be calculated. It demonstrates that as the relative noise level increases, reliable transmission is possible by increasing bandwidth [13, 14].

2.3.1 FH-SS

An FH-SS system is similar to a *frequency shift keyed* (FSK) modulation. The difference is that in FSK systems two frequency tones are used for the modulation of 1 and 0 information, whereas in FH-SS a code-generator-controlled frequency synthesizer is used to sequentially modulate the information onto a very large set of frequency tones. The set of tones can be very large; an actual system is reported to have 2^{20} different frequencies [15].

A simple block diagram of a BPSK FH-SS system is shown in Figure 2.14. The code-controlled oscillator sequentially modulates the information onto a plane of frequencies. Because a very large number of modulating frequencies are used, the signal spectrum is spread over a very wide bandwidth.

The BPSK modulated signal, represented by $d(t)$, is equal to:

$$d(t) = \sqrt{2P}\ b(t) \exp(J\omega t) \tag{2.14}$$

where P is the transmitted power, $b(t)$ is the data stream consisting of a train of i.i.d. data bits with duration T_b and which take the values of ± 1 with equal probability, $\omega = 2\pi f$ is the carrier frequency, and $J = \sqrt{-1}$. The

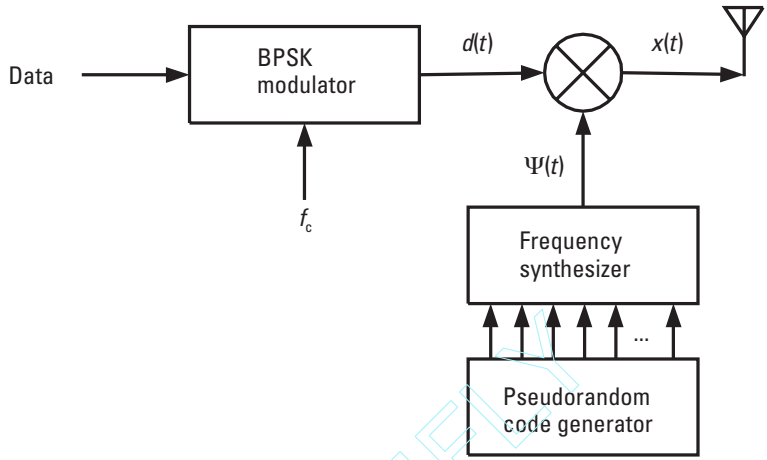

Figure 2.14 Block diagram of an FH-SS transmitter.

TEAM-FLY

spreading hopping sequence is the sum of a sequence of tones with a chip time duration T_c. It is represented by $\Psi(t)$ and is written as follows:

$$\Psi(t) = \sum_{n=-\infty}^{\infty} 2p(t - nT_C)\exp(J\omega_n t + j\phi_n) \tag{2.15}$$

where $p(t)$ is a unit amplitude pulse of duration T_c; and ω_n and ϕ_n are, respectively, the radian frequency and its associated phase during the nth hop.

From (2.14) and (2.15), the transmitted signal can be written as

$$x(t) = d(t)\,\Psi(t) \tag{2.16}$$

The received signal $y(t)$ is the multiplication of the transmitted signal and the channel impulse response $h(t)$ from (2.3), summed with a noise term $n(t)$:

$$y(t) = x(t)h(t) + n(t) \tag{2.17}$$

where δ is the propagation delay of the channel. At the receiver, a replica of the spreading frequencies $\Psi(t)$ is generated to despread the frequency-hopped signal, as shown in Figure 2.15. The product of $\Psi(t - \hat{\delta}_d)\Psi(t - \delta_d)$ is equal to 1 after the bandpass filter if $\hat{\delta}_d$ can be estimated to be equal to δ_d [12]. If the delay is estimated accurately, then the multiplication will

Team-Fly®

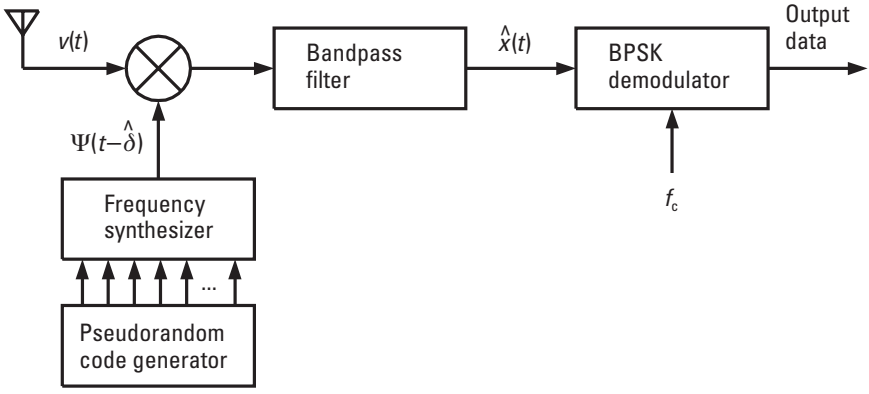

Figure 2.15 Block diagram of an FH-SS receiver.

remove the FH component and result in the original baseband signal (with the additional noise and other interference; not shown in Figure 2.15).

Based on the hopping rate, the FH-SS systems are classified into two different groups. If the frequency hop occurs at every few bit intervals, the system is called a *slow frequency hopping spread spectrum* (SFH-SS) system, but if many hops occur during a bit period, the system is known as a *fast frequency hopping spread spectrum* (FFH-SS) system. Figure 2.16 illustrates the two systems.

2.3.2 DS-SS

A simple block diagram of a BPSK DS-SS system is shown in Figure 2.17. The BPSK modulated data, represented by $d(t)$ in (2.14), is spread after multiplication by a *pseudorandom* (PN) sequence with a bandwidth much greater than the information signal. The transmitted signal $x(t)$ can be expressed as

$$x(t) = \sqrt{2P}b(t)a(t)\exp(J\omega t) \tag{2.18}$$

where $a(t)$ is the spreading PN sequence with chips of ± 1 of duration and code length of $N = T_b/T_c$. The signal spectrum at various stages of transmission is shown in Figure 2.18. As an information signal is multiplied by the PN sequence, its energy is spread over a wide bandwidth while the total

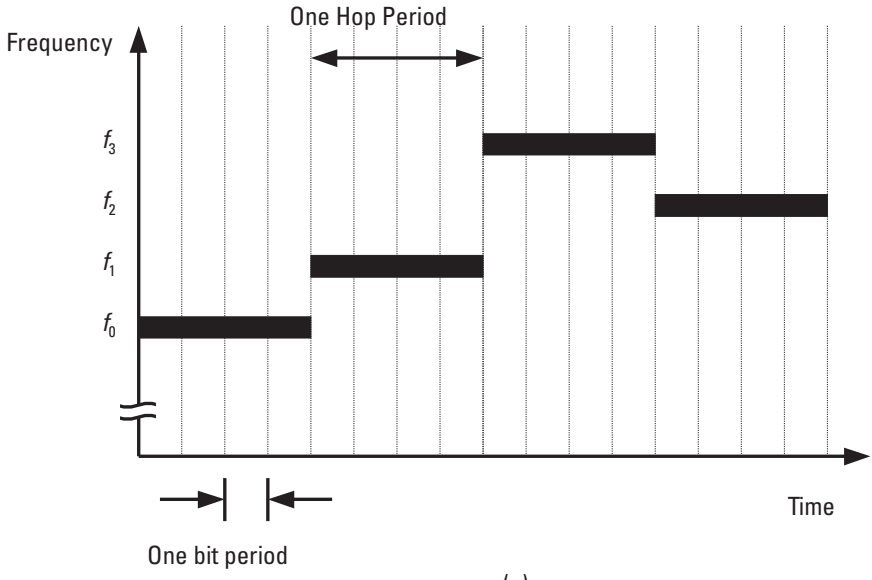

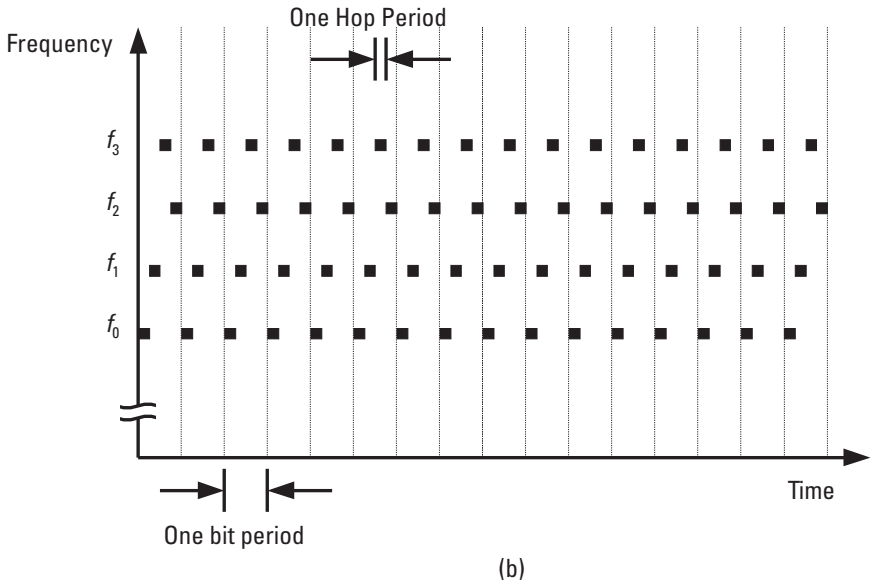

Figure 2.16 A frequency versus time diagram of the two different types of FH-SS systems: (a) SFH-SS and (b) FFH-SS.

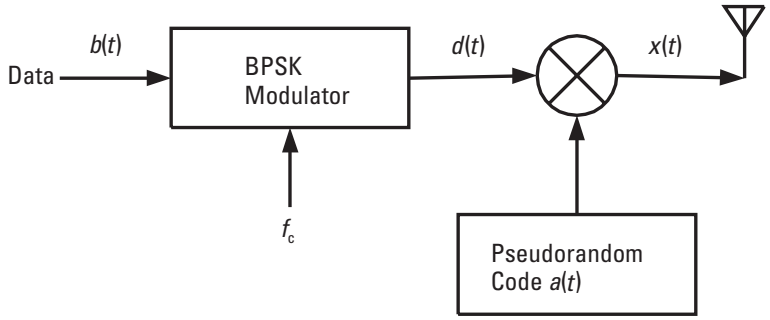

Figure 2.17 Block diagram of a DS-SS transmitter.

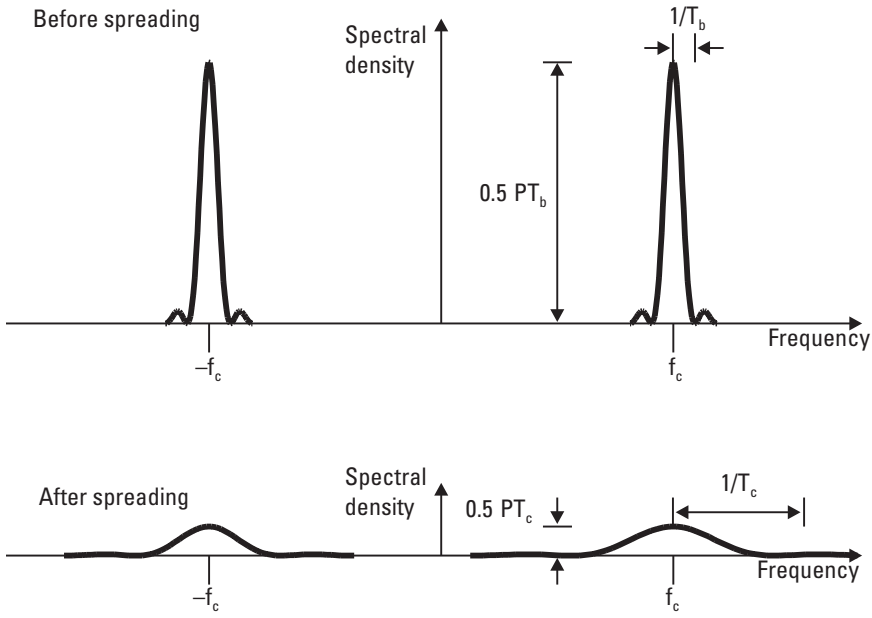

Figure 2.18 Signal spectrum of a DS-SS modulation before and after spreading.

signal energy remains constant. If the spreading ratio is large enough, the spread signal appears as very low power noise.

A block diagram of a DS-SS receiver is shown in Figure 2.19. The received signal $y(t)$ is expressed as

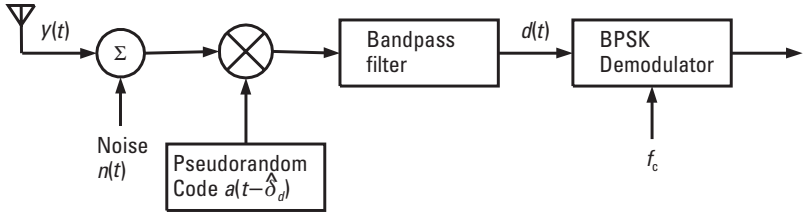

Figure 2.19 Block diagram of a DS-SS receiver.

$$y(t) = h(t)\, x(t - \delta_d) + n(t) \tag{2.19}$$

where $h(t)$ represents the propagation channel impulse response, including multipath fading, shadowing, and path loss; δ_d is the channel propagation delay; and $n(t)$ is zero mean *additive white Gaussian noise* (AWGN) with a two-sided power spectral density of $N_0/2$.

Substituting for $x(t)$ from (2.18) yields:

$$y(t) = h(t)\sqrt{2P}\, b(t - \delta_d)a(t - \delta_d)\, \exp\left[J\omega(t - \delta_d)\right] + n(t) \tag{2.20}$$

The received signal $y(t)$ of (2.19) is multiplied by a delayed replica of the spreading sequence $a(t - \hat{\delta}_d)$, where $\hat{\delta}_d$ is a local estimate of the propagation delay δ_d:

$$\begin{aligned} \hat{d}(t) &= \sqrt{2P}h(t)b(t - \delta_d)a(t - \delta_d)a\left(t - \hat{\delta}_d\right) \\ &\exp\left[J\omega(t - \delta_d)\right] + a\left(t - \hat{\delta}_d\right)n(t) \end{aligned} \tag{2.21}$$

The despreading of signal $y(t)$ is realized if $\hat{\delta}_d$ can be estimated at the receiver to be equal to δ_d, in which case $a(t - \hat{\delta}_d)a(t - \delta_d) = 1$. Noise power remains unchanged.

The DS-SS signal can be despread by a matched filter. In a matched filter, the received signal is fed to a delay line, which consists of shift registers operating at chip clock rate. A locally generated replica of the spreading sequence multiplies the output of the shift registers. The results are summed, so when there is a match between the input signal and the spreading sequence, the output is large. Otherwise the output is minimal and depends on the autocorrelation and cross-correlation properties of the PN code. In practice, less than perfect synchronization between the received signal's spreading phase and the locally generated spreading signal's phase results in

loss of performance, assuming that the receiver can perfectly estimate the delay and phase and therefore perfectly despread the received signal. The operation of a matched filter is illustrated in Figure 2.20.

The output of the matched filter is a signal with the prespreading bandwidth. All other signals that are spread with different PN sequences remain wideband, and most of their energy will be filtered out. This is the basis for the CDMA systems, where different users are assigned a different spreading code. All signals are then transmitted at the same carrier frequency and are distinguished at the receiver by their unique spreading code.

The increase in the received signal level, caused by despreading, is defined as process gain, G_p, of the spread spectrum systems and is equal to the bandwidth ratio of the spread signal and the narrowband (before spreading) signal:

$$G_P = \frac{BW_s}{BW_n} = \frac{T_s}{T_c} \tag{2.22}$$

where T_s is the symbol period and T_c is the chip period.

2.4 CDMA Communications

As discussed earlier, all of the users in a CDMA system transmit in the same frequency band and access the transmission medium simultaneously with

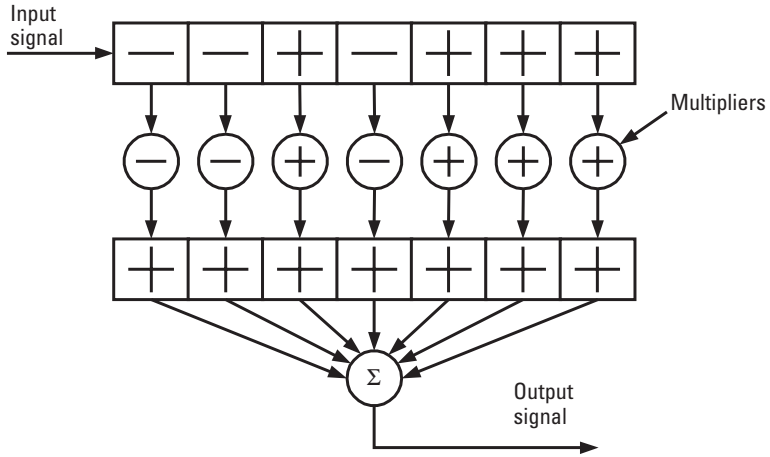

Figure 2.20 Operation of a matched filter.

many other users. The signals to and from a user are spread by a set of unique spreading code sequences, assigned by the communication system. This set of codes is assigned to the user for the entire duration of the call, and may be reassigned to other users after the call is finished. In the uplink all users' signals arrive at the base station and are distinguished by their spreading codes. In the downlink the base station transmits to all users simultaneously and each user receives the signal intended for it by despreading with its assigned code. Except for the desired signal that will be despread, all other users' signals will remain spread and appear effectively as noise. Figure 2.21 shows how the *signal-to-interference ratio* (SIR) changes as the result of despreading. As the interference and noise powers are reduced by a ratio equal to G_p:

$$(I+N)_{(\text{before})} = G_P \cdot (I+N)_{(\text{after})} \tag{2.23}$$

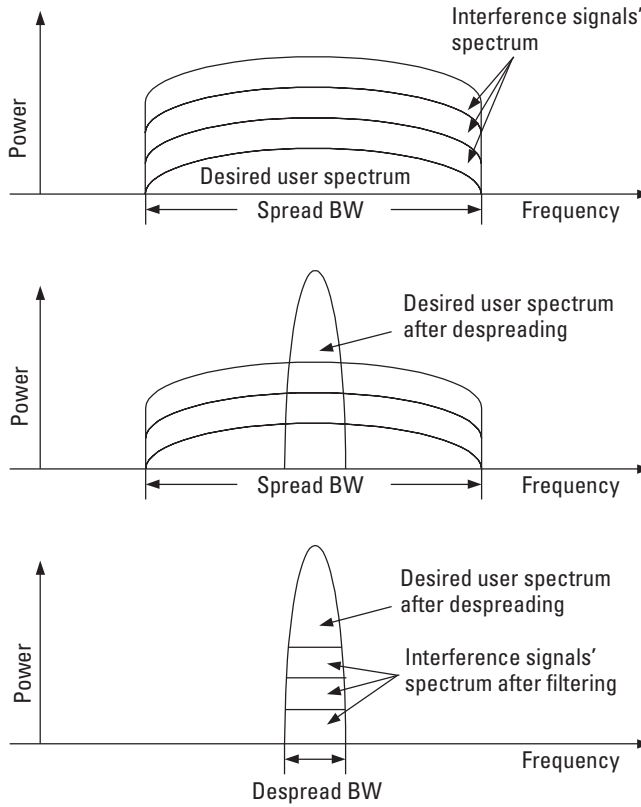

Figure 2.21 Signal and interference power before and after despreading.

the resulting SIR after despreading is increased by the same ratio compared with before despreading:

$$\frac{S}{I+N}_{(\text{after})} = G_P \cdot \frac{S}{I+N}_{(\text{before})} \tag{2.24}$$

A note is in order to clarify terms such as E_b/N_0 and E_b/I_0 and their relation to SNR and SIR. For a noise-only system (i.e., no interference), E_b/N_0 is calculated from

$$\frac{E_b}{N_0} = \frac{S}{N}_{(\text{after})} \cdot \frac{BW_n}{R} \tag{2.25}$$

where R is the symbol rate. When interference exists, a similar equation can be written as follows:

$$\frac{E_b}{I_0+N_0} = \frac{S}{I+N}_{(\text{after})} \cdot \frac{BW_n}{R} \tag{2.26}$$

In CDMA systems, interference is dominant and the term E_b/I_0, without N_0, is often used.

2.4.1 Uplink of a CDMA System

The performance of a CDMA system can be derived by examining its SIR. For a single-cell CDMA system with K users, the real part of the transmitted signal from user k may be written as

$$s(t) = \sqrt{2P_k}\, a_k(t) b_k(t) \cos(\omega_c t) \tag{2.27}$$

where P_k is the received power level, $b_k(t) \in \{-1,1\}$ is the data sequence, and $a_k(t) \in \{-1,1\}$ is the spreading sequence. The received signal over channel $h_k(t)$ is:

$$r_k(t) = \sqrt{2P_k}\, h_k(t) a_k(t-\tau_k) b_k(t-\tau_k) \cos(\omega_c t + \phi_k) \tag{2.28}$$

where τ_k and ϕ_k are the relative delay and phase to a reference user 0. The received signal at the base station for all K users is:

$$r(t) = \sum_{k=0}^{K-1} r_k(t) + n(t) \tag{2.29}$$

where $n(t)$ is AWGN with a two-sided power spectral density $N_0/2$. The received signal is despread to the original bandwidth by multiplying it by the code sequence of user 0, and integrating over one bit period (here the zeroth bit). The decision variable for user 0 can be written as:

$$Z_0 = \int_0^{T_b} r(t)a_0(t)\cos(\omega_c t)\,dt \tag{2.30}$$

Substituting from (2.27) and (2.29) in (2.30) results in (2.31):

$$Z_0 = \int_0^{T_b}\left[\sum_{k=0}^{K-1}\sqrt{2P_k}\,h_k(t)a_k(t-\tau_k)b_k(t-\tau_k)\cos(\omega_c t+\phi)+n(t)\right] \tag{2.31}$$
$$a_o(t)\cos(\omega_c t)\,dt$$

where Z_0 can be expressed as the sum of its main components:

$$Z_0 = D_0 + A + \eta \tag{2.32}$$

where D_0 is the desired signal for user 0, A is the multiuser interference, and η is noise contribution. Signal D_0 is derived by setting $k = 0$ in (2.31). Because $a_0^2(t) = 1$, the value of D_0 depends only on the transmitted symbol $b_0(t)$ and the channel factor $h_0(t)$. The interference part, A, is found by setting $k \neq 0$ in (2.31). Its value is calculated by considering the statistics of the multiplication of $a_0(t)a_k(t-\tau_k)$. This value, summed over the entire spreading code period, is referred to as the cross-correlation between the spreading codes of users 0 and k. The cross-correlation value is an important factor when deciding on the codes. A number of spreading codes groups are designed to exhibit orthogonality to each other if $\tau_k = 0$, that is, $a_0(t)a_k(t) = 0$ for all k. This is important because it means that the interference due to cross-correlation can be zero. The condition of $\tau_k = 0$ can be realized in the downlink transmission of signals where the base station transmits to all users at synchronously. However, this is only fully realized when the channel consists of a single path, that is, for the case of a flat fading channel where the maximum delay spread is less than T_c. In multipath channel conditions, the signals arriving through multipaths cannot be synchronous to each other and therefore the condition of $\tau_k = 0$ will not be realized. An orthogonality factor is defined for different channels. This factor expresses what ratio of the downlink multiuser interference is removed due to orthogonality of the codes and what ratio remains due to multipath signal reception [5, 6].

2.5 System Configuration

Although spread spectrum systems were mainly used for military applications for the first half century of their existence, during the 1990s they gradually began to be used for a great many civil applications. We have already talked about the application of DS-SS-based CDMA systems to cellular mobile communications. DS-SS and FH-SS systems are used also in cordless and ad hoc networks in public and private communications systems. In this section we briefly define the characteristics of cellular and ad hoc systems. The detailed definition of usage of a TDD-CDMA system in each configuration is given in Chapters 7 and 8.

2.5.1 Public Systems

In this group we classify all public land and satellite mobile communication systems. In these systems, a central station, generally referred to as a *base station* (BS), serves all mobile users within its coverage area. The position of a BS may be fixed for a great majority of the systems. For example, GSM, PDC, or CDMA BSs are installed at a place where they remain for a long time. Other examples are geostationary satellite mobile systems such as those operated by InmarSat. These satellites are also maintained at a relatively stationary position in reference to a point on Earth. Another example is the proposal for using large airships over metropolitan areas. In some special cases, a base station might be installed temporarily in response to a temporary increase in traffic in a hot spot, and then later removed as the system configurations are upgraded to take care of the increased traffic demand.

The base station may also be nonstationary, such as a number of *low-Earth-orbit* (LEO) satellite mobile communication systems. In these systems although the BSs move, a mobile user is able to establish a connection to a new station as it loses sight of the present server.

All of these systems share a common characteristic: They are owned and operated by an entity other than the users. A user subscribes to these systems and uses the communication services at a cost.

The system topography is generally a star network. A central station serves a number of mobile users, although the users may at times be connected to two or more stations. The central system is usually connected to the public landline system that carries the traffic over the network backbone.

The TDD-CDMA technique is standardized to operate in the TD-CDMA mode of the UMTS 3G system. It is further being standardized

for the Chinese TD-SCDMA system. We will define these standards in detail in Chapter 7.

2.5.2 Private and Ad Hoc Systems

A number of spread spectrum CDMA-based systems exist that are owned and operated privately. These range from cordless telephones to ad hoc systems, and to wireless local-area networks. In general, these are systems that need very little expertise to be installed and can be easily moved from place to place. They also cost significantly less than the public mobile systems. Most of these systems use the TDD mode of CDMA due to its lower cost and simplicity of operation. Most (if not all) operate in unlicensed bands.

The topology is a star network in most cordless and wireless standards. However, the ad hoc networks use a master/slave configuration that can dynamically change from user to user.

In Chapter 8 we will describe a TDD-CDMA based cordless phone system, and the Bluetooth ad hoc system.

TEAM-FLY

2.6 Summary

This chapter presented a brief technical background for the subjects that will be discussed in this book. We will discuss power control, diversity transmission, and capacity enhancement techniques as they are realized in a TDD-CDMA system. Therefore, a summary of the mathematics related to these technologies was presented here.

References

[1] ITU-T, G.723, G.721, G.729 standards; http://www.itu.net.

[2] ITU-T, H.261, H.263 standards; http://www.itu.net.

[3] Lin, S., and D. J. Castello, *Error Control Coding, Theory and Practice,* Upper Saddle River, NJ: Prentice Hall, 1993.

[4] Holma, H., and A. Toskala, *WCDMA for UMTS,* New York: Wiley, 2001.

[5] Rappaport, T. S., *Wireless Communications,* Upper Saddle River, NJ: Prentice Hall, 1996.

[6] Jakes, C., *Microwave Mobile Communications,* New York: Wiley, 1974.

Team-Fly®

[7] Turin, G. L., "Introduction to Spread Spectrum Anti Multipath Techniques and Their Application to Urban Digital Radio," *IEEE Proc.,* Vol. 68, No. 3, March 1980, pp. 328–353.

[8] Schwartz, M., W. R. Bennet, and S. Stein, *Communication Systems and Techniques,* New York: McGraw-Hill, 1966.

[9] Ariyavsitakul, S., and L. F. Chang, "Signal and Interference Statistics of a CDMA System with Feedback Power Control," *Proc. IEEE Globecom,* December 1991, pp. 1490–1495.

[10] Cameron, R., and B. D. Woerner, "An Analysis of CDMA with Imperfect Power Control," *Proc. IEEE Vehicular Technology Conference,* May 1992, pp. 977–980.

[11] Heath, M. R., and P. Newson, "On the Capacity of Spread Spectrum CDMA for Mobile Radio," *Proc. IEEE Vehicular Technology Conference,* May 1992, pp. 985–988.

[12] Simon, M. K., et al., *Spread Spectrum Communications,* Rockville, MD: Computer Science Press, 1985.

[13] Zeimer, R. E., and R. L. Peterson, *Digital Communications and Spread Spectrum Systems,* New York: Macmillan, 1985.

[14] Viterbi, A. J., *CDMA: Principles of Spread Spectrum Communication,* Reading, MA: Addison-Wesley, 1995.

[15] Dixon R. C., *Spread Spectrum Systems,* New York: Wiley Interscience Publication, 1976.

3

TDD Transmission

Duplex transmission of information between two users can be accomplished in several ways. The most common method is FDD transmission, in which separate frequency channels are used for duplex transmission. TDD systems accomplish two-way communication by allowing each party to communicate over the same frequency band by alternately transmitting and receiving. This chapter defines TDD operation in CDMA systems and how TDD differs from the FDD mode of operation.

3.1 TDD System

Figure 3.1 illustrates how TDD and FDD modes carry out data transmission over a mobile communication system [1]. In an FDD system two separate frequency channels are used for full-duplex transmission. One frequency channel is used for downlink, or BS to *mobile terminal* (MT), transmission. Also, a separate frequency channel is used for the uplink, or MT to BS, transmission.

A TDD system, however, uses the same frequency channel for full-duplex transmission and reception of signals on the downlink and uplink. This is accomplished by sharing the channel between the uplink and downlink transmissions by way of allocating certain times for each transmission and switching alternately between the two links. TDD systems are also known as Ping-Pong systems, because data are alternately sent and received.

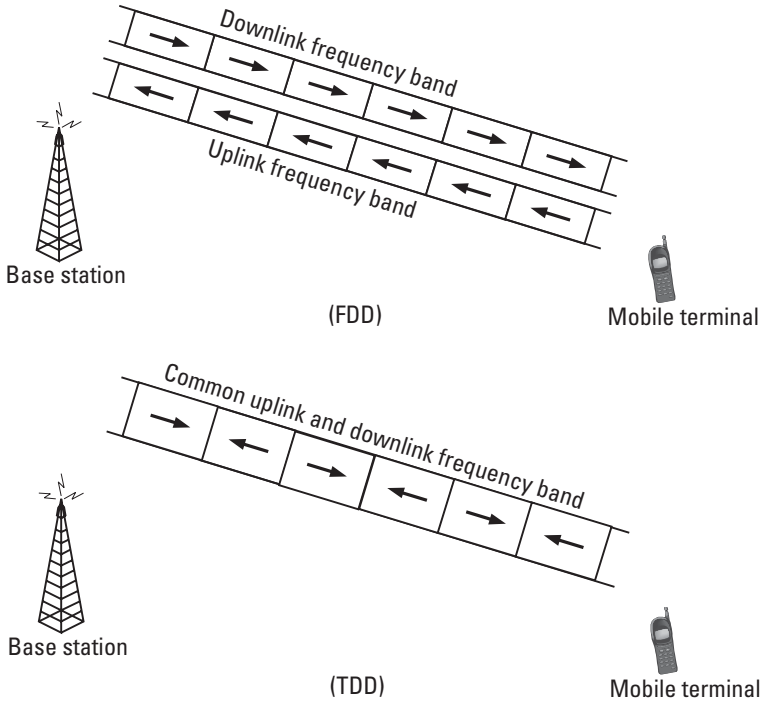

Figure 3.1 TDD and FDD.

The lengths of uplink and downlink slots, τ_{ul} and τ_{dl}, respectively, are either set by the communication system and broadcast to mobile terminals who wish to connect to the system or are fixed by the standards.

A frequency guardband is required in an FDD system to minimize the mutual interference between the uplink and downlink. The level of interference that can be tolerated by the system determines the size of the guard band. In a TDD system both uplink and downlink transmit in the same frequency band and therefore a frequency guardband is not necessary. However, a time guard at the BS, τ_b, and a smaller guard time at the MT, τ_m, are necessary to prevent interference between the uplink and downlink transmissions (Figure 3.2).

The lengths of slots can be unequal, $\tau_{ul} \neq \tau_{dl}$, as illustrated in Figure 3.3, or the number of the uplink and downlink slots per frame can be different as in Figure 3.4 [2]. This results in unequal system capacity for the uplink and downlink of a system, which is very important for cases where traffic requirements for uplink and downlink are different. For voice traffic, the capacity

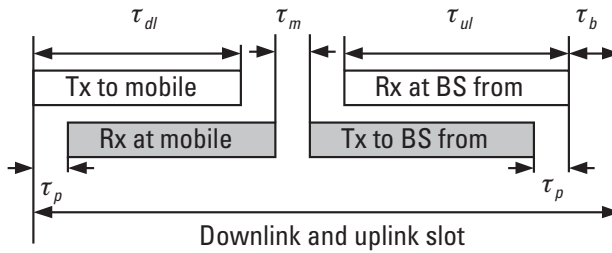

Figure 3.2 One uplink and one downlink TDD slot.

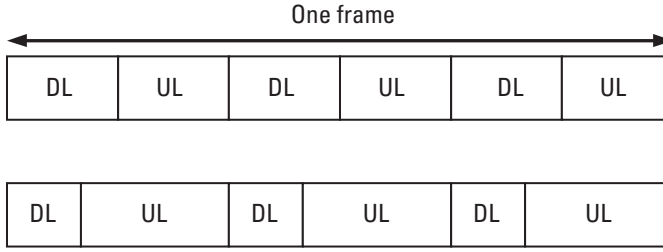

Figure 3.3 Unequal uplink and downlink slot lengths.

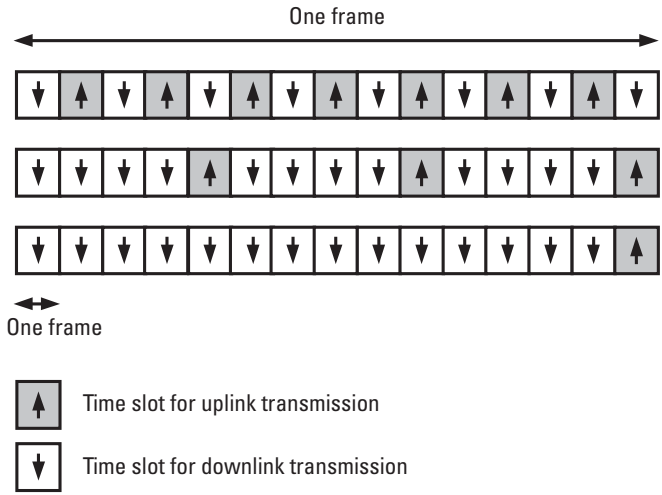

Figure 3.4 Unequal number of uplink and downlink slots per frames.

requirements are more or less the same, although the capacity is limited by the downlink. This is mostly due to the processing limitations of MTs. However, for data traffic, the capacity requirements of the downlink and uplink can be significantly different as traffic requirements are expected to be much larger in the downlink. This is due to the fact that Internet usage is mostly downloading rather than uploading, a trend that is expected to be repeated for mobile data communications. The TDD mode of operation is flexible in sharing the total bandwidth capacity between the uplink and downlink as traffic requirements change. It is reasonable to assume that mobile communication traffic will be more voice to start with, but that gradually data traffic will become more significant. The TDD mode can flexibly respond to this change in traffic profile. In contrast, in FDD operation, the uplink or downlink frequency bands, once assigned, cannot be readily reassigned.

In an FDD system the uplink and downlink frequency channels are separated [1, 3]. The separation is called a frequency guardband, and its purpose is to reduce the mutual interference between the transmissions to and from a communication device. Figure 3.5 shows the frequency plan for the European, North American, and Japanese mobile communication systems. It can be seen that for FDD systems, such as WCDMA-FDD, two equal portions of frequency bandwidth, one for uplink transmission and one for downlink transmission, have been assigned. The uplink assigned band of IMT-2000 is 1,920–1,980 MHz, and the downlink, 2,110–2,170 MHz [4]. A guardband of 190 MHz separates the assigned frequency bands. Standardization bodies decide the frequency assignment and, therefore, the channel separation. The decision depends on factors such as the requirements of public and private communications, as well as the costs of filtering used to reduce the mutual interference between uplink and downlink transmissions.

Figure 3.5 also shows that some bands have been assigned on a continuous basis. That is, no matching frequency bands have been assigned. These are sometimes unlicensed bands. For these bands communication devices can be developed using any available technology. The only limitation is the output transmission power level, which must remain below a set value. These bands are sometimes shared with other systems, such as radars, and medical and industrial devices. An example is the Industrial, Scientific and Medical (ISM) band, which in Europe and North America is assigned at 2.4–2.483 GHz. This band is used also for cordless telephones and *wireless local-area networks* (WLANs.) There are also licensed unpaired bands. These are usually, although not necessarily, intended for a TDD operation. Examples are shown in Figure 3.5 for DECT in Europe and PHS in Japan as well as the IMT-2000 TDD assigned bands [5, 6].

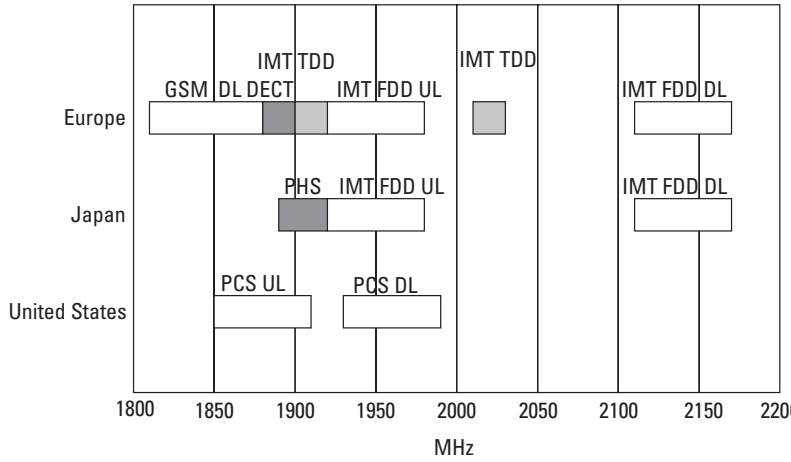

Figure 3.5 A frequency plan for mobile communication systems.

It follows that the required bandwidth for the transmission of the same bit rate over the uplinks and downlinks for an FDD and a TDD system needs to be equal to the sum of the allocated bandwidth for the uplinks and downlinks in a comparable FDD system with similar capacity.

As explained in Chapter 2, in contrast to a TDMA or FDMA system, where separate frequencies are assigned to the transmission of signals in each cell, CDMA systems do not require frequency planning because the same frequency band is used in all cells. As defined above, in an FDD-CDMA system, separate frequency bands are used for the uplink and downlink transmissions [7]. In contrast, in a TDD-CDMA system the same frequency is used for the uplink and downlink transmissions. As in any CDMA systems, the users are distinguished by the spreading codes they use. A CDMA system, operating in the TDD mode, is illustrated in Figure 3.6. A BS uses one or more set of codes for conveying control information, such as pilot bits, power control, broadcast channels, and so forth. One or more set of codes is used for uplink common channels such as a random-access channel. In addition, each user's data traffic will be spread using a unique code set [3].

As discussed, in a TDD system, data are transmitted in bursts. This could pose some problems since the spread spectrum receiver may lose synchronization and tracking during the periods of no signal reception. Isolated bursts of transmission require initial synchronization, which means that a permanent part of each burst is then needed for synchronization preambles. However, the TDD systems do not need these preambles for each burst

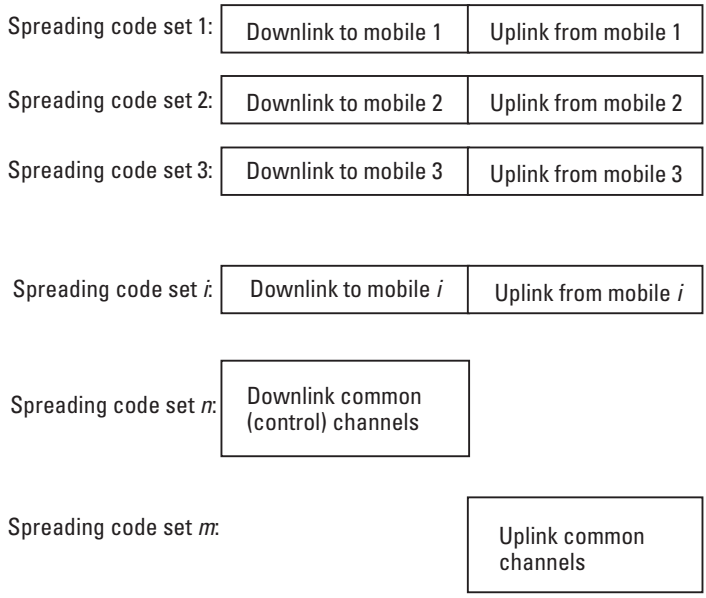

Figure 3.6 The TDD-CDMA system.

because the receiver is reasonably expected to maintain synchronization between successive burst receptions. This is due to the fact that the channel delay profile does not change significantly during a TDD burst of typically less than a millisecond. The configuration of the TDD CDMA system and the subject of acquisition of spread spectrum signals are discussed in [8], where it is shown that acquisition can be made even under high levels of interference for typical TDD burst lengths.

3.2 Synchronous Transmission

From Figure 3.6 we can also see that downlink transmission is carried out synchronously. Generally the downlink transmission is carried out in a chip-synchronous and symbol-synchronous fashion in both TDD and FDD systems. In addition to this, TDD systems are also time-frame synchronous. The reason is quite clear: A mobile cannot be transmitting uplink, while a neighboring mobile is receiving a downlink transmission. The mutual interference can be prohibitive. All TDD-CDMA base stations must transmit in a time-frame synchronous fashion. BS synchronization can be accomplished

by using a central timing system, such as the *Global Positioning Satellite* (GPS) positioning system, or by using a master/slave topology where a cluster of BSs are synchronized through a master BS. This is a disadvantage compared with FDD systems and one reason why TDD systems are not more widely used.

As illustrated in Figure 3.7, τ_b is decided by the maximum cell radius r_c, and calculated as

$$\tau_b \geq \frac{2r_c}{c} \tag{3.1}$$

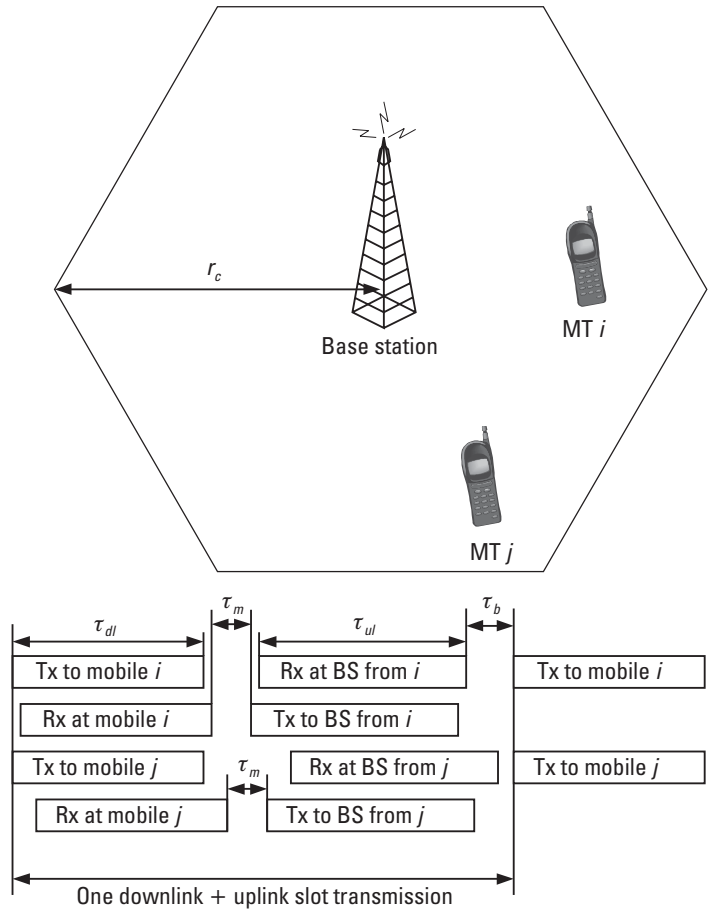

Figure 3.7 Guard time in a TDD system.

where c is the speed of light. The guard time is usually set by standards, and the maximum cell size of a TDD base station is calculated from it. For example, if τ_b is set to 5 μs, the maximum cell radius can be 750m.

TDD uplink/downlink slots also facilitate chip-synchronous transmission in the uplink. The regular time intervals allow a mobile to accurately detect changes in the propagation delay and to adjust its transmission time such that its signal may arrive synchronously with other users in the same cell. Although this is possible for FDD operation as well, it is more easily implemented in TDD [9]. We will discuss this further in Chapter 6.

3.3 Why TDD?

First proposed in a report at a Japanese IEICE Communication Society seminar in August 1991 [10], TDD-CDMA followed from the earlier TDD-TDMA systems. As noted in Chapter 1, all half-duplex systems, such as amateur radio, are in fact TDD systems. The communications parties alternately talk and listen, or send and receive information, using a manual switch. In "modern" TDD systems, the switching between uplink and downlink is automatic. Furthermore, in a multiple-access scheme it is done in a star topology; that is, it is carried out between a central unit and multiple terminals.

The first public cellular-mobile communication systems to use the TDD mode were PHS in Japan and DECT in Europe [5, 11]. The evolution of these systems occurred during the late 1980s and the systems have been in operation since 1993. Both of these systems were based on the TDMA method. A number of vendors also offered cordless phones based on a TDD mode in unlicensed bands [12, 13].

There are two main reasons for selecting a TDD mode of operation. One is its more efficient bandwidth utilization that is realized in nonpaired, continuous bands, as illustrated in Figure 3.8. Using an FDD mode would result in a tradeoff between the utilized bandwidth and the cost of bandpass filtering. Low-order, low-cost filters necessitate a large guard frequency and, therefore, inefficient use of the spectrum. Better usage of frequency spectrum can be accomplished using higher order, more expensive filters. Using the same set of filters and equalizers for both reception and transmission also results in cost savings. Another reason is the channel reciprocity between the uplink and downlink and the several advantages that result from it. Reciprocity is discussed further in the next section. The advantages resulting from reciprocity are discussed in Chapters 4, 5, and 6.

Team-Fly®

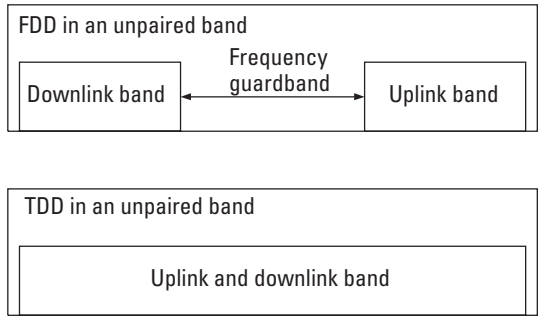

Figure 3.8 Uplink and downlink channel assignment in TDD and FDD modes of an ISM band operation.

3.3.1 Reciprocity

Communication channel characteristics were defined in Chapter 2, where we noted that the fading pattern caused by the multipath arrival of a signal at various points in a geographical area was the result of the combination of signal coming from different paths.

Figure 3.9 shows a model of the fading channel in which the received signal at the mobile unit is shown as a sum of received vector signals. Each received signal component goes through a distinct path and has a different carrier phase shift, signal strength, and propagation delay. If $x(t)$ is the transmitted signal from a BS, the received signal $y(t)$ at an MT can be written as follows:

$$y(t) = \sum_{k=1}^{K} b_k x(t - \delta_k) e^{J\theta_k} + n(t) \tag{3.2}$$

where b_k is the signal gain factor, δ_k is the propagation delay, and θ_k is the carrier phase shift all for path k.

Except for noise, all other factors of (3.2) are the same for forward and reverse links. If a path exists in the forward link, it must also exist in the reverse link because the same antennas are used for transmission and reception. Thus, if the same signal $x(t)$ were transmitted from an MT toward a BS at the same time t, it would be received at base station with the same fading character. Because fading occurs because of the constructive or destructive summing of signals from different paths, if the paths are identical, the sum in (3.2), with the exception of noise, remains the same for both uplink and downlink [3].

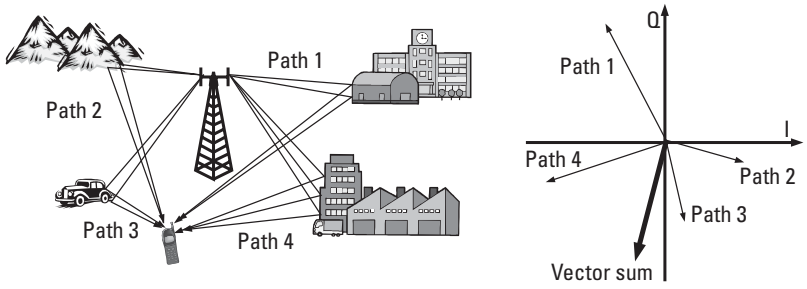

Figure 3.9 Fading pattern reciprocity in TDD systems.

Figure 3.10 shows the shift in center frequency due to the movement of a mobile unit and possible movements of the signal reflector. It can be shown that the Doppler shift is identical for both the uplinks and downlinks of a TDD communication channel.

Let f_c denote the downlink carrier frequency. The reflected signal has a different carrier frequency due to the Doppler shift resulting from the reflector movement. The new carrier frequency f_{c1} can be written as

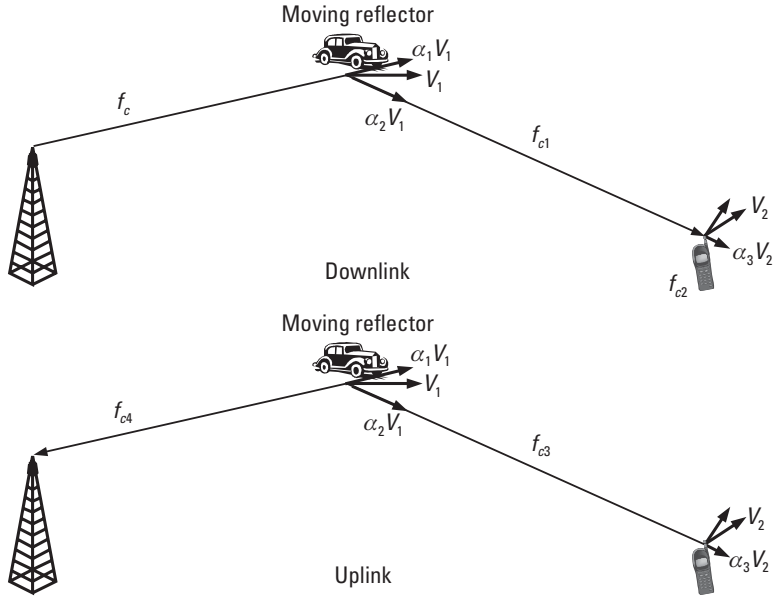

Figure 3.10 Fading reciprocity with a moving reflector.

$$f_{c1} = f_c + \frac{(\alpha_2 - \alpha_1)V_1 f_c}{c} \tag{3.3}$$

where $\alpha_1 V_1$ is the component of reflector velocity in the direction of transmitted signal ray, and $\alpha_2 V_1$ is the component in the reflected direction.

The received signal at the moving mobile unit has a carrier frequency equal to f_{c2} which can be written as

$$f_{c2} = f_{c1} + \frac{\alpha_3 V_2 f_{c1}}{c} \tag{3.4}$$

where $\alpha_3 V_2$ is the velocity component in the direction of the received signal. Substituting for f_{c1} from (3.3) yields

$$f_{c2} = f_c + \frac{(\alpha_2 - \alpha_1 V_1 f_c)}{c} + \frac{\alpha_3 V_2 f_c}{c} + \frac{\alpha_3 V_2 (\alpha_2 - \alpha_1) V_1 f_c}{c^2} \tag{3.5}$$

On the other hand, the signal transmitted from the mobile unit (uplink) has a Doppler shifted carrier frequency because of the unit movement, represented as f_{c3}:

$$f_{c3} = f_c + \frac{\alpha_3 V_2 f_c}{c} \tag{3.6}$$

The reflected signal also experiences a shift in its carrier frequency due to the movement of the reflector. This frequency f_{c4} can be written as

$$f_{c4} = f_{c3} + \frac{(\alpha_2 - \alpha_1)V_1 f_{c3}}{c} \tag{3.7}$$

Substituting for f_{c3} yields

$$\begin{aligned} f_{c2} &= f_c + \frac{(\alpha_2 - \alpha_1)V_1 f_c}{c} \\ &+ \frac{\alpha_3 V_2 f_c}{c} + \frac{\alpha_3 V_2 (\alpha_2 - \alpha_1) V_1 f_c}{c^2} \end{aligned} \tag{3.8}$$

which is equal to (3.5). Hence, in a TDD environment the Doppler shift is equal for both uplinks and downlinks. Note that in the case of a stationary reflector, both α_1 and α_2 are equal to zero.

3.3.2 Impulse Response Estimation

Reciprocity is the main feature of TDD systems. In practice, a TDD receiver analyzes the received signal to determine the channel impulse response. The received signal, or an associated auxiliary channel, usually contains some pilot symbols, which provide the receiver with a reference signal. Although the received pilot symbols are affected by noise in the same way as data symbols, averaging over several symbols reduces the effect of noise and other reference to give a fairly accurate estimate of the complex channel impulse response. The present estimates can be used to forecast the impulse response for the next transmission slot. Accuracy also depends on the correlation between the power levels of two consequently received and transmitted bursts. As discussed in Chapter 2, in mobile communication the channel impulse response varies with time and in a rate directly related to Doppler frequency, f_d. Therefore, the accuracy of the estimation is related with how stationary the channel response is. This can be found from the autocorrelation function of the channel impulse response [14–16]. If we model the channel as a single-path Rayleigh fading channel, the autocorrelation function, $R_{xx}(\tau)$, for an interval τ is equal to the Bessel function of the zeroth degree $J_0(x)$:

$$R_{xx}(\tau) = J_0(2\pi f_d \tau) \tag{3.9}$$

Equation (3.9) gives an indication of how accurately the channel estimates can be estimated. The function has been drawn in Figure 3.11, and $R_{xx}(\tau_s)$, $\tau_s = 0.666\,\mu$s, has been calculated for several fading rates in Table 3.1. These results indicate that given accurate estimates of the channel impulse response for a present slot, the channel impulse response for the next slot may be quite accurately forecast at low fading rates. The degree of estimation accuracy decreases as fading rate increases.

The ability to estimate the channel can be utilized in several ways. One important outcome is accurate open-loop power control, a subject discussed

Table 3.1
Autocorrelation Function $R_{xx}(\tau_s)$ for Several Fading Rates, with Time Slot $\tau_s = 667\,\mu$s

f_d	1 Hz	3 Hz	5 Hz	10 Hz	30 Hz	50 Hz	100 Hz	300 Hz	500 Hz
$2\pi f_d \tau_s$	0.004	0.013	0.021	0.042	0.126	0.210	0.419	1.257	2.095
$J_0(2\pi f_d \tau_s)$	99.99%	99.99%	99.99%	99.96%	99.61%	98.91%	95.66%	64.25%	16.99%

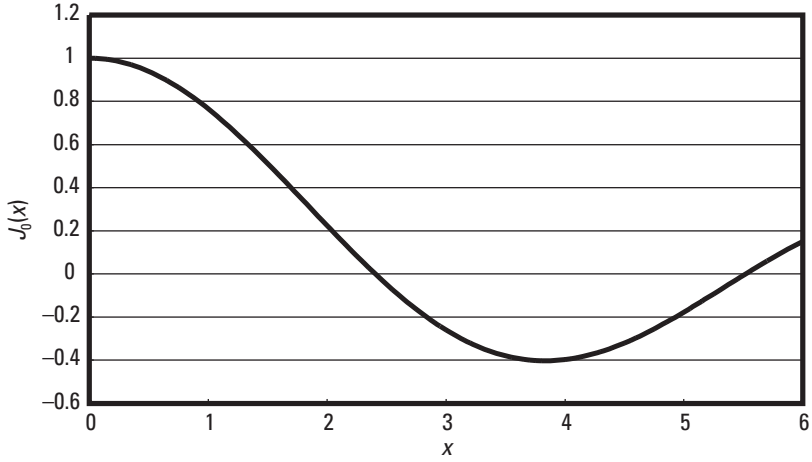

Figure 3.11 Bessel function $J_0(x)$ for $x = 0$ to 6.

in Chapter 4 [17]. It is also utilized to adapt transmission in response to the expected channel impulse response and to take advantage of expected channel path diversity [18]. This will be discussed in Chapter 5.

3.4 CDMA Group Transmission: TDD

The group transmission mode of TDD-CDMA, initially proposed in [3], was intended to increase the correlation between uplink and downlink slots in systems operating under high fading frequencies. The proposal, as illustrated in Figure 3.12, was to divide the users in a cell into N groups, where the transmission and reception to and from each group was done consecutively, and in a TDMA fashion. Because communication between mobiles

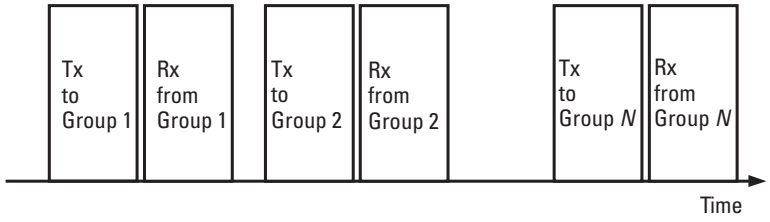

Figure 3.12 Group transmission concept.

and a BS is done in a fraction of time, the correlation between the uplink/downlink could be increased, in effect reducing τ in (3.9).

The concept is now used for a different purpose. The transmission length of a slot is kept constant, but the spreading rate is decreased. Because fewer users are served in a time slot, more advanced receivers and transmitters can be used. One example is the joint detection function, which can become very complex if there are too many users are to be detected. Similarly joint transmission can be prohibitively complex if it has to be carried out to all users within the cell. Group transmission facilitates the realization of such methods. We will discuss these in Chapter 6.

3.5 Summary

A general overview of the TDD system was given in this chapter. The differences between the FDD and TDD modes of transmission were discussed. These differences lead to several advantages for the TDD mode, as well as some disadvantages. The most important advantage is the reciprocity of the channel impulse response between the uplink and downlink. This leads to better power control and diversity transmission techniques, which are the subjects of the next two chapters.

TDD systems, however, require time-frame synchronous transmission across all BS, which leads to network synchronization requirements. Furthermore, the cell size is limited by the set guard time and is usually smaller than that for a comparable FDD system. Because of these disadvantages, TDD systems have not been more widely utilized.

References

[1] Akaiwa, Y., "A Conceptual Design of Micro-Cellular Radio Communication System," *Proc. IEEE Vehicular Technology Conference,* Orlando, FL, May 1990, pp. 156–160.

[2] 3GPP Technical Specification No. 25.200–224, Ver. 5.0.0, December 2001.

[3] Esmailzadeh, R., "Time Division Duplex Transmission of Direct Sequence Spread Spectrum System," Ph.D. thesis, Yokohama, Japan: Publications of Dept. of Electrical Engineering, Keio University, March 1994.

[4] Dahlman, E., et al., "UMTS/IMT-2000 Based on Wideband CDMA," *IEEE Communications Magazine,* Vol. 36, No. 9, September 1998, pp. 70–80.

[5] Kondo, Y., and K. Suwa, "Transmitter Diversity in TDMA/TDD Transmission," *IEICE National Convention Records*, Spring 1990.

[6] Ochsner, H. "DECT—Digital European Cordless Telecommunications," *Proc. IEEE Vehicular Technology Conference,* 1989, pp. 718–721.

[7] Dixon, R. C., *Spread Spectrum Systems,* New York: Wiley Interscience Publications, 1976.

[8] Mori, N. R., et al., "Frame Timing Acquisition for Direct Sequence Spread Spectrum Signals in Time Division Duplex Transmission," *Proc. IEEE Vehicular Technology Conference*, 1993, pp. 815–818.

[9] Esmailzadeh, R., and M. Nakagawa, "Quasi-Synchronous Time Division Duplex CDMA," *IEICE Trans. on Fundamentals of Electronics, Communications and Computer Sciences,* September 1995, pp. 1201–1205.

[10] Esmailzadeh, R., and M. Nakagawa, *Frequency Shaping of DS-SS Signals for Frequency Common Use Systems*, IEICE Technical Report No. SST91-13, Nagaoka, Japan, August 1991.

[11] Bailey, R. J., and M. R. Heath, "Radio Channel Characterization for the Digital European Cordless Telecommunications (DECT) System," *IEE Colloquium on CT2/CAI and DECT Cordless Telecommunications*, 1990, pp. 8/1–8/7.

[12] Tanaka, K., "A Spread Spectrum Cordless Telephone," *IEICE Trans.*, Vol. J77-B-II, No. 11, November 1994, pp. 703–710 (in Japanese).

[13] Flores, C., and S. Behtash, "DCP Systems Specifications: A Low-Cost Flexible CDMA Architecture for Cordless and PCS Applications," *Proc. IEEE PIMRC,* 1994, pp. 680–684.

[14] Jakes, C., *Microwave Mobile Communications,* New York: Wiley, 1974.

[15] Owen, F. C., "The DECT Radio Interface," *IEE Colloquium on CT2/CAI and DECT Cordless Telecommunications,* 1990, pp. 7/1–7/6.

[16] Schwartz, M., W. R. Bennet, and S. Stein, *Communication Systems and Techniques,* New York: McGraw-Hill, 1966.

[17] Esmailzadeh, R., and M. Nakagawa, "Time Division Duplex Method of Transmission of Direct Sequence Spread Spectrum Signals for Power Control Implementation," *IEICE Trans. on Communications,* August 1993, pp. 1030–1038.

[18] Esmailzadeh, R., and M. Nakagawa, "Pre-RAKE Diversity Combination for Direct Sequence Spread Spectrum Mobile Communications Systems," *IEICE Trans. on Communications,* August 1993, pp. 1008–1015.

4

Power Control in TDD-CDMA Systems

Power control is a major aspect of spread spectrum–based systems such as CDMA. As discussed in Chapter 2, these systems are not bandwidth limited; instead they are interference limited. Because all CDMA users appear as interference to other users, any excessive transmission power will increase the overall interference, which results in reduced capacity for the system as a whole. A great portion of the promised capacity of CDMA systems can be lost without an effective power control system [1–3].

In cellular mobile communications, transmission power must be controlled in both uplink and downlink. Uplink power control is required for combating the near–far problem. In a cellular environment, the received signal from a near user can have a much larger amplitude than that of a user farther away. The interference caused by a near user appears as strong interference to users farther away, and can disable their communication with the BS. Thus, both near and far users must adjust their transmission power in a way that their signals arrive at the BS with equal levels, as illustrated in Figure 4.1, in which the mobiles control the transmission power for each of their signals such that they arrive at the serving BS with equal power.

Power control in the downlink is used to increase the capacity of the system. Ideal power control in this mode delivers necessary power for each individual user, while minimizing the interference to mobile users of neighboring cells. To minimize the mutual interference, BSs transmit at a prescribed total power level. This value is determined by the network design and

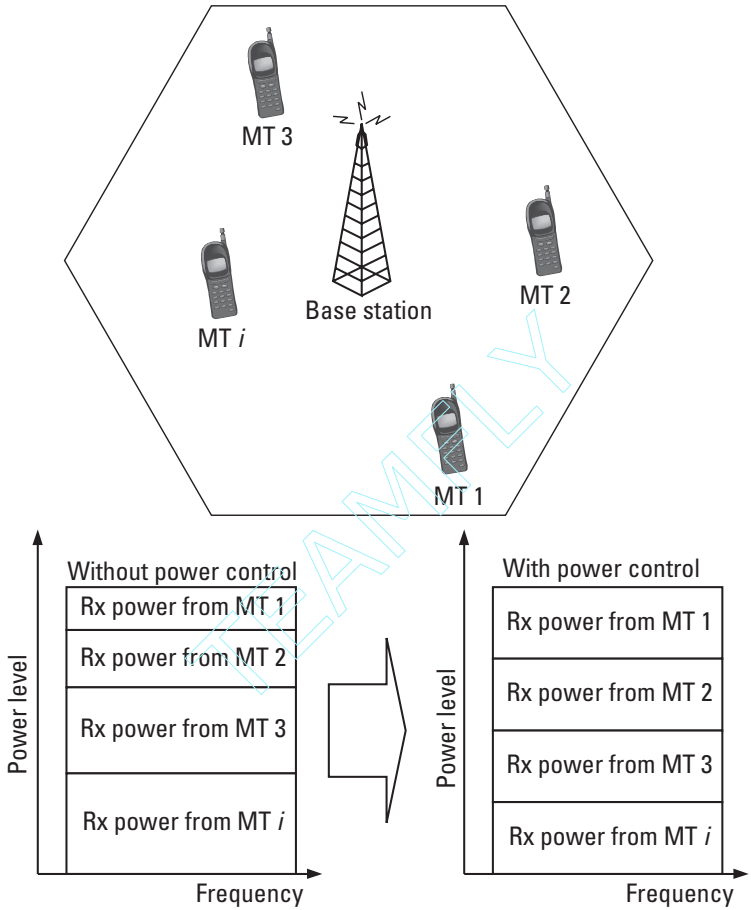

Figure 4.1 Uplink power control.

the required capacity of the BS. The BS must then use this available transmission power to serve MTs in a way such that they achieve their *quality of service* (QoS) requirements.

In general, power control is carried out in a closed-loop fashion. That is, the receiver terminal, whether it is the BS or an MT, calculates the received power level, and determines if it is adequate and according to design parameters. If necessary, it will then request/order the transmitter to vary the transmit power in order to correct any deviation from the required level. A block diagram of a singular closed-loop power control system is shown in Figure 4.2. This operation is generally similar for both the uplink and the

Team-Fly®

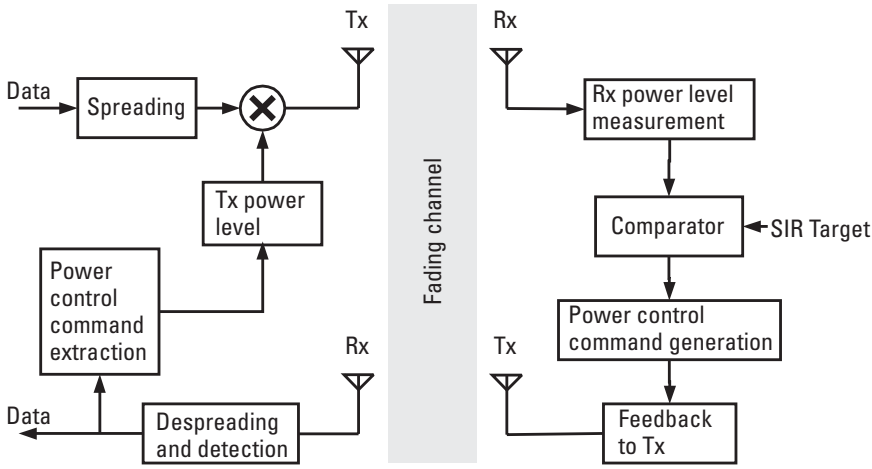

Figure 4.2 A block diagram of a closed-loop power control system.

downlink. One main difference is that fed-back power control messages are "requested" for the downlink, whereas they are "commanded" for the uplink. In closed-loop power control systems, the receiver constantly measures the received signal level. The measured level is compared to a *signal-to-interference ratio* (SIR) target, and a command/request message is fed back to the transmitter so that the target level can be reached and then maintained. The SIR target is calculated based on a desired performance level. This is generally a target *frame error rate* (FER). Note that the SIR target itself is a variable depending on the fading characteristics of the channel, such as the number of paths and the Doppler fading.

To maintain a suitable SIR target, dual-loop power control becomes necessary in which the second loop is designed to constantly update the SIR target level. For example, the WCDMA system in its FDD mode uses a dual loop for uplink and downlink power control, and a dual loop for the downlink in its TDD mode. (For more details on such a system configuration, as well as a comparison with power control in FDD mode, see [4–8].) In their uplink operation, however, the TDD systems can take advantage of the channel reciprocity and use a simple open-loop power control. The open-loop operation, as illustrated in Figure 4.3, relies only on the received signal to estimate its transmission power level. Open-loop power control operation is discussed in Section 4.1. The TDD downlink power control operation is briefly discussed in Section 4.1.2.

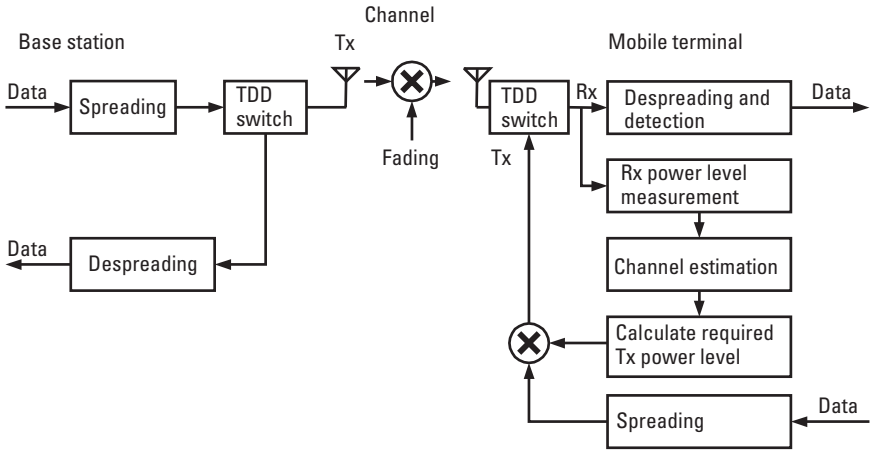

Figure 4.3 A block diagram of the uplink open-loop power control TDD system.

4.1 Uplink Power Control in TDD

The transmission power of a mobile can be controlled in an open-loop fashion due to the fading reciprocity characteristic of the TDD operation. In the open-loop operation, a mobile measures its received power level and from it calculates the path loss from the base station. If the transmission power level of a broadcast channel is known, the path loss, L_{path}, can be measured. The BS also broadcasts its required SIR, SIR_{BS} and the present interference level I_{BS}. The required transmission power, P_{req}, can then be calculated from the following equation:

$$P_{req} = \frac{SIR_{BS}}{I_{BS} L_{path}} \cdot C \tag{4.1}$$

where C is a constant, and depends on factors such as the required QoS. Path loss is the product of several factors: fading due to multipath, fading due to shadowing, and propagation loss due to distance. The last two factors vary relatively slowly, and their effect can be found by averaging P_{req} over several fading periods. The variation of the multipath fading as discussed in Chapter 2 is a function of the Doppler rate and mobile velocity. Figure 4.4 shows the power variations due to multipath fading on the decibel scale. As discussed in Chapter 2, for the received power level in a single multipath channel, variations follow an exponential distribution:

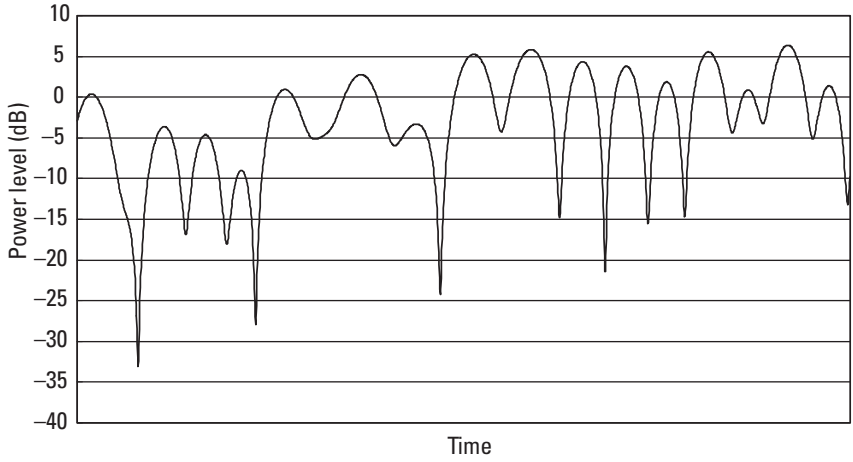

Figure 4.4 Received power variations due to multipath fading.

$$p(\gamma) = \frac{1}{\Gamma_0} \exp\left(-\frac{\gamma}{\Gamma_0}\right) \tag{4.2}$$

where Γ_0 is the average SNR. This can be interpreted as the effects of the long-term channel effects, averaged over several fading periods. Its cumulative distribution function is written as:

$$P_\gamma(\gamma < t) = \int_0^t p(\gamma)\, d\gamma = 1 - \exp\left(-\frac{t}{\Gamma_0}\right) \tag{4.3}$$

To remove the effects of multipath fading, the signal level needs to be increased by a factor equal to the inverse of the fading level. To achieve this, the channel impulse response must be accurately measured in the presence of noise and interference. A suitable algorithm then uses the measured values to estimate the future channel impulse response. A *least-mean-square* (LMS) method has been used in [9]. Better accuracy can be obtained from more sophisticated prediction algorithms such as that proposed in [10]. In any case the channel cannot be perfectly estimated. The estimation error depends on the fading rate, and can be small at low f_d values.

We first assume that the channel can perfectly be estimated, and derive the BER equations. We then take the estimation errors into consideration and derive corresponding equations.

If the channel is perfectly estimated, the exact necessary transmission power to compensate for fading can be calculated. Figure 4.5 illustrates this necessary transmission power. Let us denote this parameter as φ. By definition, it follows that

$$\varphi = \frac{\Gamma_0}{\gamma} \tag{4.4}$$

The cumulative distribution function for φ can be written as

$$P_\varphi(\varphi < t) = \Pr\left[\frac{\Gamma_0}{\gamma} < t\right] = \Pr\left[\gamma > \frac{\Gamma_0}{\gamma}\right] = 1 - \Pr\left[\gamma < \frac{\Gamma_0}{\gamma}\right] \tag{4.5}$$

$$P_\varphi(\varphi < t) = \exp\left(-\frac{1}{t}\right) \tag{4.6}$$

Differentiating (4.6) with respect to t yields the probability distribution function for the power control parameter φ:

$$p(\varphi) = \frac{1}{\varphi^2}\exp\left(-\frac{1}{\varphi}\right) \tag{4.7}$$

The two probability distribution functions of (4.2) and (4.7) are illustrated in Figure 4.6 for $\Gamma_0 = 1$.

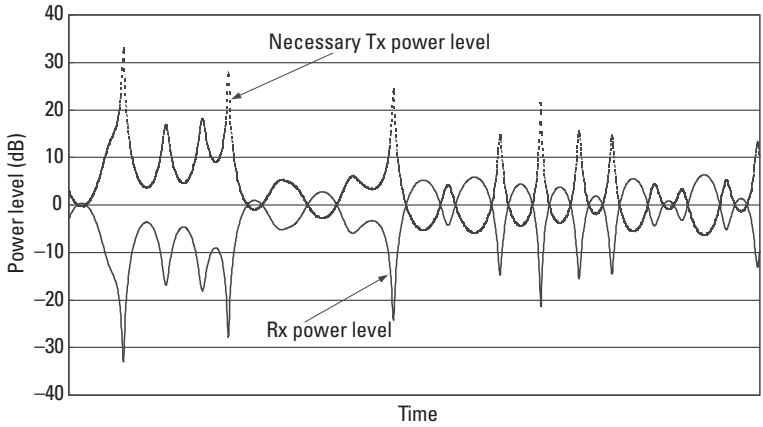

Figure 4.5 Fading compensation by varying the transmission power level.

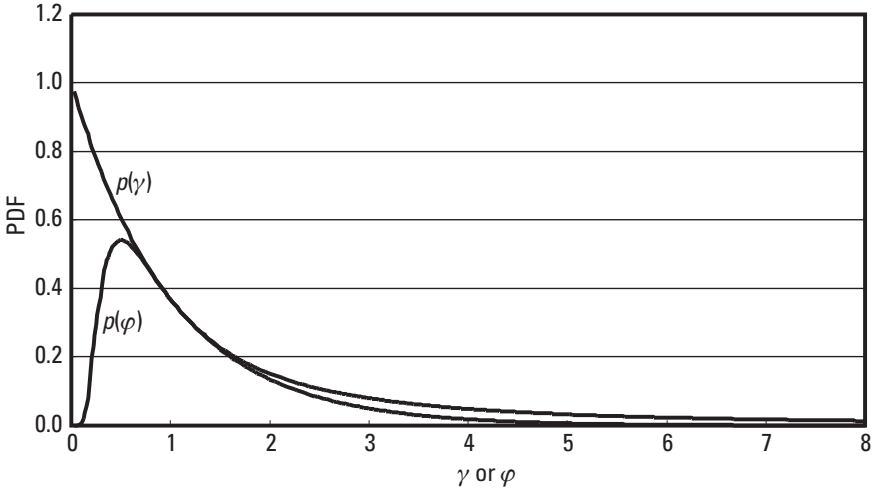

Figure 4.6 PDF of γ and φ.

The average necessary transmission power, $\overline{P}$, required to carry out perfect power control can be calculated by multiplying (4.7) by φ and integrating over all values of φ:

$$\overline{P} = \int_0^\infty \varphi p(\varphi)\, d\varphi \tag{4.8}$$

Alternatively, $\overline{P}$ can be calculated through (4.2) by substituting for a normalized $\overline{\gamma} = \dfrac{\gamma}{\Gamma_0}$ and integrating over all values of $\overline{\gamma}$ as:

$$\overline{P} = \int_0^\infty \frac{1}{\overline{\gamma}} \exp(-\overline{\gamma})\, d\overline{\gamma} \tag{4.9}$$

Although $p(\varphi) \to 0$ as $\varphi \to \infty$, $\overline{P}$ *monotonously increases as* $\varphi \to \infty$. Equation (4.7) suggests that a transmitter will need infinite power to compensate for instantaneous fading effects of the channel. In practice, the mobile transmitter can output signals at a finite power level, and therefore a transmission level cap is required. Figure 4.7 shows how the transmission level looks if a cap of 10 dB is maintained, and what the received signal level variations will be.

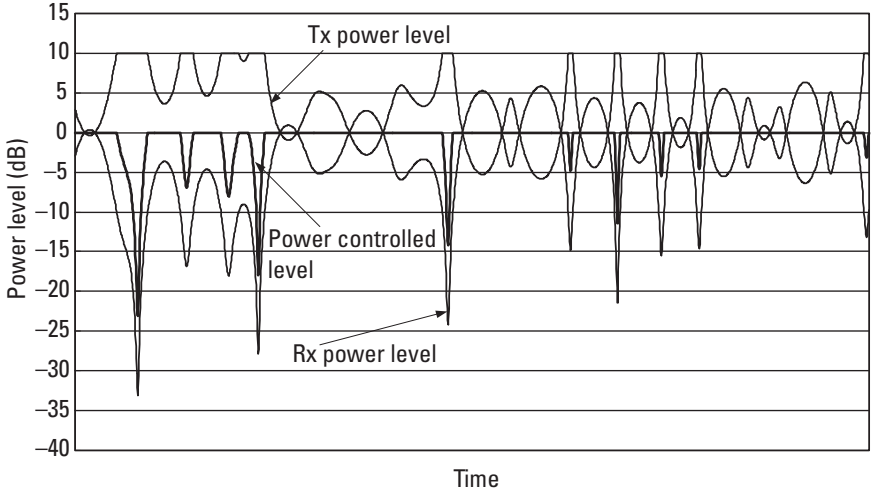

Figure 4.7 Fading compensation when a power control cap is in effect.

The *probability distribution function* (PDF) of the resulting variable can be derived as follows:

$$\begin{aligned}\overline{P}_{\text{cap}}(\gamma) &= \frac{1}{\Gamma_0 \cdot \kappa}\exp\left(-\frac{\gamma}{\Gamma_0 \cdot \kappa}\right)\cdot I_{[0,\Gamma_0)}(\gamma) \\ &+ \exp\left(-\frac{1}{\kappa}\right)\cdot \delta(\gamma - \Gamma_0)\cdot I_{[\Gamma_0,\infty)}(\gamma)\end{aligned} \tag{4.10}$$

where κ is the cap value, $I_{[.)}(\gamma)$ is equal to 1 for the γ values in the interval and zero otherwise, and $\delta(.)$ is the delta function.

The average necessary transmission power, $\overline{P}_{\text{cap}}$, in order to carry out power control in the case when there is a power cap, can be calculated by substituting from (4.8) with the exception that we need to set $\varphi = \kappa$ for all values of $\varphi > \kappa$. Equation (4.8) will be written as

$$\overline{P}_{\text{cap}} = \int_0^{\kappa} \varphi p(\varphi)\, d\varphi + \int_{\kappa}^{\infty} \kappa p(\varphi)\, d\varphi \tag{4.11}$$

This equation has been calculated for several values of κ and drawn in Figure 4.8. We observe that $\overline{P}_{\text{cap}}$ increases monotonically as κ increases, although at a much slower rate, and it tends to flatten. The optimal κ can be selected by determining the required BER level.

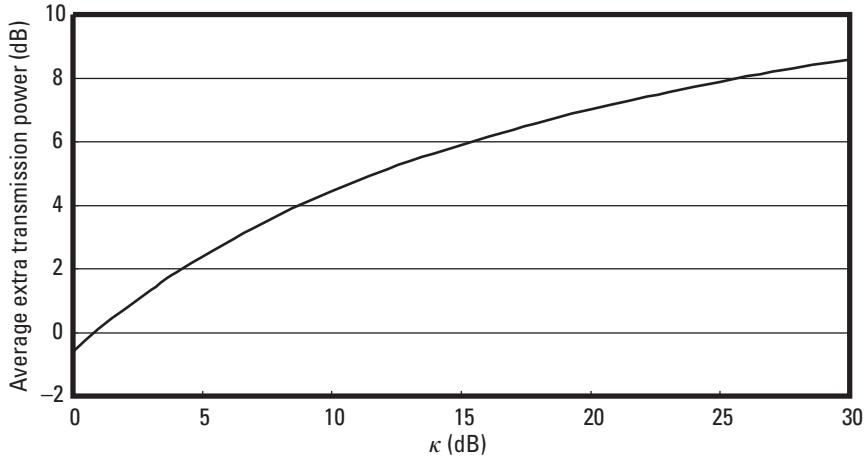

Figure 4.8 The average extra transmission power for carrying capped power control.

The BER for the power-capped case can be calculated by substituting for $p_{cap}(\gamma)$ from (4.10) in

$$P_e = \frac{1}{2}\int_0^{\infty} \operatorname{erfc}\sqrt{\gamma}\, p_{cap}(\gamma)\, d\gamma \tag{4.12}$$

which results in

$$P_e = \frac{1}{2}\int_0^{\Gamma_0} \operatorname{erfc}\left(\sqrt{\gamma}\right)\frac{1}{\Gamma_0\kappa}\exp\left(\frac{-\gamma}{\Gamma_0\kappa}\right)d\gamma + \frac{1}{2}\operatorname{erfc}\left(\sqrt{\Gamma_0}\right)\exp\left(\frac{1}{\kappa}\right) \tag{4.13}$$

However, the BERs need to be adjusted by taking into effect of the average extra transmission power for the capped power control. This works to shift the curves to the right by taking into consideration the amount of extra power that needs to be transmitted to carry out power control, as calculated from (4.11). Although the SIR level remains the same, this compensates for the fact that the transmitter is using extra power, which could be used to increase the transmission level of an equivalent system that does not use power control. Therefore, we define $\overline{\Gamma}_0 = \Gamma_0 + \overline{P}_{cap}$ and rewrite (4.13) as

$$P_e = \frac{1}{2}\int_0^{\overline{\Gamma}_0} \operatorname{erfc}\left(\sqrt{\gamma}\right)\frac{1}{\overline{\Gamma}_0\kappa}\exp\left(\frac{-\gamma}{\overline{\Gamma}_0\kappa}\right)d\gamma + \frac{1}{2}\operatorname{erfc}\left(\sqrt{\overline{\Gamma}_0}\right)\exp\left(\frac{1}{\kappa}\right) \tag{4.14}$$

Equation (4.14) is drawn in Figure 4.9. Note that one can select the power cap for a desired operating performance. For example, for the case of BER = 1E–3, a power cap of 20 dB provides a better performance than a power cap of 30 dB.

Note that in practice the power control range is limited by hardware design considerations such as battery type and linearity of power amplifiers. The above approach shows, however, that increasing the power control range may not be helpful in achieving a better BER than design requirements in most cases.

4.1.1 Imperfect Channel Estimation

Calculations in the previous section assumed that the channel could be perfectly measured and then perfectly estimated. In practice, the channel measurements are corrupted due to measurement errors and the interference and noise present in the system. Moreover, the estimation algorithms are imperfect, and therefore the estimated values include some errors. This error increases as the Doppler fading increases, as the correlation between the fading values of consecutive slots decrease. Figure 4.10 shows the received power level when the estimations are done through simulations. The fading frequency is 80 Hz. We can see that the received power varies as the channel estimates become inaccurate.

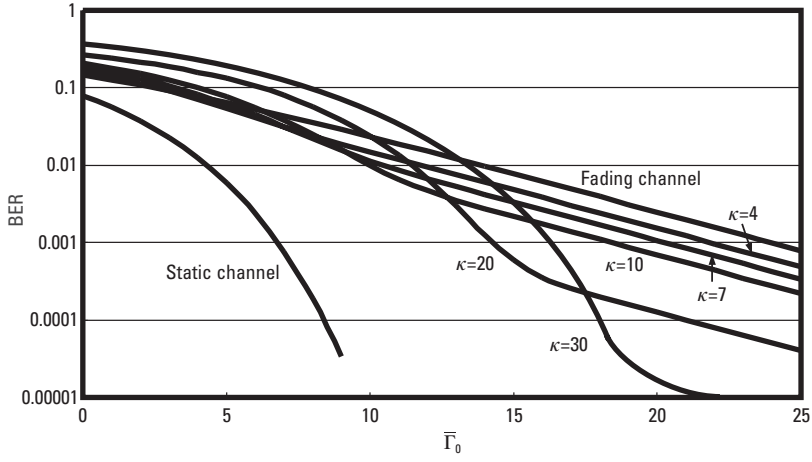

Figure 4.9 The BER curves for the capped power-controlled system adjusted by the necessary extra transmission power for power control purposes.

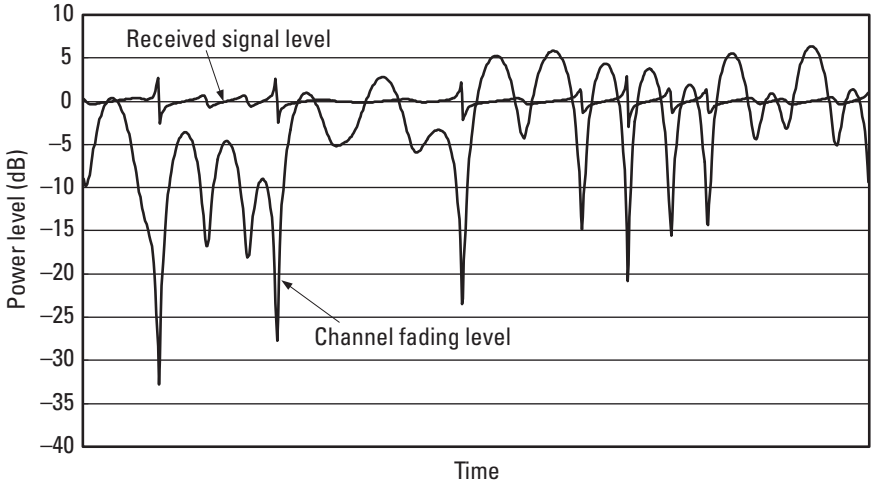

Figure 4.10 Power control error due to channel estimation error.

The resulting difference between the received signal and the desired Γ_0 is denoted by ε. This factor is usually modeled by a log-normal function with a 0 dB mean and a variable variance σ_ε^2 that increases nonlinearly with the fading factor. Figure 4.11 shows the simulation result for σ_ε^2 for a range of fading frequencies, when an LMS method is used for fading factor estimation. Although not inversely proportional, these results inversely correlate with Table 3.1, which shows the autocorrelation results for the Rayleigh parameter.

The power control estimation errors affect BER performance. The effect can be included as an extra factor in (4.14) as follows:

$$P_e = \frac{1}{2}\int_0^{\varepsilon\bar{\Gamma}_0} \operatorname{erfc}\left(\sqrt{\gamma}\right)\frac{1}{\bar{\Gamma}_0\kappa}\exp\left(\frac{-\gamma}{\bar{\Gamma}_0\kappa}\right)d\gamma + \frac{1}{2}\operatorname{erfc}\left(\sqrt{\varepsilon\bar{\Gamma}_0}\right)\exp\left(\frac{1}{\kappa}\right) \quad (4.15)$$

Equation (4.15) is drawn in Figure 4.12 for σ_ε^2 = 3, 6, and 9 dB, corresponding to a fading frequency range of 150 Hz to 250 Hz. A Monte Carlo simulation method, with 10,000 iterations of ε values has been used, over which P_e has been averaged. The power cap κ is set to 20 dB. The results show that the performance is degraded by a few decibels at BER = 1E–3 for high fading rates (more than 200 Hz). However, for most Doppler frequencies of interest the degradation is not very significant.

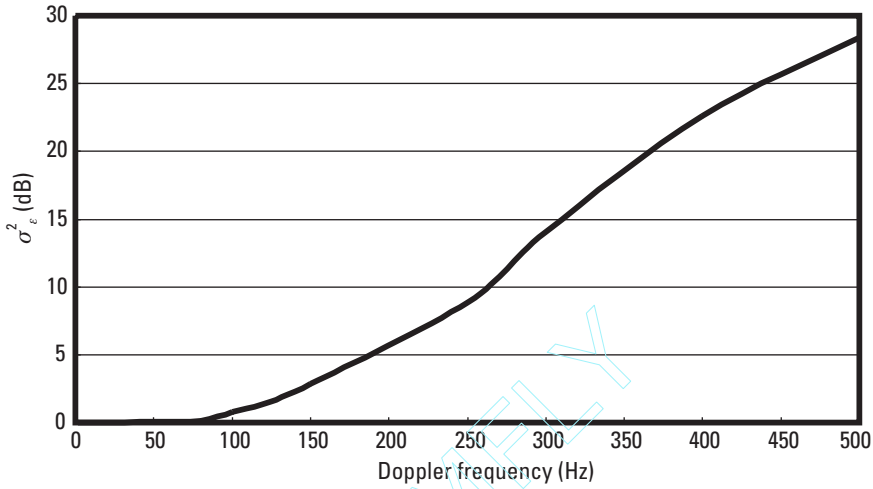

Figure 4.11 Power control error versus Doppler frequency.

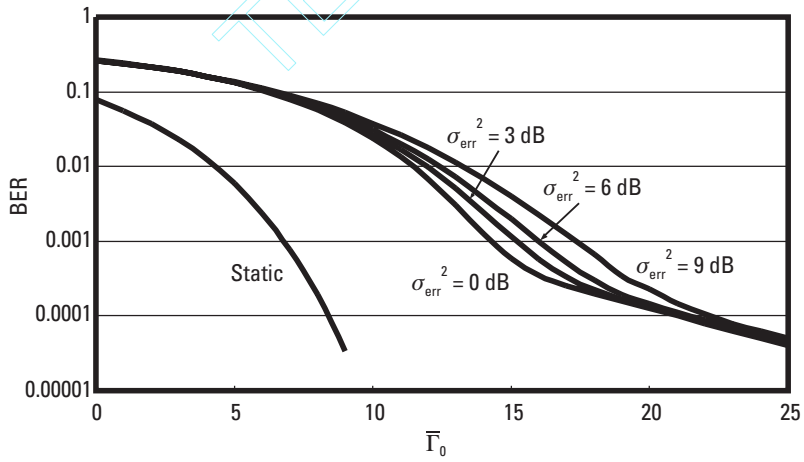

Figure 4.12 The BER curves with erroneous channel estimation.

4.2 Downlink Power Control

The downlink power control in TDD systems is achieved in a manner similar to FDD systems, that is, in a closed-loop fashion as illustrated in Figure 4.2. An MT regularly measures the received SIR level and compares it to a local

Team-Fly®

SIR target. Based on this comparison, it requests the BS to increase or decrease its transmission power in order to maintain a required performance level.

This is mainly because of the varying nature of the interference in the downlink. The interference in the uplink of a CDMA system consists of the plurality of signals coming from all MTs in the user's cell, all of which transmit to the BS, and MTs in other cells whose signals to their own BS nevertheless appears as interference to the target BS. The total value of all interference does not vary greatly with time, and therefore the SIR variation is predominantly a function of the signal rather than interference. Because the signal level is highly correlated between the uplink and downlink, the uplink SIR may be accurately estimated at the MT.

In contrast, the interference in the downlink is the sum of signals from BSs of the cells beside that of the target MT. One or two BSs may be the dominating cause of the interference. Therefore, the resulting total may vary significantly because the interference path is also affected by shadowing and multipath fading. As a result, the downlink SIR cannot be accurately estimated at the BS and open-loop power control is not useful.

This said, however, TDD transmission can be useful for downlink transmission. If a BS transmits to users using multiple antennas, it can estimate which antenna is best situated to transmit to any MT. This is called transmission diversity, and is discussed in the next section.

4.3 Power Control in Multipath Diversity

We now turn our attention to the case in which multiple antennas or long multipath delay profiles allow the receiver to have access to more than one independent transmission path. We deal with selection multipath diversity, where the path with the largest received SIR is selected for detection. We then derive the equations for a power-capped BER and for the necessary transmission power.

Multipath selection diversity is of particular interest for TDD systems. Due to the reciprocity of the uplink and downlink fading patterns, a transmission diversity system can be implemented in TDD systems [11–13]. In transmission diversity, a BS transmits to mobiles from one of its transmitter antennas. It selects the antenna based on the uplink signal received from the mobile in the previous slot through its antennas, based on which the fading patterns of mobiles to each antenna are estimated. This helps the BS save transmit power and increase its user capacity. The power control process at the MT side is done toward the selected antenna. This results in transmission

power savings as shown later in this section. Transmitter diversity systems have been implemented in practice, and experimental results have been reported for example in [14, 15].

We start our analysis of a power-controlled selection diversity system by reviewing that the PDF of the received SNR for an *m*-path selection diversity system is written as follows [16]:

$$p(\gamma) = \frac{m}{\Gamma_0} \exp\left(-\frac{\gamma}{\Gamma_0}\right)\left[1 - \exp\left(\frac{\gamma}{\Gamma_0}\right)\right]^{m-1} \tag{4.16}$$

The selection diversity combining method is capable of reducing fading periods significantly. This is due to the independent fading character of the received paths, and the fact that for the received signal level to be lower than a value *t*, all paths' levels must be lower than *t*. That is, the *cumulative distribution function* (CDF) for selection diversity combining is:

$$P(\gamma < t) = \left[1 - \exp\left(\frac{t}{\Gamma_0}\right)\right]^m \tag{4.17}$$

The power control process in selection diversity systems works in similar fashion to the single path described above. The only difference is that the power control factor is calculated for the strongest path. The procedure is illustrated in Figure 4.13. We follow a similar approach as above to find the

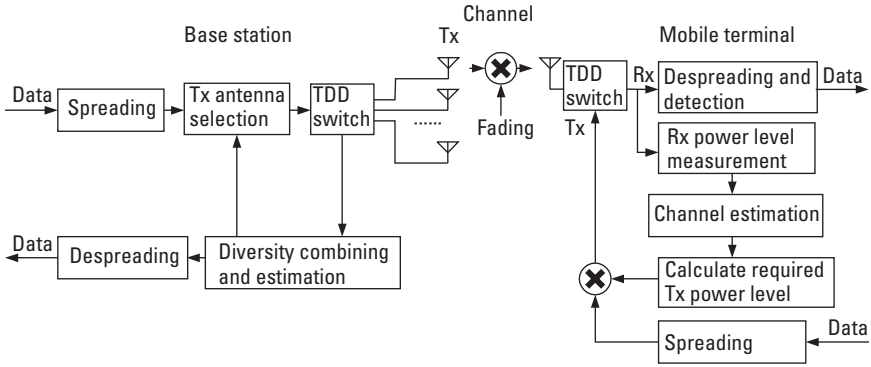

Figure 4.13 A block diagram of a closed-loop power control system for selection diversity systems.

BER performance for the power-controlled system, considering the case when a power cap exists, and when the channel estimation is not perfect.

We define the power control parameter as φ. Again by definition:

$$\varphi = \frac{\Gamma_0}{\gamma} \tag{4.18}$$

From (4.17)

$$P_\varphi(\varphi < t) = 1 - \left[1 - \exp\left(-\frac{1}{t}\right)\right]^m \tag{4.19}$$

The PDF of ϕ can be found by differentiating with respect to t:

$$p(\varphi) = \frac{m}{\varphi^2}\exp\left(-\frac{1}{\varphi}\right)\left[1 - \exp\left(-\frac{1}{\varphi}\right)\right]^{m-1} \tag{4.20}$$

The PDFs for (4.16) and (4.20) are drawn for illustration in Figure 4.14 for $\Gamma_0 = 0$.

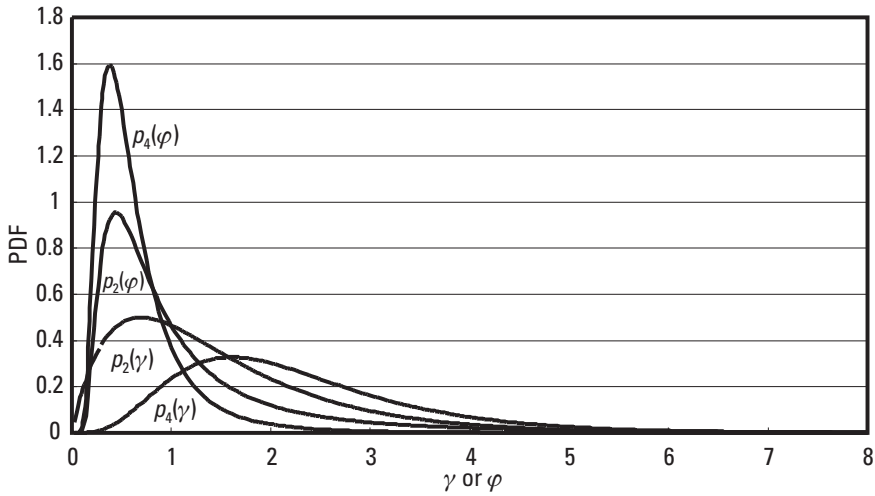

Figure 4.14 PDF for γ and φ for selection diversity systems of two and four paths.

Again, the average necessary transmission power, $\overline{P}$, in order to carry out perfect power control can be calculated by multiplying (4.7) by φ and integrating over all values of φ as in (4.7). Although in the case of single-path transmission $\overline{P}$ monotonously increases as $\varphi \to \infty$, here the third term in (4.20) ensures that $\overline{P}$ is bounded. However, (4.19) still suggests that a transmitter will need infinite power to compensate for the instantaneous fading effects of the channel. In practice, these deep fading periods are very rare. Therefore, a power cap is not of practical importance, since it is rarely required. The PDF for a power-capped system can be written in a manner similar to that for the single-path system:

$$p_{\text{cap}}(\gamma) = \frac{m}{\Gamma_0 \cdot \kappa} \exp\left(\frac{\gamma}{\Gamma_0 \cdot \kappa}\right)\left[1 - \exp\left(\frac{\gamma}{\Gamma_0 \cdot \kappa}\right)\right]^{m-1} \cdot I_{[0,\Gamma_0)}(\gamma) + C \cdot \delta(\gamma - \Gamma_0) \cdot I_{[\Gamma_0,\infty)}(\gamma) \tag{4.21}$$

where

$$C = 1 - \left[1 - \exp\left(-\frac{1}{\kappa}\right)\right]^m$$

The average necessary transmission power, $\overline{P}_{\text{cap}}$, required to carry out power control in the case when there is a power cap can be calculated from

$$\overline{P}_{\text{cap}} = \int_0^{\kappa} \varphi p(\varphi)\, d\varphi + \int_{\kappa}^{\infty} \kappa p(\varphi)\, d\varphi \tag{4.22}$$

This equation has been calculated for several values of κ for the cases of m = 1, 2, 3, and 4 and drawn in Figure 4.15. We can see that whereas for a single path the transmitter needs extra power on average to compensate for fading, as the number of transmission paths increases, the average extra power decreases. In fact, if three or more independent paths exist from a transmitter to a receiver, the average power needed is less than what a non-power-controlled system would use.

This can be explained that as the degree of diversity increases, the probability of selecting a fading path decreases. Conversely, the probability of selecting a constructive combination increases. Therefore, the power control process is aimed more at reducing power than increasing power, and as a result the average transmission power decreases.

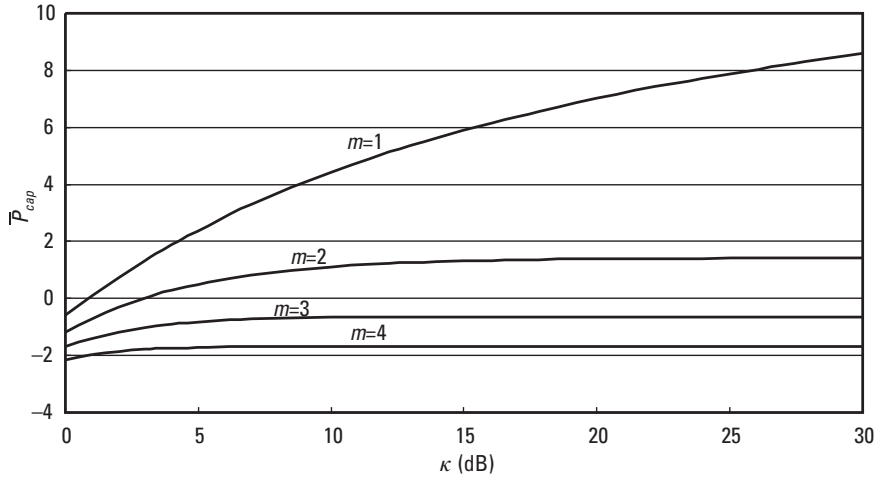

Figure 4.15 The average extra transmission power for carrying capped power control.

The BER for the power-capped case can be calculated by substituting for $p_{\text{cap}}(\gamma)$ from (4.21) in

$$P_e = \frac{1}{2}\int_0^{\infty} \text{erfc}\sqrt{\gamma}\, p_{\text{cap}}(\gamma)\, d\gamma \tag{4.23}$$

The results are drawn in Figure 4.16 for the cases of $m = 2$ and 4. The results have been adjusted by $\overline{P}_{\text{cap}}$. This means that in some cases the performance is better than the static channel performance. Again this is due to the adjustment, which allows for the fact that now less power is being used at the transmitter. Keep in mind that SIR or SNR refers to values measured at the receiver rather than the transmitter.

4.3.1 Imperfect Channel Estimation

Similar to the approach of Section 4.1, a factor can be included in the analysis to account for the channel estimation error. Again the resulting difference between the received signal and the desired Γ_0 is denoted by ε, as a log-normal function with a 0-dB mean and a variable variance σ_ε^2. The effect of the error is included as an extra factor in (4.21) and (4.23). The result is drawn in Figure 4.17 for σ_ε^2 = 3, 6, and 9 dB, for the cases of $m = 2$ and 4. Again a Monte Carlo simulation method, with 10,000 iterations of ε values,

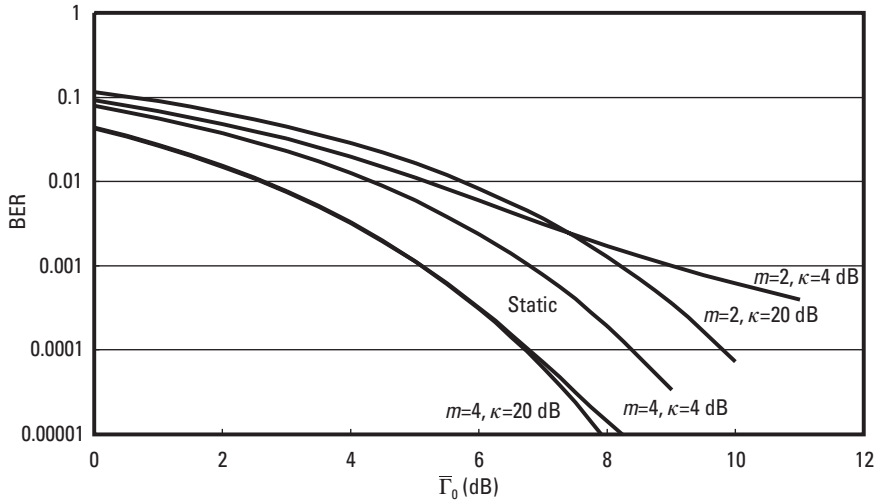

Figure 4.16 The BER curves for the capped power-controlled system adjusted by the necessary extra transmission power for power control purposes.

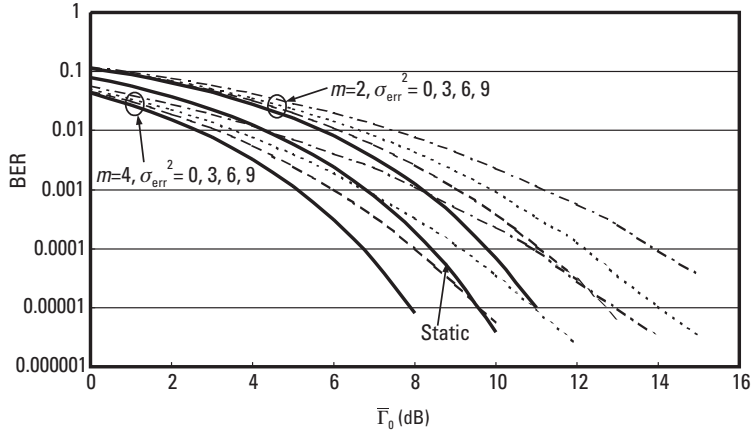

Figure 4.17 The BER curves with erroneous channel estimation.

has been used over which P_e has been averaged. The power cap κ is set to 20 dB. The results show that the performance is degraded by a few decibels at BER = 1E–3 for high fading rates (more than 200 Hz). However, for most Doppler frequencies of interest the degradation is not very significant.

4.4 Summary

The performance of the uplink power control process in TDD systems was evaluated. An open-loop power control process can be realized in the uplink of a TDD CDMA system, resulting in improved performance in single-path systems. Further improvement in performance was shown for the transmission diversity system.

References

[1] Ariyavsitakul, S., and L. F. Chang, "Signal and Interference Statistics of a CDMA System with Feedback Power Control," *Proc. IEEE Globecom,* December 1991, pp. 1490–1495.

[2] Cameron, R., and B. D. Woerner, "An Analysis of CDMA with Imperfect Power Control," *Proc. IEEE Vehicular Technology Conference,* May 1992, pp. 977–980.

[3] Chang, L. F., and S. Ariyavsitakul, "Performance of a CDMA Radio Communications System with Feed-Back Power Control and Multipath Dispersion," *Proc. IEEE Globecom,* December 1991, pp. 1017–1021.

[4] Esmailzadeh, R., and N. Doi, "A Comparison on the Performance of the FDD and TDD Modes of B-CDMA Communications," *Proc. IEEE ICUPC,* 1995, pp. 339–343.

[5] Wegmann, B., and M. Hellmann, "Analysis of Power Control Target Levels in UTRA-TDD," *Proc. IEEE PIMRC,* 2000, pp. 1216–1220.

[6] Chang, J., W. Wang, and D. Yang, "Investigation of a Combined Power Control Scheme for a Time-Division Duplex CDMA System," *Proc. IEEE Asia-Pacific Conference on Circuits and Systems,* 2000, pp. 46–49.

[7] Ghauri, I., and R. Knopp, "Power Control for Diversity Reception in Time-Division Duplex CDMA," *Proc. IEEE Vehicular Technology Conference,* 1998, pp. 2343–2347.

[8] Forkel, I. P., et al., "Performance Evaluation of Power Control Algorithms in Cellular UTRA Systems," *Proc. 2nd Int. Conference on 3G Mobile Communication Technologies,* 2001, pp. 11–15.

[9] Esmailzadeh, R., and M. Nakagawa, "Time Division Duplex Method of Transmission of Direct Sequence Spread Spectrum Signals for Power Control Implementation," *IEICE Trans. on Communication,* August 1993, pp. 1030–1038.

[10] Zhang, Y., and D. Li, "Power Control Based on Adaptive Prediction in the CDMA/TDD System," *Proc. ICUPC,* 1997, pp. 790–794.

[11] Esmailzadeh, R., "Time Division Duplex Transmission of Direct Sequence Spread Spectrum Signals," Ph.D. dissertation, Yokohama, Japan: Keio University, November 1993.

[12] Hayashi, M., et al., "CDMA/TDD Cellular Systems Utilizing a Base-Station-Based Diversity Scheme," *Proc. IEEE Vehicular Technology Conference,* 1995, pp. 799–803.

[13] Miya, K., et al., "CDMA/TDD Cellular Systems for the 3rd Generation Mobile Communication," *Proc. IEEE Vehicular Technology Conference,* 1997, Vol. 2, pp. 820–824.

[14] Horikawa, I., et al., "Performance of Wideband CDMA with TDD Scheme," *Proc. Asia-Pacific Microwave Conference,* 1997, pp. 145–148.

[15] Hiramatsu, K., et al., "Transmit Diversity Applied on the CDMA/TDD Cellular Systems," *Proc. IEEE Vehicular Technology Conference,* 2000, pp. 1170–1174.

[16] Schwartz, M., W. R. Bennet, and S. Stein, *Communication Systems and Techniques,* New York: McGraw-Hill, 1966.

5

Pre-Rake Diversity Combining

Pre-rake diversity combining is a method specific to the TDD mode of CDMA communications. The premise of this method is that if the transmission channel is known at the transmitter, it can shape the signal in a way to take advantage of multipath diversity. Simply stated, pre-rake is doing the rake combining before transmission. In this way the receiver can remain a simple nondiversity combining device with significantly reduced complexity. The difference between the two systems is illustrated in Figure 5.1. The implication of this is clearly very important: In cellular communication one would like to reduce the complexity of the MTs and concentrate most of the functions in the BSs. This method generated great interest when it was first presented [1, 2], and has attracted much further research since, some of which we will refer in the course of this chapter.

In this chapter we will describe the function of a pre-rake system, and show that its performance is the same as that for a rake in a single-user system (that is, a DS-SS mobile communications system) and is very similar to that of a multiuser CDMA system. We will use two approaches for performance analysis. First we use a separate SNR and BER analysis in the single-user case to show that the performances are the same. We then use a Gaussian approximation to derive BER results for the multiuser CDMA case.

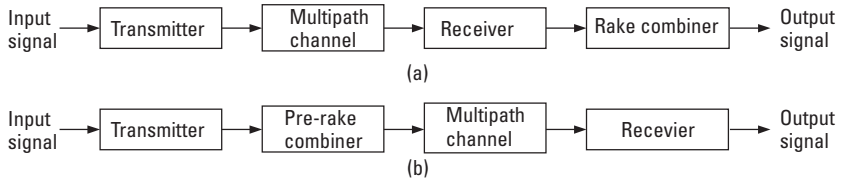

Figure 5.1 (a) Rake and (b) pre-rake systems.

5.1 Introduction

In fading mobile environments, diversity combination techniques are used to improve the performance of communications systems. For the DS-SS systems operating in a multipath environment, the signals of paths with a propagation delay difference of more than the chip duration T_c can be separated. These signals appear at the output of the receiver's matched filter as distinct peaks. Because these peaks have independent fading patterns, they can be combined to reduce the fading effects of the channel. The combining methods directly applicable to DS-SS communications are listed in Chapter 2. The rake combining in DS-SS communications is a form of maximum ratio combining.

The diversity combining receivers achieve a significant improvement over the noncombining single-path receivers. Among these, maximum ratio combining is the most effective.

The DS-SS mobile communication systems often make use of the rake combiners to improve the communication quality. A diversity combining receiver is necessarily more complicated than a single-path receiver. Moreover, the rake combiner needs some extra signal processing for setting the weighing factors and for the combining functions, which makes a rake-combining receiver more complex and a serious power consumer.

In cellular mobile communications, we want to keep the complexity, and hence size and cost, of the mobile unit to a minimum; hence, we concentrate all of the complexities at the BS. A single-path receiver is the simplest receiver and hence the most desirable. The improvements of diversity combining are, however, too significant to ignore. The pre-rake method makes it possible to retain the advantages of rake combining and at the same time use a simple single-path receiver at the mobile unit.

In pre-rake the diversity combining function is performed *before* transmission (hence, the term *pre*-rake). All of the combining functions are carried out in the BS and the mobile unit is kept as simple as a single-path receiver. The SNR and BER analyses show that the performance of the pre-rake combiner is equal to that of the rake combiner.

Team-Fly®

Ideal conditions of operation are assumed for these analyses. It is assumed that the channel parameters are exactly known at the receiver (for the rake combiner) and can be exactly estimated at the transmitter (for the pre-rake combiner).

To set the pre-rake combiner parameters, the future channel fading state must be estimated. These parameters can be estimated from the present channel impulse response, which is derived from the received signals of TDD transmission.

Note that pre-rake operation is intended for traffic channels or point-to-point transmission and thus is not suitable for broadcast or multicast channels.

5.2 Multipath Channel Model

We utilize the simplified tapped delay line multipath channel model of [3, 4]. The uplink channels are assumed to be statistically independent for all users. Also, with the utilization of uplink power control we assume that all channels are statistically identical, even if the MTs are at different distances from the BS. The complex low-pass impulse response of the channel of user k is given by

$$h_k(t) = \sum_{l=0}^{L-1} \beta_{k,l} \exp\left(J\gamma_{k,l}\right)\delta\left(t - lT_c\right) \tag{5.1}$$

where L is the number of channel paths, the path gains $\beta_{k,l}$ are i.i.d. Rayleigh random variables for all k and l, the angles $\gamma_{k,l}$ are i.i.d. uniformly distributed in $[0, \pi)$, and T_c is the PN code chip duration. (We further drop the subscript k, corresponding to user k for the analysis of a single user in the DS-SS system.) Without loss of generality we can take the normalization $E[\beta_{k,l}{}^2] = 1$.

In a TDD system under slow fading conditions, which are typical for portable communication systems, we assume that $h_k(t)$ does not change during two successive up and down time slots. In particular, when a slot is received at the BS through $h_k(t)$, it estimates $h_k(t)$ for use in its own rake receiver. We assume that $h_k(t)$ will not have changed when the BS transmits the following time slot to the user's MT. A diagram of this model is shown in Figure 5.2, where the *line-of-sight* (LOS) propagation delay is assumed to be zero for simplicity.

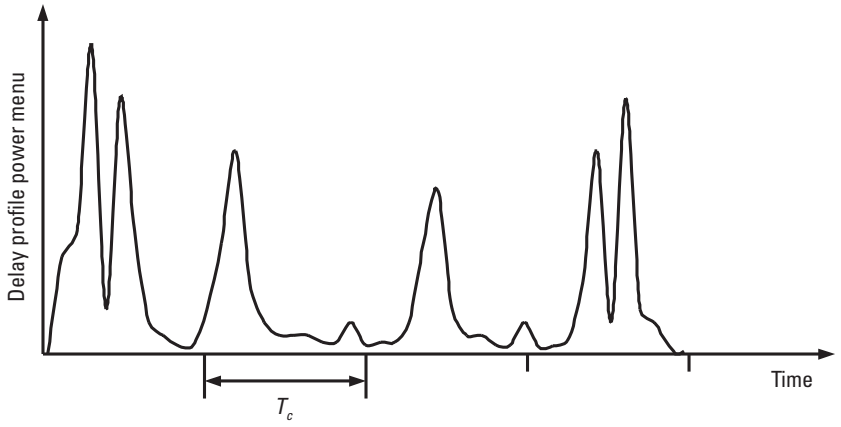

Figure 5.2 The multipath channel model.

The delay length is divided into L bins, with each bin centered on an integer multiple of T_c. The first bin is on the LOS delay. At the output of the receiver matched filter, the signals of paths with a propagation delay difference of more than T_c appear as distinct peaks. Paths with a delay difference of less than T_c are not resolved and are output as a single path with a common delay and combined power 0.

The diversity combination methods select and add the received signals that are more credible. A diagram of a DS-SS diversity combiner is shown in Figure 5.3. It is represented as a delay line after the matched filter. The length of the delay line is equal to the longest significant path delay of the channel. The delay line is divided into L segments, each T_c seconds long. The values of each segment are multiplied by factor a a_l, which is determined by the employed diversity method [5, 6].

5.3 The Rake Combination

The rake combination is a form of maximum ratio combining method. In [5] the optimum weighing factors of Figure 5.3 are derived for the rake combination diversity method to be proportional to the individual path strengths; $a_l \propto \beta_l^*$, where β_l^*, is the complex conjugate of the estimated path strength.

In the rake method, the diversity combiner of Figure 5.3 can be a transversal filter whose impulse response is the time reversal of the channel

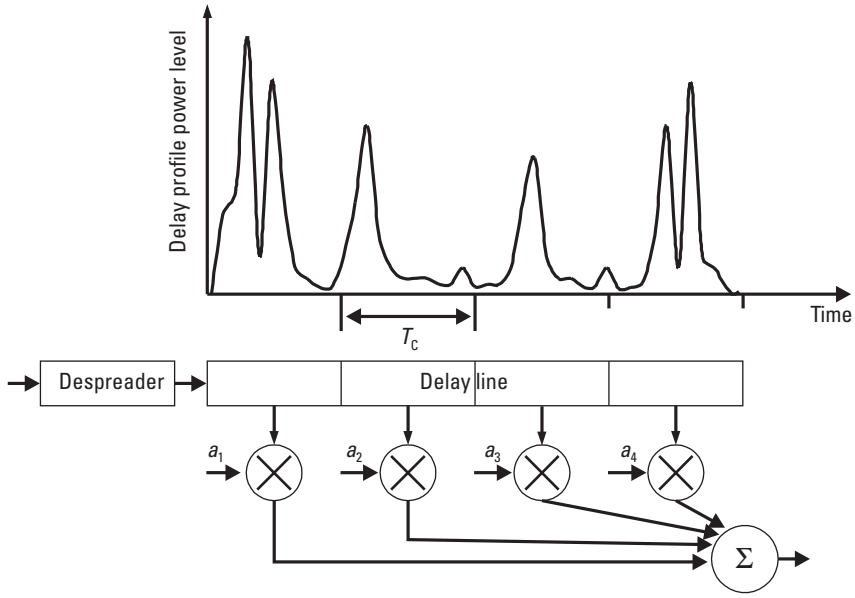

Figure 5.3 A diversity combining receiver.

impulse response. Figure 5.4 shows the time-domain response of the product of the channel impulse response and the rake combiner. The desired output occurs at time $t-(L-1)T_c$. This is the main peak of the combined signal and is proportional to $\sum_{l=0}^{L-1} a_l \beta_l$.

The rake combiner makes use of a transversal filter (or an equivalent device) and a channel estimator. Both of these devices are complicated and power consuming and, thus, undesirable for use in handheld mobile units.

In the pre-rake combining system the same response is produced in the mobile unit receiver without using the rake combiner.

5.4 The Pre-Rake Combination

The purpose of the pre-rake combination is to facilitate the arrival of a signal that is already a rake-like combination of the multipath signals. The rake signal is a sum of the multipath signals, where the received signal from each path is scaled by a factor related to the strength of that path. This operation is an equivalent operation to the multiplication of the received signal by the time-reversed channel impulse response. This is illustrated in Figure 5.5.

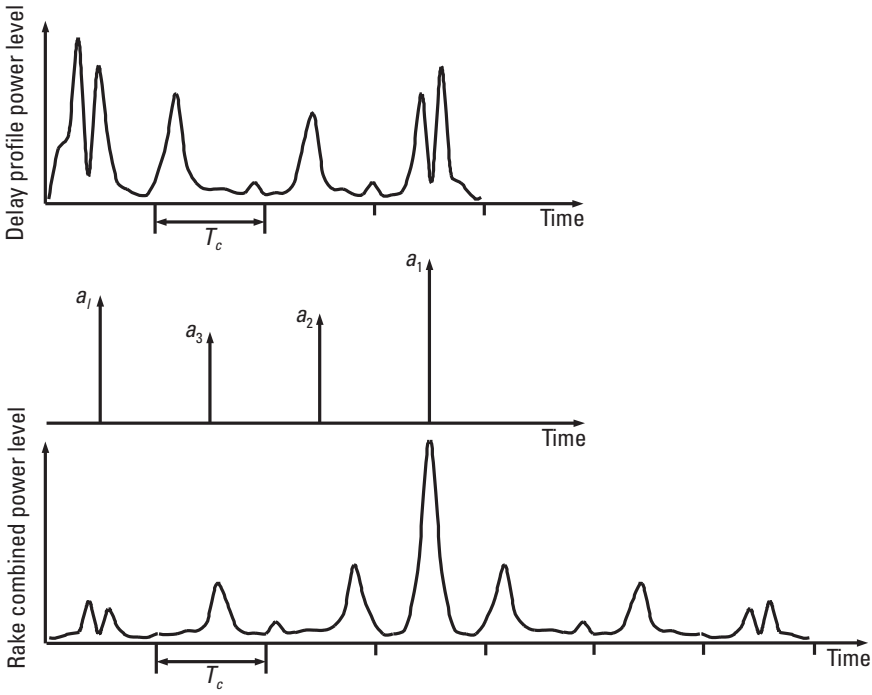

Figure 5.4 Time-domain impulse response convolved by transversal filter impulse response.

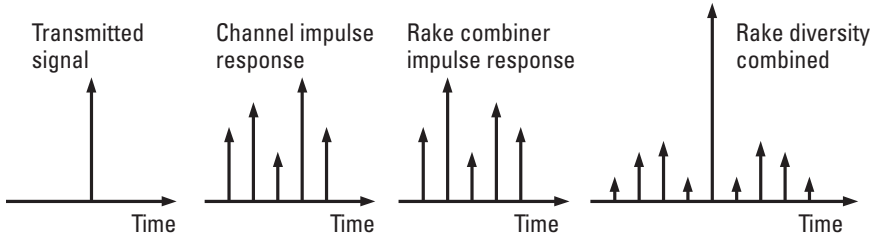

Figure 5.5 The rake diversity combining process.

The pre-rake concept is shown in Figure 5.6 and can be stated as follows: If the future channel impulse response, that is, the strength and the corresponding relative phase of the multipaths, can be estimated, the above-mentioned multiplication can be carried out at the transmitter side. The received signal will then be equivalent to the rake-combined signal

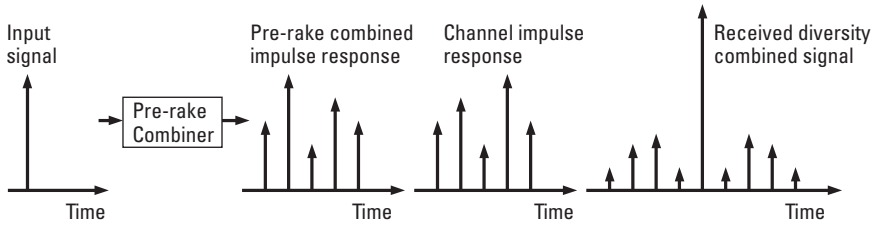

Figure 5.6 The pre-rake diversity combining process.

because the same linear operation is performed in both systems, although in a different order.

The channel impulse response consists of a series of impulses. The amplitude and phase of each impulse represent the specifics of a single path. The time delay associated with the impulse is determined from the propagation delay of that path. The output signal of the pre-rake combiner is the result of the convolution of the DS-SS signal and the time reversed channel impulse response.

The receiver in the pre-rake combiner is a simple single-path receiver, which decodes only the L – 1th peak of the matched filter in each received symbol.

For the pre-rake method, the combiner parameters need to be set in advance of signal transmission. This means that the future path strength, path delay, and path phase must be estimated. In the TDD DS-SS transmission method, the present channel parameters can be directly measured from the received signal, because both forward and reverse links have similar channel parameters. The future values can then be estimated by using a suitable predictive algorithm.

5.5 Theoretical Analyses

5.5.1 SNR

Evaluations of the SNR at points III and VI, before decision circuit, are presented below for the L paths' diversity channel of Figure 5.7. In these analyses knowledge of exact path strength parameter β_l is assumed.

The total transmission power of the pre-rake combiner/transmitter is kept equal to that of the rake combining system by dividing the signal by a factor N. This factor can be derived by considering the total power gain from

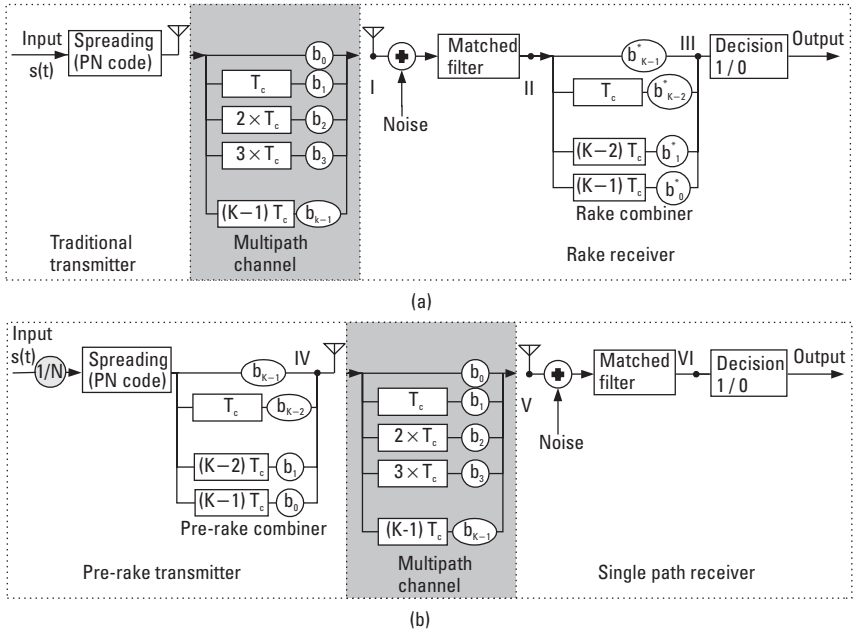

Figure 5.7 Block diagram of (a) rake and (b) pre-rake processes.

the pre-rake system. The PN sequence cross-correlation, shifted by one chip, is assumed to be small, and is ignored in this evaluation. We will show in the Gaussian approximation that cross-correlation values are equal for rake and pre-rake processes.

The input signal is $s(t)$ with a transmission power equal to $<|s(t)|^2>=1$, where <.>signifies the time average. The signal at point I of Figure 5.7(a) is

$$\sum_{l=0}^{L-1} \beta_l s_s\left(t - lT_c\right) \tag{5.2}$$

where $s_s(t)$ is the spread signal of $s(t)$. The signal at point II is

$$\sum_{l=0}^{L-1} \beta_l s_{\mathrm{MF}}\left(t - lT_c\right) + n(t) \tag{5.3}$$

where $s_{\mathrm{MF}}(t)$ is the peak output of the matched filter. It has a signal power equal to $<|s_{\mathrm{MF}}(t)|^2>=G<|s(t)|^2>$, where G is the process gain. Noise is

added as $n(t)$, a band-limited AWGN with a variance of σ^2. The output of the rake combiner and the matched filter (at point III) is

$$\sum_{l=0}^{L-1} \beta^*_{l-1-j}\, n(t - lT_c) + \sum_{j=0}^{L-1}\sum_{l=0}^{L-1} \beta_l \beta^*_{l-1-j}\, s_{\mathrm{MF}}\left(t - (l + j)T_c\right) \tag{5.4}$$

The desired output of the rake combiner occurs at time $t = (L-1)\,T_c$ and is

$$\sum_{l=0}^{L-1} \beta_l \beta_l^* s_{\mathrm{MF}}\left(t - (L-1)T_c\right)$$

(Note: $l + 1 = L - j$ or $l = L - 1 - j$.) It has a signal strength of

$$\left(\sum_{l=0}^{L-1} \beta_l \beta_l^*\right)^2 G \tag{5.5}$$

The noise power is

$$\left(\sum_{l=0}^{L-1} \beta_l \beta_l^*\right)\sigma^2 \tag{5.6}$$

From (5.5) and (5.6) the SNR is equal to

$$\left(\sum_{l=0}^{L-1} \beta_l \beta_l^*\right)\frac{G}{\sigma^2} \tag{5.7}$$

On the other hand, the signal strength at the output of the pre-rake combiner must be equal to unity. From Figure 5.7(b), it can be shown that N, the normalizing parameter, needs to be equal to

$$N = \left(\sum_{l=0}^{L-1} \beta_l \beta_l^*\right)^{\frac{1}{2}} \tag{5.8}$$

The signal at point IV will be

$$\frac{1}{N}\sum_{l=0}^{L-1} \beta_l^* s_s\left(t - lT_c\right) \tag{5.9}$$

at point V,

$$\frac{1}{N}\sum_{j=0}^{L-1}\sum_{l=0}^{L-1}\beta_l^*\beta_{l-1-j}s_s\left(t-(l+j)T_c\right) \tag{5.10}$$

and at point VI,

$$\frac{1}{N}\sum_{j=0}^{L-1}\sum_{l=0}^{L-1}\beta_l^*\beta_{l-1-j}s_{\mathrm{MF}}\left(t-(l+j)T_c\right)+n(t) \tag{5.11}$$

The desired signal occurs again at time $t = (L-1)T_c$ and has a power equal to

$$\frac{G}{N^2}\left(\sum_{l=0}^{L-1}\beta_l\beta_l^*\right)^2 \tag{5.12}$$

and noise power equal to σ^2. From (5.8) and (5.12) the SNR for the pre-rake system is equal to that of the rake system of (5.7).

5.5.2 BER

To calculate the theoretical BER, the probability distribution function of the instantaneous SNR at the input of the decision circuit must be derived. The desired signal at point VI can be written as follows:

$$\frac{1}{N}\sum_{l=0}^{L-1}\beta_l\beta_l^*s_{\mathrm{MF}}(t) \tag{5.13}$$

Because only one path is demodulated, the noise part includes only one term, $n(t)$, with instantaneous noise power of $\frac{1}{2}<|n(t)|^2>$. The SNR, γ, can be written

$$\gamma=\frac{1}{2}\frac{\left(\frac{1}{N}\sum_{l=0}^{L-1}\beta_l\beta_l^*\right)^2\left\langle|s_{\mathrm{MF}}(t)|^2\right\rangle}{\frac{1}{2}\left\langle|n(t)|^2\right\rangle} \tag{5.14}$$

Substituting for N from (5.8) and using $<|s_{\mathrm{MF}}(t)|^2>$:

$$\gamma = \frac{\sum_{l=0}^{L-1} \left| \beta_l \beta_l^* \right|}{\left\langle \left| n(t) \right|^2 \right\rangle} G \tag{5.15}$$

The instantaneous SNR for a single path can be written as follows, where the noise signal is the same for all the pre-rake combined paths, because they all arrive at the same time:

$$\gamma_l = \frac{\left| \beta_l \beta_l^* \right|}{\left\langle \left| n(t) \right|^2 \right\rangle} G \tag{5.16}$$

From (5.15) and (5.16):

$$\gamma = \sum_{l=0}^{L-1} \gamma_l$$

which is the same as that for maximum ratio combining, for example, as derived in [6]. The theoretical BER can be calculated with a method similar to that used in [6] for an ideal coherent PSK method:

$$P_e = \frac{1}{2} \int_0^\infty \operatorname{erfc} \sqrt{\gamma}\, p(\gamma)\, d\gamma$$

This result is for the ideal pre-rake combiner. The measurement and estimation errors cause system performance to be somehow inferior to the ideal case. The simulation results in [2] showed that the performances of the nonideal rake and pre-rake systems are poorer than the ideal case by 0.5 dB to 1.5 dB. Furthermore, it was shown that BER performance is degraded as the estimation and measurement errors increase due to the increase in the fading rate.

5.6 TDD-CDMA System with Pre-Rake

We now deal with the multiuser application of the pre-rake technique, which is applied when the pre-rake method is used in CDMA systems. We extend the above analysis and study the performance of the pre-rake system in a multiuser TDD-CDMA, and we provide analytical treatment. In this

section, we introduce a TDD-CDMA system that uses the pre-rake technique. For the sake of comparison, we analyze both pre-rake and conventional rake receivers.

As discussed before in TDD-CDMA, only one carrier is used for the uplink and downlink transmissions. Each user is distinguished by its specific PN code. If there is no fading, the BS transmits the downlink time slots for all users synchronously.

In a multipath-fading channel, a conventional rake receiver is used, in which each rake finger is synchronized to one of the channel paths. The rake receiver fingers provide matching to the channel impulse response. Using maximal ratio combining, each rake finger despreads the spread spectrum signal on its assigned channel path and multiplies the despread output with the complex conjugate of the path gain of that path. Hence, the receiver in both the BS and MTs must be equipped with sufficient rake fingers and the corresponding channel estimation.

In TDD-CDMA systems, we can utilize the fact that for a period of time the channel impulse response is the same for the uplink and downlink. Hence, only the BS needs to estimate it. As shown in Figure 5.6, to pre-rake the downlink signal of a certain user, the BS multiplies this signal by the time-reversed, complex conjugate of the uplink channel impulse response of that user. Estimation of the uplink multipath complex gains can be practically achieved using pilot symbol-aided techniques. Known symbols are added to the uplink frames at known locations. The BS receiver extracts the pilot symbols and uses them to estimate the uplink channel impulse response. This method is an alternative to the dedicated pilot channel used in the downlink of the current CDMA cellular standard in the United States. In fact, pilot symbol-aided channel estimation is used in both the uplink and downlink of the experimental wideband CDMA system [7] proposed by NTT in Japan. Although this system is not TDD, the concept of using pilot symbols is applicable to TDD. The conventional transmitted signal without pre-rake for user k with BPSK modulation is given by

$$s_k(t) = \sqrt{2P}\, b_k(t) a_k(t) \exp(J\omega t) \tag{5.17}$$

where P is the transmitted power, ω is the carrier frequency, and $b_k(t)$ is the data stream for user k consisting of a train of i.i.d. data bits with duration T, which take the values of ± 1 with equal probability. The current bit is denoted by b_k^0 while next or previous bits are denoted by adding or subtracting the superscript by one; $a_k(t)$ is the PN code of user k with ± 1 chips of duration T_c and code length $N = T/T_c$ (i.e., one code period per bit); and $J =$

Team-Fly®

$\sqrt{-1}$. The bits and chips waveforms are rectangular. Now, in a pre-rake system, instead of (5.17) the downlink transmitted signal will be

$$s_k(t) = \sqrt{\frac{2P}{U_k}} \sum_{l=0}^{L-1} \beta_{k,L-l-1} b_k(t - lT_c) a_k(t - lT_c) \exp\left(J\omega(t - lT_c) - J\gamma_{k,L-l-1}\right) \tag{5.18}$$

where U_k is a normalizing factor that keeps the instantaneous transmitted power constant regardless of the number of paths. The term U_k is given by

$$U_k = \sum_{l=0}^{L-1} \beta_{k,l}^2 \tag{5.19}$$

Note that the uplink channel impulse response is independent for all users. The signal received by user k is (5.18) convolved with the channel impulse response of user k. This produces a strong peak at the output of the channel, equivalent to the conventional rake receiver's combining. Therefore, the receiver of the MT does not need to estimate the channel impulse response and can only use one rake finger tuning to this peak. The pre-rake concept is shown graphically in Figure 5.6 for a $\delta(t)$ transmitted signal. It is worthwhile to mention that an optimal receiver for this pre-rake signal must provide a match with *all* components at the output of the channel. However, because the pre-rake system puts most of the power in one component, matching with this component provides sufficient performance. The performance improvements when a more complex receiver is utilized at the mobile are given in [8–10].

5.7 Performance Analysis of the Pre-Rake TDD-CDMA

Assuming a CDMA system with K users, the received signal at user i during the downlink time slot is given by

$$r_i(t) = n(t) + \text{Re} \sum_{k=1}^{K} \sum_{j=0}^{L-1} \beta_{i,j} s_k(t - jT_c) \exp\left(J\gamma_{i,j}\right) \tag{5.20}$$

where $n(t)$ is the zero-mean AWGN with two-sided power spectral density $N_0/2$. Using (5.18) in (5.20), one can see that the channel output includes

$2L-1$ paths with a strong peak when $j+l=L-1$. Only one rake finger is needed in the MT to synchronize to this path. Without loss of generality, we assume that user $i=1$ is the desired user. The output of the finger employed in the receiver of user 1 is given by

$$\begin{aligned} Z &= \int_{(L-1)T_c}^{(L-1)T_c+T} r_1(t)a_1\left[t-(L-1)T_c\right]\cdot\cos\left[\omega t-\omega T_c(L-1)\right]dt \\ &= D+S+A+\eta \end{aligned} \tag{5.21}$$

where η is a zero-mean Gaussian random variable with variance $N_0T/4$, and D is the desired part for the current bit given by the $k=1$ part of $r_1(t)$ and $j+l=L-1$ in (5.20). After simple manipulations, D is found to be

$$D=\sqrt{\frac{P}{2}}b_1^0T\sqrt{U_1} \tag{5.22}$$

The S and A values in (5.21) are the self- and multiple-access interference, respectively. Using the Gaussian approximation, we treat S and A as Gaussian random variables, and it is readily shown that they are independent with zero mean. Hence, we are only interested in their variances. The variances of S and A are evaluated conditioned on $\{\beta_{1,l}\}$, and the final results are averaged over $\{\beta_{1,l}\}$.

5.7.1 Self-Interference

This interference exists even in a single-user system and is caused by the multipath. It has been neglected in [4, 11, 12], which assume a low out-of-phase autocorrelation of the PN codes. However, we consider its effect here. From (5.18) to (5.20), S is found by putting $k=1$ (self-interference) and $j+l\neq L-1$ (undesired part). Self-interference S can be written after some manipulations as (substituting $m=L-l-1$)

$$\begin{aligned} S=\sqrt{\frac{P}{2U_1}}\sum_{j=0}^{L-1}\sum_{m=0,m\neq j}^{L-1}\beta_{1,j}\beta_{1,m}\cos\left[\omega T_c(j-m)+\gamma_{1,j}\right] \\ \cdot\int_0^T b_1\left[t-(j-m)T_c\right]a_1\left[t-(j-m)T_c\right]a_1(t)\,dt \end{aligned} \tag{5.23}$$

The summation of (5.23) includes correlated terms when j and m swap their values. We use the following identity:

$$\sum_{j=0}^{L-1}\sum_{m=0,m\neq j}^{L-1} f(j,m) = \sum_{j=0}^{L-2}\sum_{m=j+1}^{L-1} f(j,m) + f(m,j) \tag{5.24}$$

for any function $f(j,m)$. Also, we have

$$\begin{aligned}&\int_0^T b_1(t-mT_c)a_1(t-mT_c)a_1(t)dt\\ &=\begin{cases}T_c\left[b_k^{-1}C_{k,1}(m-N)+b_k^{0}C_{k,1}(m)\right] & \text{for } m\geq 0\\ T_c\left[b_k^{0}C_{k,1}(m)+b_k^{1}C_{k,1}(N+m)\right] & \text{for } m<0\end{cases}\end{aligned} \tag{5.25}$$

where $C_{k,1}(m)$ is the discrete aperiodic cross-correlation function defined in [11]. Denoting $C_{i,i}(m)$ by $C_i(m)$ and utilizing $C_i(m) = C_i(-m)$, we get

$$\begin{aligned}S = &\sqrt{\frac{P}{2U_1}}\sum_{j=0}^{L-2}\sum_{m=j+1}^{L-2}\beta_{1,j}\beta_{1,m}\cos\left[\omega T_c(j-m)+\gamma_{1,m}-\gamma_{1,j}\right]\\ &\left\{b_1^{-1}C_1(N-m+j)+b_1^{1}C_1(N-m+j)+2b_1^{0}C_1(m-j)\right\}\end{aligned} \tag{5.26}$$

For any value of j and m, any term in (5.26) is a zero mean and all terms are uncorrelated due to the independent phase angles. Hence, we can add their variances. Taking the second moment of (5.26), we get

$$E\left[S^2\middle|\{\beta_{1,l}\}\right] = \frac{PT_c^{\,2}}{2U_1}\sum_{j=0}^{L-2}\sum_{m=j+1}^{L-1}\beta_{1,j}^2\beta_{1,m}^2\left[C_1^2(N-m+j)+2C_1^2(m-j)\right] \tag{5.27}$$

5.7.2 Multiple-Access Interference

The multiple-access interference A due to other users is found by the $k > 1$ part of (5.20) in (5.21) and can be written after some manipulation as

$$\begin{aligned}A = &\sqrt{\frac{P}{2U_1}}\sum_{k=2}^{K}\sum_{j=0}^{L-1}\sum_{m=0}^{L-1}\frac{\beta_{1,j}\beta_{k,m}}{\sqrt{U_k}}\cos\left[\omega T_c(j-m)+\gamma_{k,m}-\gamma_{1,j}\right]\\ &\int_0^T b_k\left[t-(j-m)T_c\right]a_k\left[t-(j-m)T_c\right]a_1(t)dt\end{aligned} \tag{5.28}$$

Equation (5.28) can be divided into two parts: one for $m = j$ and one for $m \neq j$. The first part can be written

$$A\Big|_{m=j} = T_c \sqrt{\frac{P}{2}} \sum_{k=2}^{K} \sum_{j=0}^{L-1} \frac{\beta_{1,j}\beta_{k,j}}{\sqrt{U_k}} \cos\left[\gamma_{k,j} - \gamma_{1,j}\right] b_k^0 C_{k,1}(0) \tag{5.29}$$

For $m \neq j$ we use (5.24) and (5.25) to obtain

$$\begin{aligned} A\Big|_{m\neq j} &= \sqrt{\frac{P}{2}} \sum_{k=2}^{K} \sum_{j=0}^{L-2} \sum_{m=j+1}^{L-1} \frac{T_c}{\sqrt{U_k}} \\ &\cdot \Big\{ \beta_{1,j}\beta_{k,m} \cos\left[\omega T_c (j-m) + \gamma_{k,m} - \gamma_{1,j}\right] \\ &\cdot \left[b_k^0 C_{k,1}(j-m) + b_k^1 C_{k,1}(N+j-m) \right] \\ &+ \beta_{1,m}\beta_{k,j} \cos\left[\omega T_c (m-j) + \gamma_{k,j} - \gamma_{1,m}\right] \\ &\cdot \left[b_k^{-1} C_{k,1}(N-m-j) + b_k^0 C_{k,1}(m-j) \right] \Big\} \end{aligned} \tag{5.30}$$

It is easy to check that both (5.29) and (5.30) have a zero mean and all terms are uncorrelated since all angles inside the cos(.) are independent. Also, it is important to note that in (5.29) the full-period cross-correlation $C_{k,1}(0) = 0$ if orthogonal codes such as the Walsh–Hadamard codes are used. We introduce a pointer W for this purpose, as shown below. Taking the second moment of (5.29) and (5.30), we get

$$\begin{aligned} E\left[A^2 \middle| \{\beta_{1,l}\}\right] &= \frac{P T_c^{\,2} Q}{4} \sum_{k=2}^{K} \Bigg\{ W C_{k,1}^2(0) \sum_{m=0}^{L-1} \beta_{1,m}^2 \\ &+ \sum_{j=0}^{L-2} \sum_{m=j+1}^{L-1} \beta_{1,j}^2 \left[C_{k,1}^2(j-m) + C_{k,1}^2(N+j-m) \right] \\ &+ \sum_{j=0}^{L-2} \sum_{m=j+1}^{L-1} \beta_{1,m}^2 \left[C_{k,1}^2(m-j-N) + C_{k,1}^2(m-j) \right] \Bigg\} \end{aligned} \tag{5.31}$$

where W is a pointer with $W = 0$ if orthogonal codes are used and $W = 1$ otherwise, and Q is given by:

$$Q = Q_{k,j} = E\left[\frac{\beta_{k,j}^2}{U_k}\right] = \frac{1}{L}, \text{ for } j = 0, 1, \ldots, L-1$$

This is easily found by noting that since $\{\beta_{k,j}\}$ are i.i.d, $Q = Q_{k,0} = Q_{k,1} = \ldots = Q_{k,L-1}$, and from the definition in (5.19), $Q_{k,0} + Q_{k,1} + \ldots + Q_{k,L-1} = 1$. To evaluate (5.27) and (5.31), we assume random code sequences. Random codes are shown in [3] to provide a performance between the best and the worst code selections. In this case, we replace all $C_{k,1}(m)$ in (5.27) and (5.31) by their expected values given by

$$\begin{aligned} E\left[C_i^2(m)\right] &= N - |m| \quad \text{for } m \neq n \\ E\left[C_{k,j}^2(m)\right] &= N - |m| \\ E\left[C_{k,i}(m)C_{k,i}(n)\right] &= 0 \quad \text{for } m \neq n, k \neq i \end{aligned} \tag{5.32}$$

The last part in (5.31) will be needed later. If orthogonal codes are used, we set $W = 0$ [or equivalently $C_{k,i}(0) = 0$]. However, for the out-of-phase cross-correlations of orthogonal codes [i.e., $m \neq 0$ in (5.32)], we still use (5.32). Using (5.32) in (5.27) and (5.31), and assuming Z in (5.21) as Gaussian random variable, we can find that the probability of error, conditioned on $\{\beta_{1,n}, n = 0,1,\ldots,L-1\}$, is given by

$$P\left(e\middle|\{\beta_{1,n}\}\right) = 0.5\,\mathrm{erfc}\left(\sqrt{Y}\right) \tag{5.33}$$

where Y is the SNR, given by $Y = \frac{D^2}{2\,\mathrm{var}(Z)}$, where $\mathrm{var}(Z)$ is the variance of the random variable. By noise we mean the sum of the effects of AWGN noise, self-interference, and multiple-access interference. After some manipulations, Y is found to be

$$Y = \left[\frac{L}{\bar{\gamma}_b U_1} + \frac{4\chi}{NU_1^2} - \frac{2\mu}{N^2 U_1^2} + \frac{(K-1)(L-1+W)}{NL}\right]^{-1} \tag{5.34}$$

where $\bar{\gamma}b = PTL/N_0$ is the average received signal-to-AWGN ratio, $\chi = \sum_{j=0}^{L-2}\sum_{m=j+1}^{L-1}\beta_{2,j}\beta_{2,m}$, and $\mu = \sum_{j=0}^{L-2}\sum_{m=j+1}^{L-1}(m-j)\beta_{1,j}^2\beta_{1,m}^2$. The PDFs of χ and μ are very difficult to obtain. The final probability of error P_e is evaluated from (5.33) and (5.34) using the Monte Carlo integration. At each iteration, L Rayleigh random variables are computer generated, U_1, χ, and μ are evaluated, and Y is found and substituted in (5.33). For each value, (5.33) is averaged over a sufficiently large number of iterations.

5.8 Performance Analysis of the Rake TDD-CDMA

The rake receiver analysis is introduced for the sake of comparison, using the same assumptions of the pre-rake. Without using a pre-rake at the BS, the received signal at user 1 is given by (5.20) with $s_k(t)$ from (5.17) instead of (5.18). We assume the rake receiver is equipped with L rake fingers, each tuned to one of the channel paths. Each rake finger gets self-interference S and multiple-access interference A. With maximal ratio combining, the final decision statistic of the rake receiver is given by

$$Z = \sum_{n=0}^{L-1} \beta_{1,n} \int_{nT_c}^{nT_c+T} r_1(t) a_1(t - nT_c) \cos(\omega t - \omega n T_c + \gamma_n)\, dt = D + S + A + \eta \tag{5.35}$$

where η is a zero-mean Gaussian random variable with variance $N_0 TU_1/4$ [3] and D is the desired signal part, which is found by substituting $k = 1$ (desired user) and j of $r(t) = n$ in (5.20). Hence, D is given by

$$D = \sqrt{\frac{P}{2}} b_1^0 TU_1 \tag{5.36}$$

5.8.1 Self-Interference

Substituting (5.17) in (5.20) and (5.35), the self-interference S is found by putting $k = 1$ (desired user) and $n \neq j$ (output of nth rake finger due to paths other than n). It is easy to find that S is similar to that in (5.23) except that U_1 is removed and, hence, the self-interference power in the rake receiver is given by (5.27) without U_1.

5.8.2 Multiple-Access Interference

This interference is found by setting $k > 1$ in (5.35). In this case, we emphasize a major difference with respect to the pre-rake. In the pre-rake, the signal of each user is pre-raked according to its uplink channel impulse response. Hence, in the downlink the desired user's signal is maximal ratio combined, while other users' signals are not. In the rake receiver system, the desired and the multiple-access signals are maximal ratio combined. We will find that unless orthogonal codes are used the multiple-access interference in the rake receiver is much higher than that in the pre-rake receiver. The multiple-access interference is given by

$$A = \sqrt{\frac{P}{2}} \sum_{k=2}^{K} \sum_{n=0}^{L-1} \sum_{j=0}^{L-1} \frac{\beta_{1,n}\beta_{1,j}}{\sqrt{U_k}} \cos\left[\omega T_c (j-n) + \gamma_{1,n} - \gamma_{1,j}\right] \cdot \int_0^T b_k\left[t-(j-n)T_c\right] a_k\left[t-(j-n)T_c\right] a_1(t)\,dt \tag{5.37}$$

Again, A can be divided into two terms—one with $j = n$ and the other with $j \neq n$. The first term can be written as

$$A\big|_{n=j} = T_c \sqrt{\frac{P}{2}} \sum_{k=2}^{K} \sum_{j=0}^{L-1} \beta_{1,j}^2 b_k^0 C_{k,1}(0) \tag{5.38}$$

This part of multiple-access interference is maximal ratio combined. It is equal to zero only if orthogonal codes are used. Otherwise, it is easy to check that it produces more interference than the counter term in (5.30). For $j \neq n$ and using (5.24), we get

$$\begin{aligned} A\big|_{n\neq j} = {} & T_c \sqrt{\frac{P}{2}} \sum_{k=2}^{K} \sum_{n=0}^{L-2} \sum_{j=n+1}^{L-1} \beta_{1,n}\beta_{1,j} \cos\left[\omega T_c (j-n) + \gamma_{1,n} - \gamma_{1,j}\right] \\ & \cdot \left\{ b_k^0 C_{k,1}(n-j) + b_k^1 C_{k,1}(N+n-j) \right. \\ & \left. + b_k^{-1} C_{k,1}(j-n-N) + b_k^0 C_{k,1}(j-n) \right\} \end{aligned} \tag{5.39}$$

Taking the second moment of A, we get

$$\begin{aligned} E\left[A^2 \middle| \{\beta_{1,l}\}\right] = {} & \frac{PT_c^2}{4} \sum_{k=2}^{K} \left\{ 2WC_{k,1}^2(0) \left(\sum_{j=0}^{L-1} \beta_{1,j} \right)^2 + \sum_{n=0}^{L-2} \sum_{j=n+1}^{L-2} \beta_{1,n}^2 \beta_{1,j}^2 \right. \\ & \cdot \left[C_{k,1}^2(j-n-N) + C_{k,1}^2(N+n-j) \cdot C_{k,1}^2(n-j) \right. \\ & \left. \left. + C_{k,1}^2(j-n) + 2C_{k,1}(n-j) \cdot C_{k,1}(j-n) \right] \right\} \end{aligned} \tag{5.40}$$

Similar to the pre-rake receiver, we use random code sequences to evaluate the probability of error. Employing (5.32) Y is now given by

$$Y = \left[\frac{L}{\bar{\gamma}_b U_1} + \frac{4\chi}{NU_1^2} - \frac{2\mu}{N^2 U_1^2} + \frac{2(K-1)\left(WU_1^2 + \chi\right)}{NU_1^2} \right]^{-1} \tag{5.41}$$

where $W = 0$ for orthogonal codes and $W = 1$ otherwise. The final probability of error is evaluated using a Monte Carlo integration of (5.33) as explained before [13, 14].

5.9 Numerical Results and Discussion

We consider a TDD-WCDMA system with 50 users and code length $N = 128$. Figure 5.8 shows the probability of error versus the E_b/N_0 for the rake and pre-rake systems with two paths. Clearly, when orthogonal codes are used, the performance is much better for both systems, with the rake receiver performing better than the pre-rake receiver. However, the difference is not very big, and the use of pre-rake is still justified to reduce the cost and size of the MT. When nonorthogonal codes are used, the pre-rake receiver greatly outperforms the rake receiver since the latter enhances the interference as well.

To clarify the latter point, we compare the multiple-access interference terms (5.29) and (5.38) for the pre-rake and rake receivers, respectively. For orthogonal codes, the two terms disappear and the performance of the rake and pre-rake are almost the same. However, when random codes are used, we notice that in the pre-rake case this part of the multiple-access interference

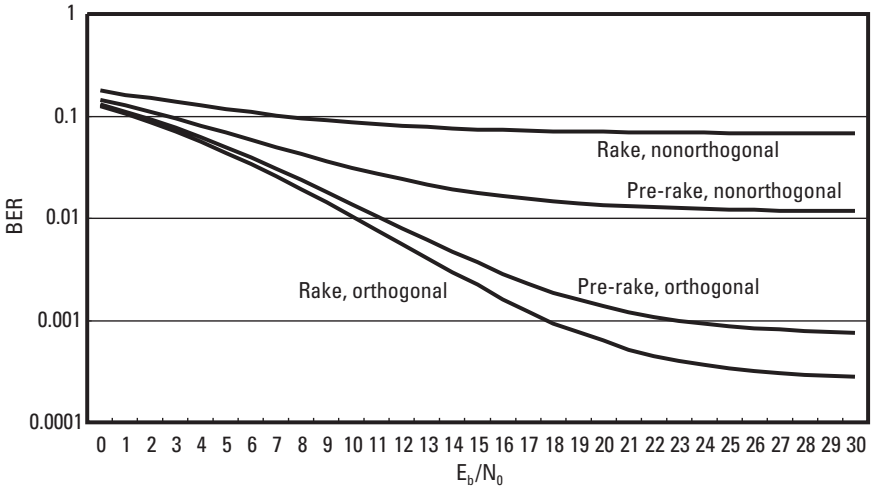

Figure 5.8 BER versus E_b/N_0.

does *not* match with pre-rake combining, that is, paths with the same delay do not have the same channel gain or phase. This is because the pre-rake process weighs the signal of user $k \neq 1$ with the channel impulse response of that user k. Hence, this part of interference power is not enhanced when it goes through the downlink channel of user 1. On the contrary, in the rake receiver case, all signals for all users go through the channel of user 1, and the part of multiple-access interference represented by (5.38) is due to the rake matching in gain and phase to the interference of all users $k \neq 1$. Hence, when using random codes, the rake system is subject to higher multiple-access interference power.

Figure 5.9 shows the probability of error versus the number of users with E_b/N_0 = 20 dB and L = 2. The same observation of the previous figure can be seen here. Figure 5.10 shows the probability of error versus the number of paths for 50 users and E_b/N_0 = 20 dB. We can see that as the number of channel paths increase, the performance improves at first due to diversity, then it starts to deteriorate due to increased interference from the large number of paths of all users. We can see then that, for the given parameter in synchronous downlink transmission, the rake diversity combining method is not useful for large numbers of channel paths, since noise and signal are both coherently combined. For a discussion on pre-rake performance with estimation error, see [15–18].

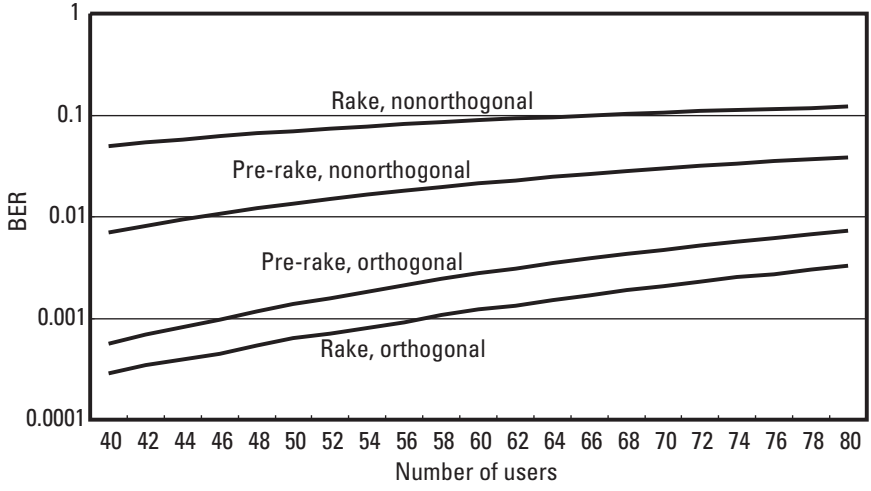

Figure 5.9 BER versus the number of users.

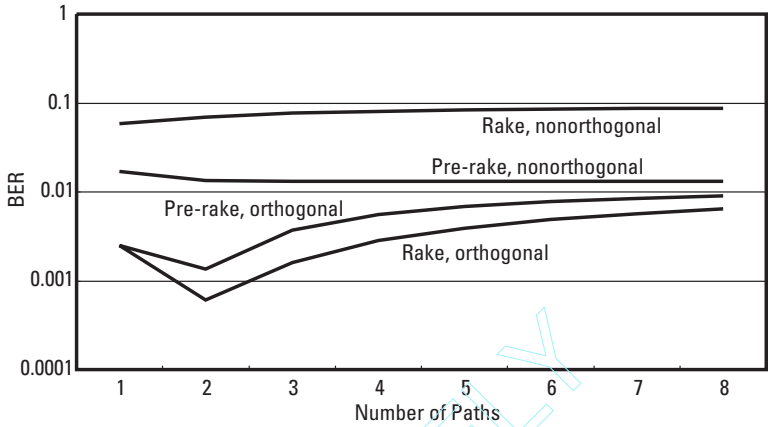

Figure 5.10 BER versus the number of paths.

TEAMFLY

5.10 Summary

The pre-rake system for TDD-CDMA mobile communications has been described. Since the uplink and downlink are on the same carrier, the BS can estimate the channel impulse response and pre-rake the signal before transmission to the portable unit. With a simple receiver, employing just one rake finger at the portable unit, the diversity effect is achieved. This greatly reduces the size and cost of the portable unit. Pre-rake receiver performance is comparable to that of a rake receiver when orthogonal codes are used, and pre-rake performs even better than the rake receiver when nonorthogonal codes are used.

References

[1] Esmailzadeh, R., and M. Nakagawa, "Pre-Rake Diversity Combination for Direct Sequence Spread Spectrum Mobile Communications Systems," *Proc. IEEE ICC*, Geneva, 1993.

[2] Esmailzadeh, R., and M. Nakagawa, "Pre-Rake Diversity Combination for Direct Sequence Spread Spectrum Mobile Communications Systems," *IEICE Trans. on Commun.,* Vol. E76-B, No. 8, August 1993.

[3] Proakis, J., *Digital Communications,* New York: McGraw-Hill, 1989.

[4] Kchao, C., and G. Stuber, "Analysis of a Direct Sequence Spread Spectrum Cellular Radio System," *IEEE Trans. on Commun.,* Vol. 41, October 1993, pp. 1507–1516.

[5] Turin, G. L., "Introduction to Spread-Spectrum Anti-Multipath Techniques and Their Application to Urban Digital Radio," *Proc. IEEE,* Vol. 68, March 1980, pp. 328–353.

Team-Fly®

[6] Schwartz, M., W. R. Bennet, and S. Stein, *Communication Systems and Techniques,* New York: McGraw-Hill, 1966.

[7] Adachi, F., et al., "Coherent DS-CDMA, Promising Multiple Access Multimedia Mobile Communications," *Proc. IEEE ISSSTA,* 1996.

[8] Wang, J. -B., et al., "FIR-Rake Multipath Diversity Combined with Antenna Array Used in TDD-CDMA Systems," *Proc. WCT 2000,* pp. 725–728.

[9] Wang, J. -B., et al., "A Novel Multipath Transmission Diversity Scheme in TDD-CDMA Systems," *IEICE Trans. on Commun. (Letter),* Vol. E82-B, No. 10, October 1999.

[10] Barreto, A. N., and G. Fettweis, "Performance Improvement in DS Spread Spectrum CDMA System Using a Pre- and a Post-Rake," *Proc. International Zurich Seminar on Broadband Communications,* 2000, pp. 39–46.

[11] Pursley, M., "Performance Evaluation for Phase-Coded Spread-Spectrum Multiple Access Communications—Part I: System Analysis," *IEEE Trans. on Commun.,* Vol. COM-25, August 1977, pp. 795–799.

[12] Borth, D. E., and M. B. Pursley, "Analysis of Direct Sequence Spread Spectrum Multiple Access Communication over Rician Fading Channels," *IEEE Trans. on Commun.,* Vol. COM-27, October 1979, pp. 1566–1577.

[13] Esmailzadeh, R., E. Sourour, and M. Nakagawa, "Pre-Rake Diversity Combining in Time Division Duplex Mobile Communications," *Proc. IEEE PIMRC*, 1995, pp. 431–435.

[14] Esmailzadeh, R., E. Sourour, and M. Nakagawa, "Pre-Rake Diversity Combining in Time Division Duplex Mobile Communications," *IEEE Trans. on Vehicular Technology,* Vol. VT-48, No. 3, May 1999, pp. 795–801.

[15] Sourour, E. E., T. A. Kadous, and S. E. El-Khamy, "The Performance of TDD/CDMA Systems Using Pre-RAKE Combining with Different Diversity Techniques and Imperfect Channel Estimation," *Proc. 2nd IEEE Symp. on Computers and Communications,* 1997, pp. 280–284.

[16] Kadous, T. A., E. E. Sourour, and S. E. El-Khamy, "Comparison Between Various Diversity Techniques of the Pre-Rake Combining System in TDD/CDMA," *Proc. IEEE Vehicular Technology Conference,* 1997, pp. 2210–2214.

[17] El-Khamy, S. E., E. E. Sourour, and T. A. Kadous, "Analysis of Incoherent Pre-Rake TDD/DPSK/CDMA Wireless Portable Communications," *Proc. 15th National Radio Science Conference,* 1998, pp. C13/1–C13/8.

[18] El-Khamy, S. E., E. E. Sourour, and T. A. Kadous, "Wireless Portable Communications Using Pre-Rake CDMA/TDD/QPSK Systems with Different Combining Techniques and Imperfect Channel Estimation," *Proc. IEEE PIMRC,* 1997, pp. 529–533.

6

System Capacity in TDD-CDMA Systems

In this chapter we discuss the capacity of a TDD-CDMA system and discuss methods that can contribute to enhancing the performance of TDD systems. We first review a method for evaluating the downlink and uplink capacity of a CDMA system. We then use this model to explore TDD performance enhancements.

It is well documented that CDMA systems are interference limited [1–8]. This is because all users share the same spectrum, and the addition of a user adds to the total interference present in the system. As illustrated in Figure 6.1, a desired user's signal shares spectrum with other users present in the system. When the signal is despread, the signal power is despread to a narrower bandwidth, whereas all interference signals remain wideband. Filtering removes a large part of the interference power, but residual interference does remain and becomes significant as the total number of interferers increases. The desired user requires a certain SIR for required performance quality. The capacity of a system is determined by the maximum number of users that can be accommodated, for which the SIR target for required performance can be delivered.

The sources of interference are signals that are transmitted in the same band and are intended for other users or are for control purposes. Figure 6.2 shows the signal and interference sources in the downlink of a cellular mobile communication system. In the downlink, an MT receives its desired signal

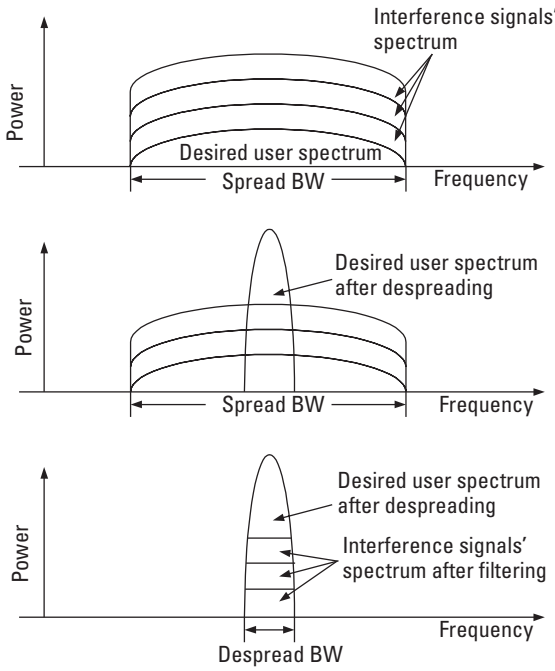

Figure 6.1 Multiuser interference, SIR.

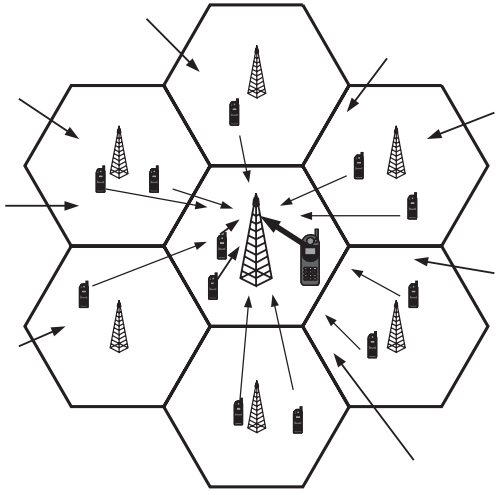

Figure 6.2 Signal and interference sources in the downlink of a cellular mobile communication system.

from the BS of the cell in which it is located, or if it is in a soft handoff mode, from other nearby cells' BSs. This signal is interfered with by the signals from all other BSs in the system and also by the signals the serving BSs send to other users within the same cell.

As we saw in Chapter 5, a self-interference term is also present and results from the interference from the multipath transmission. In contrast, the sources of interference in the uplink are all of the MTs in the system. Figure 6.3 shows the signal and interference sources in the uplink of the system. Although all other cells' MT signals are intended for BSs other than the target for the desired user, they transmit in the same spectrum and therefore appear as interference. Like the situation with the downlink, another source is the multipath induced self-interference.

6.1 Downlink Capacity

We consider a CDMA system consisting of B BSs exerting interference on a user k among K users in the central BS, denoted by subscript 0. The SIR for user k in the central BS, $\gamma_{0,k}$, can be written as follows:

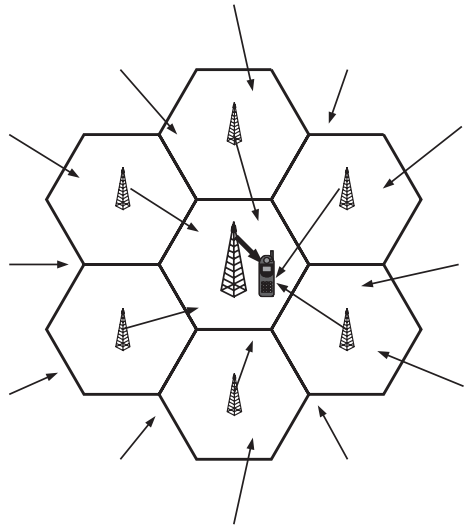

Figure 6.3 Signal and interference sources in the uplink of a cellular mobile communication system.

$$\gamma_{0,k} = \frac{P_{0,k} g_{0,k}}{\sum_{\substack{i=0 \\ i \neq k}}^{K} P_{0,i} g_{0,k} + P_C g_{0,k} + \sum_{b=1}^{B} P_b \cdot g_{b,k} + \phi P_{0,k} g_{0,k} + \eta} \tag{6.1}$$

where $P_{0,k}$ is the amount of power allocated to user k of the total power available, P_0, in the serving BS; P_C represents the power necessary to transmit the control channels, these signals appear as interference when detecting the traffic channels; $g_{b,k}$ is the channel gain from the bth BS to the kth MT; ϕ is the ratio of self-interference compared with the desired signal, and η is the receiver noise power. The denominator of (6.1) represents interference from signals intended for other users within the same cell, interference from the BSs of other cells, self-interference, and noise. Equation (6.1) can also be written

$$\gamma_{0,k} = \frac{P_{0,k} g_{0,k}}{\left(P_0 - P_{0,k} - P_C\right) g_{0,k} + P_C g_{0,k} + F_{dl} P_0 g_{0,k} + \phi P_{0,k} g_{0,k} + \eta} \tag{6.2}$$

where F_{DL} is the ratio of outer-cell to own-cell interference in the downlink. The BS tries to deliver sufficient power, $P_{0,i}$ to MT i such that the SIR requirement $\gamma_{0,i}$ is met. The capacity of the downlink can be calculated as the maximum number of users K that satisfies the inequality:

$$\sum_{i=0}^{K} P_{0,i} \leq P_0 - P_C \tag{6.3}$$

In other words, the capacity is the number of users a BS can support with the limited amount of power it has.

6.2 Uplink Capacity

For the system defined in the previous section, the SIR of the signal of user k at BS 0 can be written

$$\varphi_{0,k} = \frac{p_{0,k} g_{0,k}}{\sum_{\substack{i=0 \\ i \neq k}}^{K} p_{0,i} g_{0,i} + \sum_{b=1}^{B} \sum_{i=0}^{M} p_{b,i} g_{0,b,i} + \phi p_{0,k} g_{0,k} + \eta} \tag{6.4}$$

where $p_{b,k}$ is the signal power transmitted from the kth MT for the bth BS. Assuming perfect power control and uniform service: $p_{0,k}g_{0,i} = p_{0,k}g_{0,k}$ for all i,k. Then (6.4) can be written

$$\varphi_{0,k} = \frac{1}{(1+F_{ul})(K-1)+\phi+\dfrac{\eta}{p_{0,k}g_{0,k}}} \tag{6.5}$$

where $F_{ul} = \dfrac{\sum_{b=1}^{B}\sum_{i=0}^{M} p_{b,i}g_{0,b,i}}{\sum_{\substack{i=0 \\ i\neq k}}^{K} p_{0,i}g_{0,i}}$ is the ratio of intercell to intracell interference.

The user capacity of the uplink is the maximum K that satisfies the required SIR as defined by (6.5).

To summarize, the capacity of a cellular CDMA system is mainly limited in the reverse link by the total mutual interference from other users, and in the forward link by interference from other BSs, as well as by intersymbol multipath interference. To increase the capacity of the system, the amount of received interference needs to be reduced. This is possible through orthogonal transmission, directional/adaptive antennas, and interference cancellation or rejection.

6.3 Orthogonal Transmission

The concept of orthogonal transmission was discussed in Chapter 2. Here we quantify the benefits of orthogonal transmission in a CDMA system downlink. We further evaluate the benefits for the uplink of a TDD system.

6.3.1 Downlink

Because downlink transmission is synchronous, use of orthogonal codes in the downlink is common practice in all CDMA systems. Walsh–Hadamard codes are used in IS-95 systems; and a class of tree-structured orthogonal codes [8] providing for an orthogonal variable spreading factor for spreading and channelization is used by the WCDMA systems. As discussed in Chapter 2, the use of orthogonal codes in synchronous transmission results in zero cross-correlation and, hence, zero interference in a single-path system. Setting the multiuser interference term (6.2) to zero results in

$$\gamma_{0,k} = \frac{P_{0,k} g_{0,k}}{P_C g_{0,k} + F_{dl} P_0 g_{0,k} + \phi P_{0,k} g_{0,k} + \eta} \tag{6.6}$$

The orthogonality of downlink transmission is reduced by multipath propagation. This is because the cross-correlation of nonsynchronous orthogonal codes is nonzero. We define a nonorthogonality factor α_{dl}, where $\alpha_{dl} = 0$ for a fully onthogonal system, and $\alpha_{dl} = 1$ for a fully nonorthogonal system. Equation (6.2) can be written

$$\gamma_{0,k} = \frac{P_{0,k} g_{0,k}}{\alpha_{dl}\left(P_0 - P_{0,k} - P_C\right) g_{0,k} + P_C g_{0,k} + F_{dl} P_0 g_{0,k} + \phi P_{0,k} g_{0,k} + \eta} \tag{6.7}$$

The values of α_{dl} and F_{dl} vary for different system configurations. They are also different for different propagation environments. Typical values for a macrocell system are $\alpha_{dl} = 0.4$ and $F_{dl} = 0.65$, and for a microcell α_{dl} and $F_{dl} = 0.2$ [2].

6.3.2 Uplink

Uplink transmission is generally asynchronous, because it is not practical to make all MTs transmit their signals synchronously at the chip and symbol level. However, when the maximum propagation delay difference for users within a microcell or an indoor environment is less than the chip duration, T_c, it is possible to achieve a degree of synchronicity between various users for reverse link transmission. This method is called *quasisynchronous* (QS) CDMA and is discussed in [9]. Because there is some error in synchronization, special orthogonal codes with small cross-correlation need to be used, some of which are discussed in [10–12]. Various degrees of QS are reported in the literature, for example, a value of $0.5\,T_c$ is reported in [12].

Another method is for the BS to instruct MTs to adjust their transmission times such that their signals may arrive synchronously at the BS. This method of QS-CDMA can be implemented in both the FDD and TDD modes. However, the realization is simpler in the TDD mode, and so is explaining the method.

In the TDD mode, the length of each transmission burst to and from a BS is constant, thereby allowing a mobile unit to accurately estimate the propagation delay and adjust its transmission so its signal arrives at its BS at a

particular designated time. In this way signals from all users could arrive quasisynchronously (within a designed accuracy). The degree of accuracy is determined by a local clock at the MT with a period of T_m, equal to a fraction of T_c.

Figure 6.4 shows how one TDD slot is divided into the uplink and downlink slots with lengths of τ_{dl} and τ_{ul}; and guard time at ith MT for slot n, $\tau^n_{m,i}$ and BS $\tau^n_{b,i}$. Propagation delays at the beginning and end of a TDD frame are denoted as $\tau^{n-1}_{p,i}$ and $\tau^n_{p,i}$, respectively. In a normal TDD (nonsynchronous) system, the first three are constant for all users. In a synchronous system, however, the guard time at base station $\tau^n_{b,i}$ must be constant and the guard band at the MT $\tau^n_{m,i}$ varies in response to the changes in propagation delay times as a mobile moves in a cell.

The guard time $\tau^n_{m,i}$ at all MTs must be set up in such a way to compensate for the differences in propagation delay times of different users $\tau^n_{p,i}$. Figure 6.5 illustrates this concept. The guard time is different for the three users, facilitating their QS arrival at the BS. Note that all the times mentioned here are integer multiples of T_m, the mobile unit clock period. For example, $\tau^n_{p,i} = \left\lfloor \frac{\tau^n_{p,i}}{T_m} \right\rfloor$, where $\lfloor . \rfloor$ indicates the integer part of the operand and $\tau^n_{p,i}$ is the actual time.

The QS state of reception is achieved at call setup by an MT. A BS transmits to all users at the beginning of each TDD frame. At call setup a user i transmits its reverse link signal after a nominal guard time $\bar{\tau}_m$, which can be one of the parameters broadcast by the BS. The BS then will ask the user to increase/decrease $\tau_{m,i}$ in order to make itself QS with the current users. When the QS state is established, the guard time at the BS $\bar{\tau}_m$ is equal for all users.

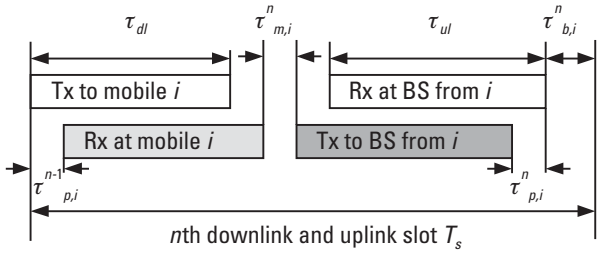

Figure 6.4 The lengths of uplink and downlink slots, propagation delays, and guard times.

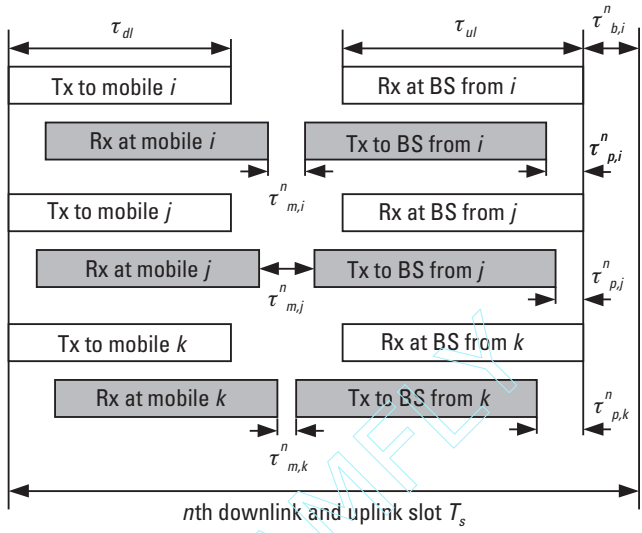

Figure 6.5 QS-CDMA transmission and reception for three users.

Upon achievement of the QS state, the mobile unit i starts the local clock, T_m. The clock measures the time elapsed after the completion of the reverse link burst, and the start of reception of the forward link burst $\tau_{c,i}$ as shown in Figure 6.6 and at the nth slot has a value equal to

$$\tau^{n}_{c,i} = 2\tau^{n}_{p,i} + \tau^{n}_{b,i} \tag{6.8}$$

where it is assumed that the propagation delay does not change significantly from the end of one slot to the beginning of the next slot.

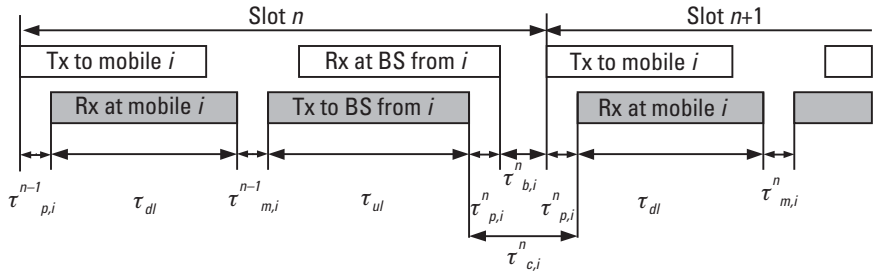

Figure 6.6 The control clock $\tau^{n}_{c,i}$.

Team-Fly®

Let us now assume that the mobile i is quasisynchronous within the design accuracy at frame $n-1$, that is, $\tau_{b,i}^{n} = \bar{\tau}_b$, and $\tau_{c,i}^{n-1} = 2\tau_{p,i}^{n-1} + \tau_{b,i}^{n-1}$. Now assume that in slot n the propagation delay $\tau_{p,i}^{n}$ is now outside QS accuracy by $\delta_{p,i}^{n} = \tau_{p,i}^{n} - \tau_{p,i}^{n-1}$. It follows that the guard time at the BS is now reduced by the increase in the propagation delay, that is, $\tau_{b,i}^{n} = \tau_{b,i}^{n-1} + \delta_{p,i}^{n}$. Defining $\delta_{b,i}^{n} = -\delta_{p,i}^{n}$, we can write

$$\tau_{b,i}^{n} = \tau_{b,i}^{n} + \delta_{b,i}^{n} \tag{6.9}$$

This applies to the case for which there has been no previous errors in propagation delay, that is, the system started in slot $n-1$ with no error. Let us define $\Delta_{b,i}^{n}$ as the total error due to changes in propagation delay up to frame n, or $\Delta_{b,i}^{n} = \sum_{j=1}^{n} \delta_{b,i}^{j}$. It can be also written

$$\Delta_{b,i}^{n} = \Delta_{b,i}^{n-1} + \delta_{b,i}^{n} \tag{6.10}$$

The guard time $\tau_{m,i}^{n+1}$ must be adjusted by $\delta_{m,i}^{n+1} = \tau_{m,i}^{n+1} - \tau_{m,i}^{n+1}$ in such a way to ensure the error of (6.10) $\Delta_{b,i}^{n}$ will be zero in the next interval. The information regarding the necessary adjustment $\delta_{b,i}^{n+1}$ is obtained from $\delta_{c,i}^{n+1} = \tau_{c,i}^{n+1} - \tau_{c,i}^{n}$.

To establish a stable system, we must set the accumulated error to represent only the changes that occurred in the propagation delay as detected by the local clock T_m in the latest slot:

$$\Delta_{b,i}^{n} = -\delta_{p,i}^{n} \tag{6.11}$$

This ensures us that by the next TDD slot the error is already reduced to zero through the operation of $\delta_{m,i}^{n+1}$. From (6.10) we can write

$$\delta_{b,i}^{n} = \delta_{p,i}^{n-1} - \delta_{p,i}^{n} \tag{6.12}$$

and, as can be seen from Figure 6.7, we can write

$$\delta_{c,i}^{n} = 2\delta_{p,i}^{n} + \delta_{b,i}^{n} \tag{6.13}$$

or, from (6.12):

$$\delta_{c,i}^{n} = \delta_{p,i}^{n} + \delta_{p,i}^{n-1} \tag{6.14}$$

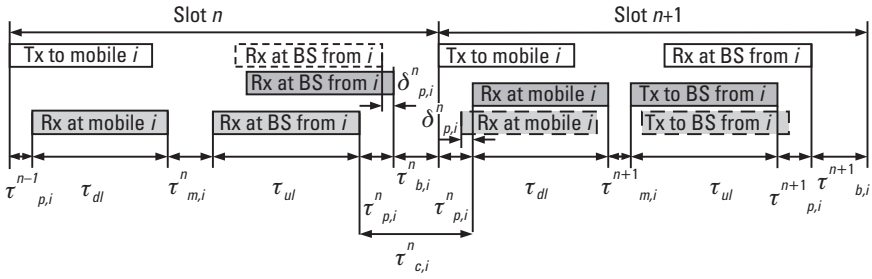

Figure 6.7 Maintaining QS timing.

The value of $\delta^{n}_{c,i}$ also can be written in terms of $\delta^{n}_{m,i}$ and $\delta^{n}_{p,i}$. Note that half of $\delta^{n}_{m,i}$ compensates for the late reception of forward link packet:

$$\delta^{n}_{c,i} = \delta^{n}_{p,i} - \frac{1}{2}\delta^{n}_{m,i} \tag{6.15}$$

Thus, $\delta^{n-1}_{p,i} = \frac{1}{2}\delta^{n}_{m,i}$, which yields

$$\delta^{n}_{c,i} = -\frac{1}{2}\delta^{n+1}_{m,i} - \frac{1}{2}\delta^{n}_{m,i} \tag{6.16}$$

which means we need

$$\delta^{n+1}_{m,i} = -2\delta^{n+1}_{c,i} - \delta^{n}_{m,i} \tag{6.17}$$

to make $\Delta^{n}_{b,i}$ go to zero.

The sensitivity of the mobile clock thus determines the degree of QS state. As the clock detects a change in propagation delay, the mobile unit adjusts its $\tau^{n}_{m,i}$ to return the system to the QS state. The clock can easily be set at 10 times the chip rate, which means that uplink transmission can be synchronous to a large degree.

In our QS CDMA system, the mobile users signals arrive at the BS within a fraction of the chip period, defined as

$$\Delta_i = \frac{\tau_i}{T_c} \tag{6.18}$$

which is determined by the accuracy of the local mobile clock. The parameter Δ_i is a random variable and is assumed distributed uniformly in

$[-\Delta_m, \Delta_m]$, where $0 < \Delta_m < 1$. For a QS CDMA system, using Walsh–Hadamard orthogonal codes, the SIR γ_{QS} for the users within the serving cell can be written as follows [12–15]:

$$\gamma_{QS} = \frac{\Delta_m^2}{3N} \tag{6.19}$$

If the local clock is operated at 10 times the chip rate, then $\Delta_m = 0.1$, and the amount of uplink intracell multiuser interference is minimal. This will modify (6.5), by removing the intracell interference term, resulting in

$$\phi_{0,k} = \frac{1}{(K-1)F_{ul} + \phi + \dfrac{\eta}{p_{0,k} g_{0,k}}} \tag{6.20}$$

6.4 Directional and Adaptive Array Antennas

The uplink and downlink interference may also be limited through usage of directional antennas. In this method, the amount of interference is limited to the area from which the incoming desired signal and the interference are received. An example of such a system is sectored antennas as shown in Figure 6.8. The interference on the desired signal is from the users in its sector of the cell. Ideally a three-sector antenna multiplies the capacity of the cell by three.

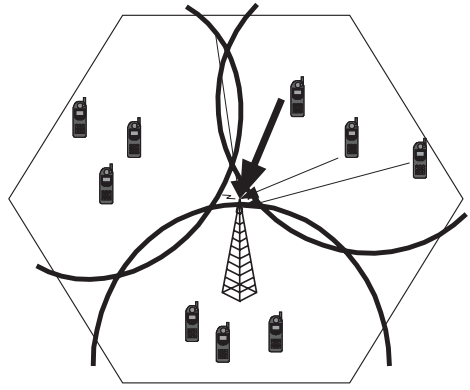

Figure 6.8 Three-sector antenna.

Theoretically it is possible to narrow the beam width of the antenna to direct the signal to any single user. Such antennas are not practical in cellular communications where an LOS channel rarely exists. Moreover, the mobiles are on the move and, therefore, fixed antenna beams are not useful. A solution is the adaptive array antennas. These antennas can direct transmissions to, and receptions from, mobile users dynamically as they move.

Figure 6.9 shows an adaptive array antenna. It consists of N antenna array elements, the output of which is summed after being multiplied by a complex number w_n. The weighting of the output of the elements causes the antenna to act as a highly directional antenna capable of emphasizing reception from a certain direction and minimizing reception from other directions. The accuracy is dependent on the number of elements and on how accurately w_n can be calculated and set.

The weights are calculated according to a training sequence $b(t)$ transmitted from a mobile. Let $x_i(t)$ denote the received signal at the ith element of the array antenna. We define $\mathbf{x}(t) = [x_1(t), x_2(t), ..., x_M(t)]^T$ and $\mathbf{w}(t) = [w_1(t),$

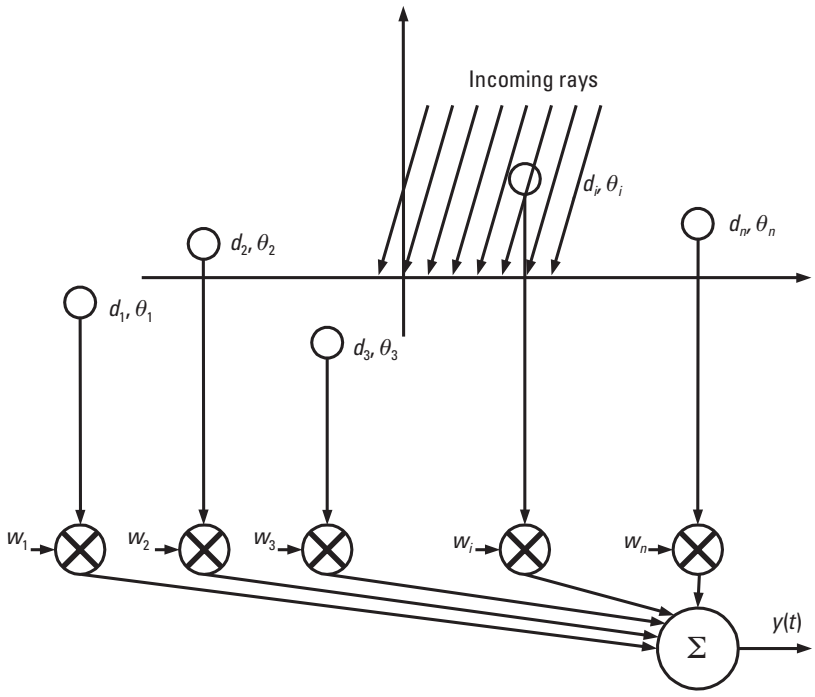

Figure 6.9 Adaptive array antenna. (*Source:* [16], ©1998 IEICE.)

$w_2(t), \ldots, w_M(t)]^T$ as the vectors of the received signal and the weighting factor. The output of the array antenna can be written

$$y(t) = \mathbf{x}^T(t)\mathbf{w} \tag{6.21}$$

Several algorithms exist for calculation of the vector of **w** values. Using the *mean square error* (MSE) method, where weights are set to minimize ε, the error signal as illustrated in Figure 6.10 is

$$\varepsilon = E\left[\left|b(t) - \mathbf{w}^T \mathbf{x}(t)\right|^2\right] \tag{6.22}$$

The training sequence $b(t)$ can then be used to iteratively update the weighting factors in order to minimize the error signal. The optimal weighting factor for minimizing the error can be shown to be equal to

$$\mathbf{w}_{\text{opt}} = R_{xx}^{-1} r_{xd} \tag{6.23}$$

where $R_{xx} = E[\mathbf{x}^*(t)\mathbf{x}^T(t)]$ is the autocorrelation value of the received signal, and $r_{xx} = [\mathbf{x}^*(t)\mathbf{d}(t)]$ is the cross-correlation with the training sequence, and $\mathbf{x}^*(t)$ is the complex conjugate value of $\mathbf{x}(t)$. The training sequence needs to be periodically inserted in the transmitted signal in order for the weight controls to be updated and the desired performance maintained [16].

The performance of adaptive array antennas has been reported on in many papers and books. They operate to reduce the total amount of interference experienced by a desired signal. The gain of an adaptive array antenna

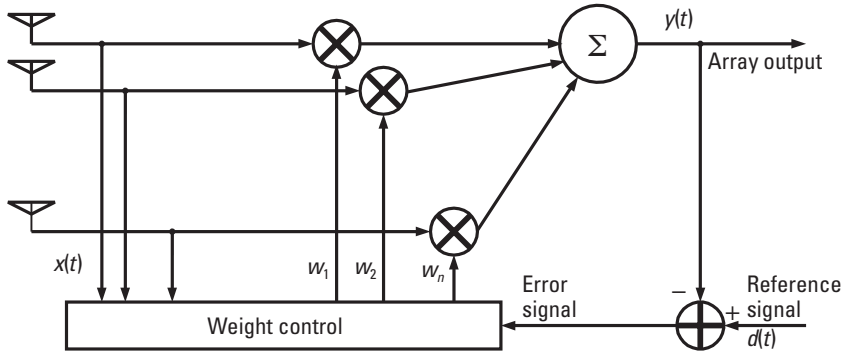

Figure 6.10 Weight factor control based on training signals. (*Source:* [16], ©1998 IEICE.)

system, g_{AA} results in reducing the denominator interference terms in (6.5) by the gain factor, resulting in

$$\varphi_{0,k} = \frac{1}{\dfrac{(1+F_{ul})(K-1)}{g_{AA}} + \phi\dfrac{\eta}{p_{0,k}g_{0,k}}} \tag{6.24}$$

Adaptive array antennas have been implemented for the BSs and, therefore, improve the performance of the uplink. It is not easy to implement array antennas in the mobile and therefore the downlink gains cannot be realized.

In TDD systems, however, it is possible to implement downlink waveforming based on the uplink channel estimate. The operation is illustrated in Figure 6.11. Here the same weighting parameter matrix **w** is used to shape the waveforms for the downlink transmission [17]. The effectiveness of this technique is again a function of the accuracy of the estimates and the fading frequency.

The increase in capacity of a CDMA system can be calculated in a manner similar to that of (6.24) from (6.7):

$$\gamma_{0,k} = \frac{P_{0,k}g_{0,k}}{\dfrac{\alpha_{dl}\left(P_0 - P_{0,k} - P_C\right)g_{0,k} + P_C g_{0,k} + F_{dl}P_0 g_{0,k}}{g_{AA}} + \phi P_{0,k}g_{0,k} + \eta} \tag{6.25}$$

resulting in reduced interference and as a result increased capacity.

6.5 Multiuser Detection

Yet another method of increasing the SIR in (6.2) and (6.5) is to calculate and subtract the interference from the denominator. *Multiuser detection* (MUD) is the method of detecting the received signal from multiple users, and in the process minimizing the multiuser interference from the received signals and thereby increasing SIR. Several MUD methods exist, and most of them are equally applicable to FDD- and TDD-CDMA. These methods, however, are very processing intensive. In particular, the most effective methods need processing power that increases exponentially with respect to the number of users being processed. For this reason, no such system has yet

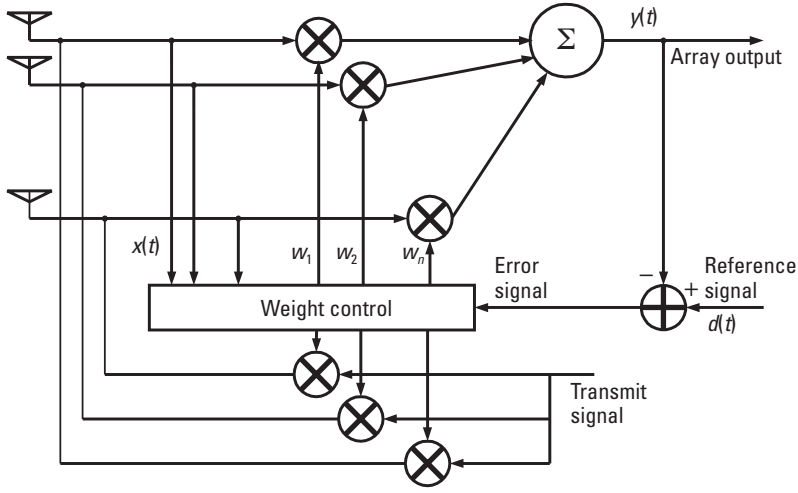

Figure 6.11 Adaptive antennas in TDD-CDMA.

been implemented for the FDD-CDMA systems. Moreover, most MUD methods are more easily implemented in BSs and thereby improve the performance of the uplink. However, the downlink is the limiting side for capacity and, therefore, these methods are not particularly useful. Two factors in TDD systems help to realize MUD: There are fewer users of the 3G TD-CDMA standard, which helps reduce the complexity of the receiver; and predistortion transmission, a form of interference minimization, can be implemented in the BS for the benefit of the downlink and, therefore, be useful in increasing whole system capacity.

In this section, we give a summary of MUD techniques, and then define the methods used for TDD systems. In general, MUD techniques are classified into two groups. One is joint detection, whereby a receiver detects the received signals from multiple users, while maximizing the individual users' received SIR. The other is *interference cancellation* (IC), in which individual users' signals are detected and removed from the total received signal in successive stages, where in each stage the SIR for all signals is increased. We first address the IC techniques, and then discuss the joint detection and joint predistortion techniques.

6.5.1 Uplink Interference Cancellation

IC is the method whereby the multiuser interference is reduced by iteratively calculating and cancelling the signals of all users received at a BS. This

method is generally useful for implementing in the uplink and at the BS. The signal of each user is detected, remodulated, and reduced from the total received signal. As all users' signals go through the same process, the total interference is reduced, and the SIR improves.

IC methods are also processing intensive, so they have yet to be implemented in FDD-CDMA BSs. However, the TD-CDMA method lowers the number of users in each interval, and thereby makes it possible to implement IC. The results of such an implementation have been reported for the TD-CDMA system in [18].

Several IC techniques have been reported on in the literature, a recent survey of which can be found in [19]. These methods are equally applicable to the FDD and TDD modes of CDMA.

6.5.2 Uplink Joint Detection

One method that can particularly benefit from the TDD mode of CDMA communication is the joint detection technique known as decorrelation. For a simple one-path system, the vector of received signal from K users at the base station may be written in matrix format as shown below. The matrix and vector notation combine the signals, which are received from all users in the system.

$$\mathbf{y} = \mathbf{XHd} + \mathbf{n} \tag{6.26}$$

where $\mathbf{X}$ is the users' spreading code matrix of size $K \times 1$, $\mathbf{H}$ is the diagonal matrix of channel impulse response of size $K \times K$, $\mathbf{d}$ is the transmitted data vector of size $1 \times K$, and $\mathbf{n}$ is the noise vector of size $K \times 1$. After a matched filter despreading, the received signal form all users can be expressed as follows:

$$\mathbf{Z} = \mathbf{S}^T \mathbf{y} = \mathbf{S}^T \mathbf{XHd} + \mathbf{S}^T \mathbf{n} = \mathbf{RHd} + \mathbf{S}^T \mathbf{n} \tag{6.27}$$

where $\mathbf{R}$ is the $K \times K$ size correlation matrix between the spreading code of the mobile users connected to the BS.

A decorrelator receiver (Figure 6.12) calculates the matrix $\mathbf{R}^{-1}$, the inverse of the correlation matrix. The product of the inverse matrix and the despread signal decorrelates all multiuser interference and yields an interference-free received vector $\hat{\mathbf{d}}$:

$$\hat{\mathbf{d}} = \mathbf{R}^{-1}\mathbf{Z} - \mathbf{Hd} + \mathbf{R}^{-1}\mathbf{S}^T \mathbf{n} \tag{6.28}$$

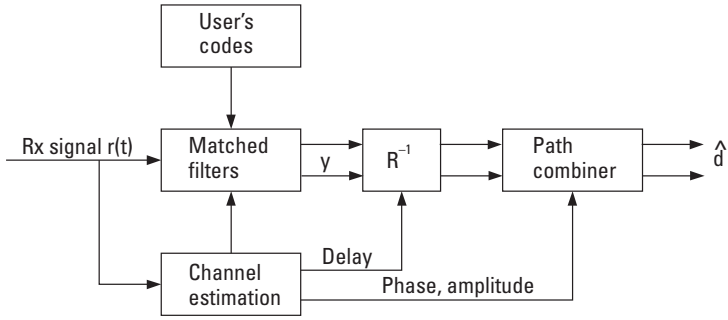

Figure 6.12 The operation of a decorrelating detector.

The symbol detection is now only affected by noise. The BS can also detect the signal of all users connected to it simultaneously. However, the power of noise is considerably increased through the right-hand-side multiplication. In addition, the calculation of the matrix $\mathbf{R}^{-1}$ is very processing intensive.

A variant of the decorrelating detector is the *zero-forcing block linear equalizer* [20], where now the interference source is defined as the convolution of the transmitted signal and the corresponding channel impulse response. Let us define

$$\underline{d}^{(k)} = \left(\underline{d}_1^{(k)}, ..., \underline{d}_N^{(k)}\right)^T \tag{6.29}$$

where $k = 1, ..., K$, as the kth user's vector of N symbols for one data block to be transmitted. Combining all user data into one vector,

$$\underline{d} = \left(\underline{d}^{(1)T}, ..., \underline{d}^{(K)T}\right)^T = \left(\underline{d}_1, ..., \underline{d}_{K \cdot N}\right)^T \tag{6.30}$$

Each user is spread using a spreading code of $\underline{c}^{(k)} = (\underline{c}_1^{(k)}, ..., \underline{c}_M^{(k)})^T$ of length M chips. The signal is then transmitted over the transmission channel's impulse response, $\underline{h}^{(k)} = (\underline{h}_1^{(k)}, ..., \underline{h}_W^{(k)})^T$, of length W samples taken at each chip interval. The combined effect of the channel and spreading for user k is found by the convolution of the transmitted signal with the channel impulse response as

$$\underline{b}^{(k)} = \underline{c}^{(k)} * \underline{h}^{(k)} = \left(\underline{b}_1^{(k)}, ..., \underline{b}_{M+W-1}^{(k)}\right)^T \tag{6.31}$$

The combination of $\underline{b}^{(k)}$ for all user data sequences is arranged in a matrix $\underline{A} = (\underline{A}_{ij})$, $i = 1, \ldots, N \cdot M + W - 1$, $j = 1, \ldots, K \cdot N$, as illustrated in Figure 6.13. The received signal at the estimator can be written

$$\underline{e} = \underline{A} \cdot \underline{d} + \underline{n} \tag{6.32}$$

where $\underline{n}$ is a noise term of length $N \cdot M + W - 1$ with a zero mean and variance of $R_n = E(\underline{n} \cdot \underline{n}^{*T}) = \sigma^2 I$, where I is the identity matrix, defined by

$$\underline{n} = \left(\underline{n}_1, \ldots, \underline{n}_{N \cdot M + W - 1}\right)^T \tag{6.33}$$

Klein, Kaleh, and Baier [21] have shown that the linear unbiased estimator should take the form of $(\underline{A}^{*T} \cdot \underline{A})^{-1} \cdot \underline{A}^{*T}$. The output of the estimator will then be

$$\hat{\underline{d}} = \left(\underline{A}^{*T} \cdot \underline{A}\right)^{-1} \cdot \underline{A}^{*T} \cdot \underline{A} \cdot \underline{d} + \left(\underline{A}^{*T} \cdot \underline{A}\right)^{-1} \cdot \underline{A}^{*T} \cdot \underline{n} \tag{6.34}$$

Note this output is free from all multiuser interference. Other joint detection techniques have also been proposed, which aim to remove the multiuser interference without increasing the noise part of (6.34). For a comprehensive survey, see [21].

The uplink SIR may therefore be significantly improved if the intracell multiuser interference can be totally removed. This will modify (6.5) as follows:

$$\phi_{0,k} = \frac{1}{(K-1)F_{ul} + \phi + \dfrac{\eta}{p_{0,k} g_{0,k}}} \tag{6.35}$$

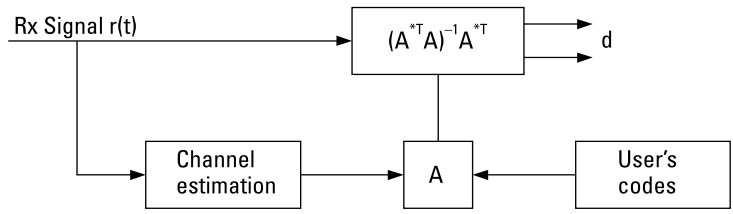

Figure 6.13 Zero forcing block linear equalizer.

TEAM FLY

Team-Fly®

6.5.3 Downlink Joint Predistortion

In the TDD system, all parameters of the $\underline{A}$ matrix are known at the transmitter. Therefore, it is possible to shape the signal to be transmitted in a way that the effect of interference from signals intended for other users can be totally removed. Several such methods have been proposed. An early proposal from Bosch regarding ETSI UMTS standardization is as follows [22]:

Using the same notation as the block linear equalizer, the kth user's code matrix of $N \cdot M$ rows and N columns can be written

$$C^{(k)} = \begin{pmatrix} \underline{c}^{(k)} & 0 & 0 \\ 0 & \ddots & 0 \\ 0 & 0 & \underline{c}^{(k)} \end{pmatrix} \tag{6.36}$$

The kth user's spread data can be written

$$C^{(k)} \cdot \underline{d}^{(k)} \tag{6.37}$$

The entire spread signal for transmission to all mobiles can be then written as

$$C \cdot \underline{d}^{T} \tag{6.38}$$

where

$$C = \begin{pmatrix} C^{(1)} & 0 & 0 \\ 0 & \ddots & 0 \\ 0 & 0 & C^{(K)} \end{pmatrix} \tag{6.39}$$

These signals are then shaped, or predistorted, by a matrix P and then summed up to one antenna signal by matrix D of $N \cdot M$ rows and $N \cdot M \cdot K$ columns:

$$D = \begin{pmatrix} 1 & 0 & 0 & 1 & 0 & 0 & \cdots \\ 0 & \ddots & 0 & 0 & \ddots & 0 & \cdots \\ 0 & 0 & 1 & 0 & 0 & 1 & \cdots \end{pmatrix} \tag{6.40}$$

resulting in the transmitted signal being

$$D \cdot P \cdot C \cdot \underline{d}^{T} \tag{6.41}$$

The received signal at user k is the convolution of (6.41) with the kth channel impulse response; $\underline{h}^{(k)}$ can be formulated as multiplication with the matrix $H^{(k)}$ ($N \cdot M + W - 1$ rows and $N \cdot M$ columns):

$$H^{(k)} = \begin{pmatrix} h_1^{(k)} & \cdots & 0 \\ \vdots & \ddots & \vdots \\ h_W^{(k)} & \vdots & h_1^{(k)} \\ \vdots & \ddots & \vdots \\ 0 & \cdots & h_W^{(k)} \end{pmatrix} \tag{6.42}$$

With the kth channel's additive noise $\underline{n}^{(k)}$, the kth receiver signal can be written

$$s^{(k)^T} = H^{(k)} \cdot D \cdot P \cdot C \cdot \underline{d} + \underline{n}^{(k)} \tag{6.43}$$

This signal can be detected using one rake finger only represented by matrix $R^{(k)}$ of $N \cdot M + W - 1$ rows and N columns:

$$R^{(k)} = \begin{pmatrix} 0 & 0 & 0 \\ \vdots & \vdots & \vdots \\ 0 & & \\ \underline{c}^{(k)} & 0 & \\ 0 & \ddots & 0 \\ 0 & 0 & \underline{c}^{(k)} \end{pmatrix} \tag{6.44}$$

To get the kth estimated data vector

$$\hat{\underline{d}}^{(k)} = R^{(k)*T} \cdot \underline{s}^{(k)^T} \tag{6.45}$$

Combining all users' rake and channel matrices as follows:

$$R = \begin{pmatrix} R^{(1)} & 0 & 0 \\ 0 & \ddots & 0 \\ 0 & 0 & R^{(K)} \end{pmatrix} \tag{6.46}$$

and

$$H = \begin{pmatrix} H^{(1)} & 0 & 0 \\ 0 & \ddots & 0 \\ 0 & 0 & H^{(K)} \end{pmatrix} \tag{6.47}$$

the vector of all estimated users' data becomes

$$\hat{\underline{d}}^{T} = R^{H} \cdot H \cdot D^{T} \cdot D \cdot P \cdot C \cdot \underline{d} + R^{H} \cdot \underline{n} \tag{6.48}$$

Reference [22] has shown that if matrix P is chosen as

$$\begin{aligned} P = &\left(R^{*T} \cdot H \cdot D^{T} \cdot D\right)^{*T} \cdot \left[\left(R^{*T} \cdot H \cdot D^{T} \cdot D\right) \cdot \right. \\ &\left. \left(R^{*T} \cdot H \cdot D^{T} \cdot D\right)^{*T}\right]^{-1} \cdot \underline{d} \times \frac{1}{\left\|C \cdot \underline{d}\right\|^{2}} \cdot \left(C \cdot \underline{d}\right)^{*T} \end{aligned} \tag{6.49}$$

the given choice results in

$$\hat{\underline{d}} = \underline{d} + R^{H} \cdot \underline{n} \tag{6.50}$$

yielding a multiuser interference-free data estimate.

Further work in combining adaptive array antennas and several other joint predistortion or joint transmission methods has been reported that follows the same principle.

In the case of perfect joint predistortion, intracell interference can be totally removed. This will result in an increase of the SIR at mobile receivers and will modify (6.2) as follows:

$$\gamma_{0,k} = \frac{P_{0,k} g_{0,k}}{F_{dl} P_{0} g_{0,k} + \eta} \tag{6.51}$$

significantly improving the SIR.

6.6 Summary

In this chapter we discussed several methods exclusive to the TDD mode of CDMA that can improve system performance by taking advantage of the reciprocity of the TDD operation.

References

[1] Viterbi, A. J., *CDMA: Principles of Spread Spectrum Communication,* Reading, MA: Addison-Wesley, 1995.

[2] Holma, H., and A. Toskala (eds.), *WCDMA for UMTS,* rev. ed., New York: Wiley, 2001, pp. 194–195.

[3] Hiltunen, K., and R. de Bernardi, "WCDMA Downlink Capacity Estimation," *Proc. of Vehicular Technology Conference,* Tokyo, Japan, 2000, Vol. 2, pp. 992–996.

[4] Viterbi, A. M., and A. J. Viterbi, "Erlang Capacity of a Power Controlled CDMA System," *IEEE Journal Selected Areas in Communications,* Vol. 11, No. 6, August 1993, pp. 892–900.

[5] Lyu, D., H. Suda, and F. Adachi, "Capacity Evaluation of a Forward Link DS-CDMA Cellular System with Fast TPC Based on SIR," *IEICE Trans. on Commun.,* Vol. E83-B, No. 1, January 2000, pp. 68–76.

[6] Sipila, K., et al., "Estimation of Capacity and Required Transmission Power of WCDMA Downlink Based on a Downlink Pole Equation," *Proc. of Vehicular Technology Conference,* Tokyo, Japan, 2000, Vol. 2, pp. 1002–1005.

[7] Choi, W., et al., "Forward Link Erlang Capacity of 3G CDMA System," *IEE 2000 3G Mobile Communication Technologies Conference Publication,* pp. 213–217.

[8] Adachi, F., M. Sawahashi, and K. Okawa, "Tree-Structured Generation of Orthogonal Spreading Codes with Different Lengths for Forward Link of DS-CDMA Mobile," *Electron. Lett.,* Vol. 33, No. 1, 1997, pp. 27–28.

[9] Omura, J. K., and P. T. Yang, "Spread Spectrum S-CDMA for Personal Communication Services," *Proc. IEEE Milcom 1992,* San Diego, CA, pp. 269–273.

[10] Bottomley, G. E., "Signature Sequence Selection in a CDMA System with Orthogonal Coding," *IEEE Trans. on Vehicular Technology,* Vol. 42, February 1993, pp. 62–68.

[11] Schotten, H. D., and M. Antweiler, "Iterative Construction of Sequences with Low Cross-Correlation Values," *Proc. IEEE ICC '93,* Geneva, Switzerland, pp. 156–160.

[12] DaSilva, V. M., and E. S. Sousa, "Multi-Carrier Orthogonal CDMA Signals for Quasi-Synchronous Communication Systems," *IEEE Journal Selected Areas in Communications,* Vol. **12,** No. **5,** June 1994, pp. 842–852.

[13] Sourour, E., and M. Nakagawa, *Performance of Multi-Carrier CDMA in a Multipath Fading Channel*, IEICE Technical Report, Tokyo, Japan, March 1994.

[14] Sasaki, S., and G. Marubayashi, *A Proposal of Spread Spectrum Parallel Data Communication System and a Note of Autocorrelation Properties of Gold Sequence*, IEICE Technical Report, Tokyo, Japan, August 4–5, 1989.

[15] Esmailzadeh, R., and M. Nakagawa, "Quasi-Synchronous Time Division Duplex CDMA," *IEICE Trans. on Fundamentals of Elec. Commun.,* Vol. E78.A, No. 9, September 1995, pp. 1201–1205.

[16] Ohgane, T., and Y. Ogawa, "Adaptive Array for Mobile Radio," *IEICE Magazine,* Vol. 81, No. 12, 1998, pp. 1254–1260.

[17] Higashinaka, M., T. Ohgane, and Y. Ogawa, *A Downlink Multiplexing Method in TDD Packet Radio Networks with a Multibeam Adaptive Array*, IEICE Technical Report RCS 2000–234, pp. 87–93 (in Japanese).

[18] Cusani, R., M. Di Felice, and J. Matilla, "A Simple Bayesian Multistage Interference Canceller for Multiuser Detection in TDD-CDMA Receivers," *IEEE Trans. on Vehicular Technology,* Vol. 50, No. 4, July 2001, pp. 920–924.

[19] Moshaui, S., "Multi-User Detection for DS-CDMA Communications," *IEEE Comm. Magazine*, October 1996, pp. 124–136.

[20] Klein, A., and P. W. Baier, "Linear Unbiased Data Estimation in Mobile Radio Systems Applying CDMA," *IEEE Journal Selected Areas in Communications,* Vol. 11, No. 7, September 1993, pp. 1058–1066.

[21] Klein, A., G. K. Kaleh, and P. W. Baier, "Zero Forcing and Minimum Mean-Square-Error Equalization for Multiuser Detection in Code-Division Multiple-Access Channels," *IEEE Trans. on Vehicular Technology,* Vol. 45, 1996, pp. 276–287.

[22] "Joint Pre-Distortion; A Proposal to Allow for Low Cost UMTS TDD Mode Terminal," TDOC SMG 2 UMTS-L1, 82/98.

7

TDD-Based CDMA Standards for Public Systems

This chapter describes the TDD mode of third-generation CDMA communication signals. These are global standards to make possible the realization of an ubiquitous system for international roaming. We first give a brief history of the standardization processes that began in the early 1990s and are now being realized in working systems. We then describe the *time division* (TD)-CDMA systems of the 3GPP standards, followed by the *time division synchronous CDMA* (TD-SCDMA) system standardized (under the umbrella of 3GPP) by the China Wireless Telecommunication Standard (CWTS) body, which are both based on TDD-CDMA.

7.1 Historical Background

The standardization process that has led to the *third-generation* mobile communication standards started well before the mobile communications boom of the late 1990s. In the early 1990s, the first-generation, analog FDMA-based mobile communication systems in Europe and Japan began to be phased out in favor of second-generation, digital TDMA-based mobile systems. Two standards were adapted in Japan. One was known as the *Personal Digital Cellular* (PDC) system, and was based on FDD-TDMA with wide coverage and efficient mobility management capability. The other was the PHS, which was based on TDD-TDMA, with higher transmission rates but

lower coverage and mobility functionality. Both systems were to become very popular, although PHS lost some of its popularity later.

IS-95 CDMA-based systems entered the Japanese market a few years later in the mid-1990s. In parallel, a pan-European standard dubbed *Global System for Mobile* (GSM) became popular and was widely adopted by European and many other countries. In the early 1990s, the North American countries adopted two digital communication standards. One was the TDMA-based systems, which used the legacy AMPS protocol as one of their operating modes. The other was the IS-95 CDMA-based system, which was compatible with the older AMPS systems in 850-MHz band deployments. These collectively came to be known as the second-generation mobile communications system.

Desiring higher data rates that could enable the use of multimedia services, a search for a new generation of mobile communications system got under way in Japan in 1993–1994 under the auspices of the Association of Radio Industry and Business (ARIB). Early on, it was decided that these standards must be globally developed to allow for seamless international roaming. This would open the large global market such that manufacturers could benefit from economies of scale. Therefore, as early as 1995, major European and North American manufacturers and operators joined the Japanese standardization activities. Parallel activities started in Europe at the European Telecommunication Standards Institute (ETSI), in the United States by means of the T1 part of ATIS, and in Korea at the Telecommunication Technologies Association (TTA).

Originally dubbed the Future Public Land Mobile Telecommunications System (FPLMTS), these activities first concentrated on deciding which technology could provide the best efficiency and user capacity. A consensus emerged that these systems should be based on the CDMA technology. Early on, a comparison between the TDD and FDD modes showed that although TDD offered relatively larger user capacity (see [1–5] for performance comparison), it was not suitable for large cells since the need for finite guard times limited the cell size. However, it was recognized that TDD-based systems would complement the FDD-based ones in small, perhaps indoor, cells with larger transmission rates and lower power consumptions. The two environments are likely to have different types of traffic: Indoor users are more likely to use highly asymmetric, high-data-rate applications requiring less mobility than outdoor users who will be mobile and use slower and more symmetric applications. Two standardization tracks in ARIB and ETSI dealt separately with these two modes of CDMA.

By 1997, an FDD-CDMA-based experimental system, based on an early version of the standard, was commissioned by two Japanese operators, NTT DoCoMo and Japan Telecom. NTT DoCoMo also commissioned a TDD-based system from Matsushita Electric Inc. Some test results based on this test system are given later. The TDD standardization efforts at ARIB were largely led by Matsushita, whereas at ETSI Siemens was the major supporter. The North American markets have retained their dual characteristics. The TDMA protocols (IS-136) are converging with the ETSI path to the third generation (WCDMA), and the CDMA (IS-95) protocols are following their own path to 3G.

The global standardization activities were aligned under ITU auspices in 1997, and a name change was in order. The activities were named International Mobile Telecommunications 2000 (IMT-2000), with 2000 referring both to the time frame (2000) when the first systems were to come into service and to the frequency band where they were to be deployed (around 2,000 MHz). Further changes in the name have since resulted and these standards are also known as Universal Mobile Telecommunications Services (UMTS) and third generation. The standards activities are now divided into two groups, the *third-generation partnership program* (3GPP), which is based on the WCDMA technology, and 3GPP2, which derives from the IS-95 standards also known as CDMA2000. The two different groups exist to protect the investments in the legacy second-generation systems as well as to account for some incompatibilities in the core networks.

The TDD-CDMA system within the 3GPP activities is now harmonized with ARIB and ETSI under a hybrid TDMA and CDMA configuration referred to as TD-CDMA. In 1997, TDD standardization activities were joined by a proposal from the Chinese body, China Wireless Telecommunication Standard (CWTS). Although largely similar to the TD-CDMA system, it has a synchronous uplink configuration and is known as TD-SCDMA.

In June 1999, a harmonized approach was accepted between 3GPP and 3GPP2 on three modes of operation: an FDD-CDMA system and a TDD-CDMA system from the 3GPP, and a multicarrier FDD-CDMA system derived from IS-95 from the 3GPP2.

In the next section the TD-CDMA standard layers 1, 2, and 3 are described. The name indicates the fact that a time-division multiplexing component is also used in the system. We will then describe TD-SCDMA. The letter S indicates the fact that the uplink is also synchronous.

7.2 TD-CDMA Standard

TDD-based TD-CDMA is very similar to the FDD-based WCDMA system in all of its higher level functionalities. The major differences are confined to the physical layer, where TD-CDMA combines TDMA and CDMA elements. This is illustrated in Figure 7.1. In TD-CDMA transmission and reception is confined/scheduled to a subset of all users in a cell at any particular time.

The TDD-based CDMA system of the UMTS standards, TD-CDMA, is based on a structure common to that of the FDD mode. The architecture is shown in Figure 7.2. It consists of a *core network* (CN), the UMTS Terrestrial Radio Access Network (UTRAN), and the mobile unit, which is known as *user equipment* (UE). Two interfaces are defined: the Iu interface between the core network and the UTRAN, and the Uu interface between the UTRAN and the UE [6–9]. The UTRAN consists of *radio network subsystems* (RNS), which include a *radio network controller* (RNC) and several BSs, which in UTRAN are referred to as node B. An RNC controls communications to and from several base stations (node Bs). RNCs interface several node Bs to the CN and handle soft handover and radio resource allocation among other functions.

The communication between RNSs (or RNCs) is carried over an Iur interface, and between RNC and node B over an Iub interface. All backbone traffic is carried over an IP network, including all Iu, Iur, and Iub interface traffic. The IP network is based on an ATM network with an AAL2 or an AAL5 topology. The UTRAN architecture is common to both FDD and TDD modes. The only difference is in the physical layer and air interface, or Uu.

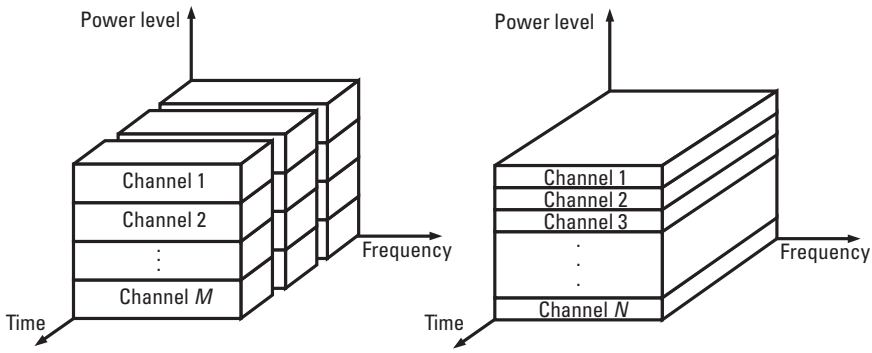

Figure 7.1 TDD and FDD modes of the 3GPP standard.

Team-Fly®

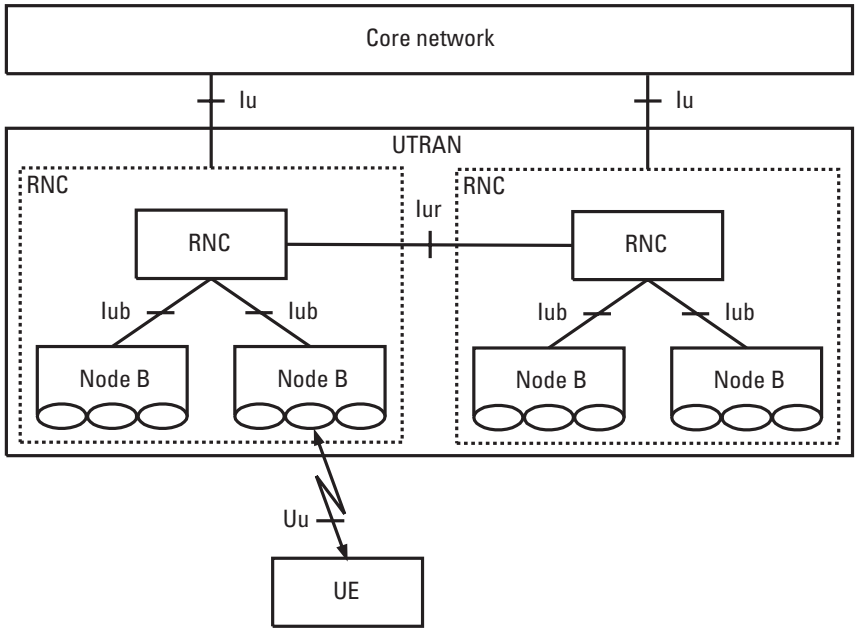

Figure 7.2 TD-CDMA system architecture. (© 2001 3GPP.)

The radio interface protocol architecture is partitioned into three layers: the physical layer, the data link layer, and the radio resource control layer (layers 1, 2, and 3, respectively) as shown in Figure 7.3.

7.2.1 Layer 3: Radio Resource Control

All control plane signaling between UTRAN and UE is handled through this layer. Further, assignment of radio resources, such as channel assignments, reconfiguration of connection specifics, and release of radio resources, is handled through this layer. It further controls and monitors the delivery of requested and assigned QoS. Other functions include dynamic channel assignment, control of the outer loop power control through signal to interference target settings, and timing advance for TDD slots.

7.2.2 Layer 2: Data Link Layer

This layer transports traffic from layer 3 to the physical layer, controlling functions such as streaming, scheduling, buffering, QoS management, and so forth. The data link layer is subdivided into four sublayers. Two of them

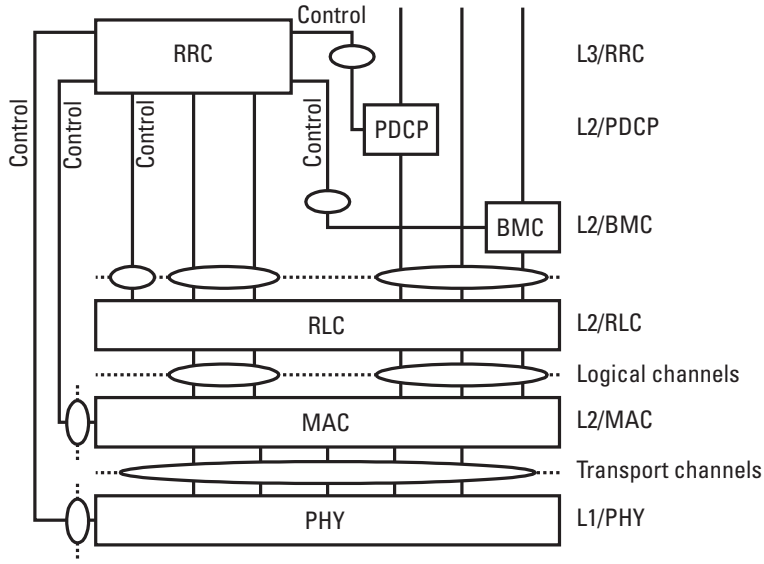

Figure 7.3 UTRAN radio interface protocol architecture. (© 2001 3GPP.)

are the *medium access control* (MAC) toward the physical layer, and the *radio link control* (RLC) toward the upper layers. Two others perform specialized functions: *broadcast/multicast control* (BMC) and *packet data convergence protocol* (PDCP). These are all further described below, but for a more detailed definition, the reader is referred to [7] and the 3GPPP standards. Traffic transport involves the radio resource control layer for configuration of dedicated channels and the RLC and MAC layer protocols. The two other sublayers (BMC and PDCP) are required for broadcast functions and IP header compression.

Data flow through layer 2 as illustrated in Figure 7.4. Voice transmission through the RLC and MAC layers is rather transparent and does not require much functionality from these layers. Layer 2 functionality for nontransparent (mainly nonvoice) information flow is shown. Here higher layer *protocol data units* (PDUs) are passed to the RLC layer, where data intended for one or more UEs is packetized into *service data units* (SDUs). Each packet may contain several different data streams. An RLC header is added and the SDU is passed to the MAC layer. At the MAC layer, a header containing routing information or logical channel mapping is added, and the resulting *transport block* (TrBK) or MAC PDU is passed to the physical layer. The CRC function is applied at this stage and the

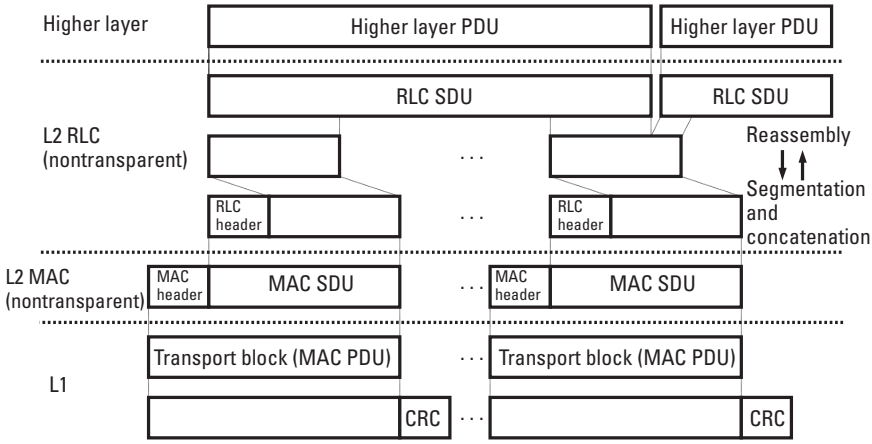

Figure 7.4 Data flow through RLC and MAC layers. (© 2001 3GPP.)

packet is passed to the physical layer as a TrBK with CRC. The IP headers are compressed at this stage to remove much redundancy.

7.2.2.1 Medium Access Protocol

The MAC layer maps the logical channels carried from the physical layer into the transport channels and the other way around. Logical channels are classified as either control channels or traffic channels. Logical control channels are used for the transfer of control plane information. A list of all of these channels is given in Table 7.1. The names are definitive, and summarize control functions for handset registration, call setup and maintenance (power control, soft handover), and so forth.

Table 7.1
Logical Control Channels

Synchronization control channel (SCCH)
Broadcast control channel (BCCH)
Paging control channel (PCCH)
Dedicated control channel (DCCH)
Common control channel (CCCH)
Shared control channel (SHCCH)

Logical traffic channels are also used for the transfer of user information. A list of these channels is given in Table 7.2. These channels are used for sending or receiving information to one or a group of UEs. More detailed information can be found in [7] and the 3GPP specifications.

These logical channels are mapped onto transport channels. These channels format the information from the logical channel into frames and packets suitable for physical transmission. Transport channels have a specific format, and several such channels can be combined to suit the parameters of the physical channels. Two types of transport channels exist: Common transport channels are used by more than one UE, and dedicated transport channels are assigned to one UE. A list of common transport channels is given in Table 7.3 and a list of dedicated transport channels in Table 7.4.

Table 7.2
Logical Traffic Channels

Dedicated traffic channel (DTCH)
Common traffic channel (CTCH)

Table 7.3
Common Transport Channels

Random access channel (RACH)
Forward access channel (FACH)
Downlink shared channel (DSCH)
Uplink shared channel (USCH)
Broadcast channel (BCH)
Synchronization channel (SCH)
Paging channel (PCH)

Table 7.4
Logical Control Channels

Dedicated channel (DCH)
Fast uplink signaling channel (FAUSCH)

7.2.2.2 RLC

This layer controls the transfer of data between the MAC layer and higher layers. Data transfer is carried out in one of three modes: transparent, which tolerates little delay and is mainly intended for voice services and does not require much functionality from the RLC; acknowledged, which is for reliable data transfer such as e-mail and which requires *automatic repeat request* (ARQ) functionality; and unacknowledged mode, which does not require ARQ and is intended for services such as multimedia streaming. Other functions of RLC include ciphering for security.

7.2.2.3 PDCP

This layer performs the function of IP header compression for Internet protocols IPv4 and IPv6. Each IP packet header contains information that allows the receiver to receive and combine the payload of the packet with the payload of other IP packets. This is necessary for information transfer in a backbone network, where each packet may take a different route to its destination. However, in mobile communication, the information transfer is point to point, and most of the IP header information is redundant. This PDCP layer compresses the header that is passed to the physical layer, and decompresses the header it receives from physical layer.

7.2.2.4 Broadcast and Multicast Control

This layer carries out the function of cell broadcast and multicast. These transmissions are messages intended for more than one user, and are usually IP traffic.

7.2.3 Layer 1: Physical Layer

In the previous section we explained how a *transport block* (TrBk), or a MAC PDU, carries the information from layer 3 to the physical layer and vice versa. A CRC is also added/checked in layer 2. The transport block is mapped to *physical channels* (PhCH) as illustrated in Figure 7.5. Functions such as forward error correction, interleaving, and rate matching are performed at this stage. Each channel bearer carries one *transport channel* (TrCH), and is defined with a specific *transmission time interval* (TTI).

7.2.3.1 Channel Coding

Each TrBk is segmented or concatenated to obtain a suitable block size for FEC coding. FEC coding may or may not be applied depending on the type of TrBk. Some transmitted information is not sensitive enough to warrant

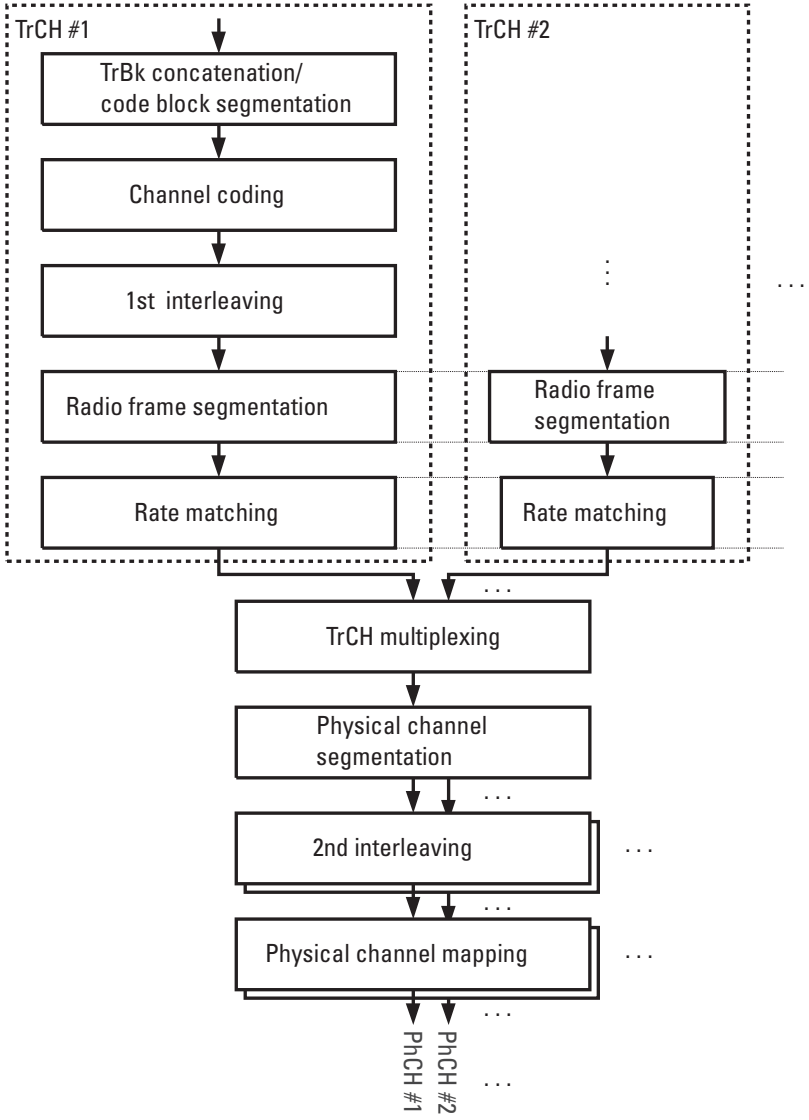

Figure 7.5 Mapping from MAC layer PDUs to physical channels. (© 2001 3GPP.)

additional FEC bits. An example is AMR voice codec output, which consists of three classes: A, B, and C. Usually Class C bits remain unprotected. Two types of FEC coding are standardized, convolutional coding with rates of 1/2 and 1/3, and turbo coding with a rate of 1/3. Service requirements such as

required bit error rates (BERs; usually 1E–3 for voice and 1E–6 for data transfer) and delay considerations determine the type of code to be used.

7.2.3.2 Interleaving

The interleaving function is carried out in order to randomize errors that occur because of the bursty fading nature of the transmission channel. This kind of fading causes errors to occur in bursts. Interleaving distributes these errors in time and helps the error correction function of the receiver.

In TD-CDMA standards, two interleaving stages are specified. The first stage is a block interleaver with intercolumn permutations. The input bits are read into a matrix. The number of columns in the matrix is determined by the type of the service and the length of the data frame (10, 20, 40, or 80 ms). The number of the rows is then determined from the size of the data block from the TrBk. The elements of the matrix are then permutated according to a function specified by the standards.

The second stage is also a block interleaver, again with intercolumn permutations. This second stage of interleaving applies to the bits within one frame, or separately within each time slot.

7.2.3.3 Radio Frame Segmentation

The encoded bit stream after interleaving is segmented into frame sizes. Both FDD and TDD modes of UTRA have frame sizes of 10 ms. Each frame is divided into 15 slots of 666 μs. As discussed before, in FDD all slots are for uplink or downlink traffic. The TD-CDMA slots in each frame are alternately allocated to uplink or downlink traffic. Slot allocation for uplink and downlink traffic is flexible and can be configured by the UTRAN. It can therefore be configured to allow for accommodating different uplink and downlink traffic capacity requirements. This is especially important for Internet traffic scenarios where it is expected that downlink traffic is much larger than the uplink. Several frame structures are illustrated in Figure 7.6. Radio frame segmentation will follow the number of slots available for the transmission.

Each slot consists of 2,560 chips, and has two data fields, a midamble, a coded power control bit (TPC), and two *transport format combination indicator* (TFCI) bits as shown in Figure 7.7. The TFCI is a unique feature of UTRA standards and acts as a pointer to a table of all possible combinations of transport formats. The TFCI field carries information on the spreading factor, FEC, repetition, and puncturing formats. The TFCI information for each 10 ms frame is spread equally over the slots. A (time) *guard period* (GP) exists at the end of each slot.

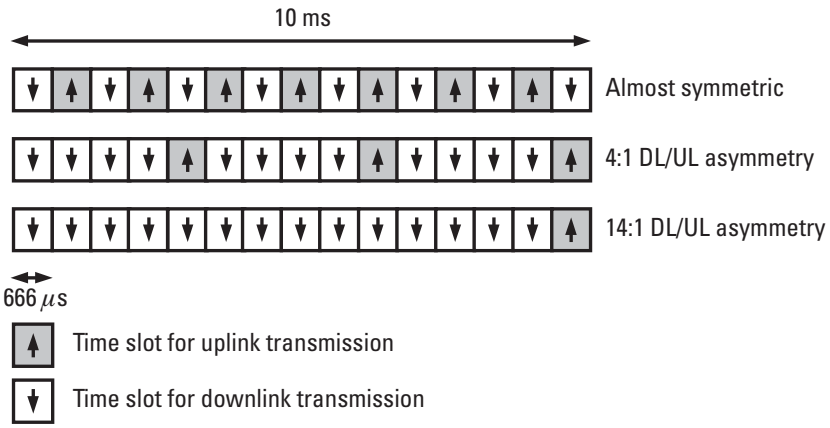

Figure 7.6 Uplink and downlink slot allocation scenarios, and slot structure. (© 2001 3GPP.)

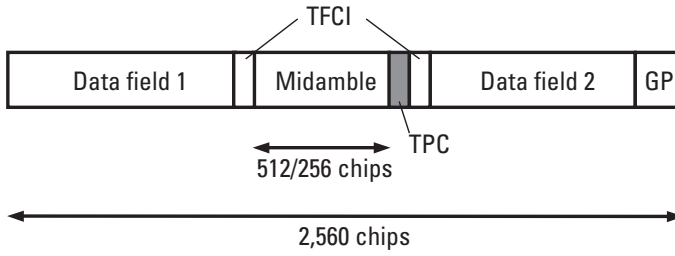

Figure 7.7 Slot structure, with TPC and TFCI fields. (© 2001 3GPP.)

Three possible types of slots exist, each type used for a particular group of physical channels. The number of chips per data field is listed in Table 7.5. Depending on the spreading factor these numbers correspond to symbol numbers.

7.2.3.4 Rate Matching

Through repeating or puncturing, the physical layer protocol ensures that all frames contain the correct number of bits. This ensures constant data burst length. Also, in cases when several bit streams with different quality requirements are transported, rate matching ensures that the required BER for each data segment within a TrBk is maintained. As discussed above, a TFCI field in each frame denotes a pointer to a table of all possible combinations for how several data streams may be combined in a TrCH.

Table 7.5
Field Length for Different Burst Types

Burst Type	Data 1	Data 2	Midamble	Guard Period
Type 1	976	976	512	96
Type 2	1,104	1,104	256	96
Type 3	976	880	512	192

7.2.3.5 Physical Channels

Physical channels are grouped into *dedicated physical channels* (DPCH) and *common physical channels* (CCPCH). A DPCH is used for carrying user data in the uplink and downlink from *dedicated transport channels* (DCH). User-dedicated information such TFCI and *transmission power control* (TPC) on the uplink are also transmitted on a DPCH as illustrated in Figure 7.7.

A *primary CCPCH* (P-CCPCH) is used for conveying the *broadcast transport channel* (BCH). A *secondary CCPCH* (S-CCPCH) is used for conveying messages from PCH and FACH. Two further common physical channels are the *page indicator channel* (PICH), which is used for transmitting paging information, and the *physical random access channel* (PRACH), which is used in the uplink for random access or to convey RACH.

7.2.3.6 Modulation and Spreading

Figure 7.8 shows how physical channels are transmitted over the air interface. The incoming bit stream is I/Q demultiplexed. The complex symbols

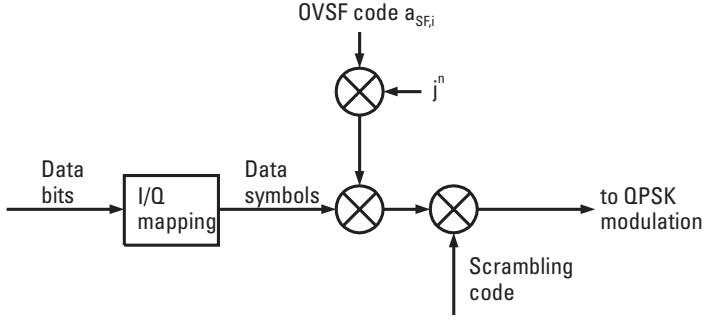

Figure 7.8 Modulation. (© 2001 3GPP.)

are then spread by a chip-wise complex rotation of a real *orthogonal variable spreading factor* (OVSF) code as shown in Figure 7.9. The *spreading factor* (SF) is a maximum of 16 in order to facilitate functions such as joint detection, as described in Chapter 6. A bode B specific scrambling code of length 16 is then applied in order to reduce mutual interference from neighboring cells. The resulting chip stream is then QPSK modulated. Further frequency up conversion is carried out before the signal is transmitted over the antenna. Table 7.6 summarizes the system parameters for the TD-CDMA system.

7.3 TD-SCMDA Standard

In parallel with ARIB and ETSI, the CWTS body has been developing a mobile communication standards system based on TDD-CDMA technology. Different from others, the new system has been specifically—and primarily—designed for TDD operation. Its physical layer specification is slightly different from that for a TD-CDMA system; it is designed to provide the following:

- *Synchronous CDMA:* Transmission is made synchronously in the uplink as well as in the downlink. Uplink synchronization is made possible through BS monitoring of signals from each mobile, and transmission timing adjustment feedback.

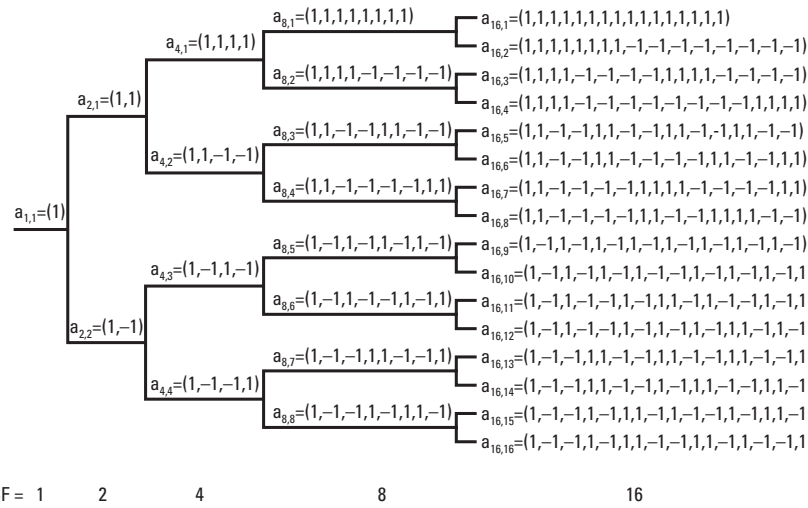

Figure 7.9 OVSF code structure. (© 2001 3GPP.)

Team-Fly®

Table 7.6
TD-CDMA Parameters

Chip rate	3.84 Mcps
Carrier spacing	5 MHz
Data modulation	QPSK
Spreading codes	OVSF orthogonal
Spreading rates	1, 2, 4, 8, and 16
Time slots per frame	15

- *Smart antennas:* BSs transmit and receive using adaptive array antennas.
- *Baton handover:* Enables faster and more reliable handover functioning, through accurate mobile positioning.

In an effort to merge the two modes, the TD-CDMA 3GPP standard has been modified to include a low-chip-rate mode of 1.28 Mcps, corresponding to the TD-SCDMA specification. In the following, we discuss the physical layer of the TD-SCDMA system, or the low-chip-rate part of the TD-CDMA standard.

7.3.1 Physical Layer

The physical layer of the low-chip-rate mode is somewhat different from high-chip-rate TD-CDMA. Table 7.7 shows the system parameters. Compared with Table 7.6, we can see that chip rate and carrier spacing are different. The number of slots per frame is also different. A lower chip rate

Table 7.7
System Parameters

Chip rate	1.28 Mcps
Carrier spacing	1.6 MHz
Data modulation	QPSK or 8 PSK (optional)
Spreading codes	OVSF orthogonal
Spreading rates	1, 2, 4, 8, and 16
Slots per frame	14

facilitates easier uplink synchronization and beam forming in the downlink and, therefore, improves performance.

In the low-chip-rate mode, transport channel multiplexing from the MAC layer to the physical layer channel mapping, shown in Figure 7.10, is similar to that of the high-chip-rate mode of Figure 7.5. The differences are (1) a radio frame equalization block is specified to ensure that the FEC coding output is the right size for interleaving block; and (2) a new subframe segmentation block after the second interleaver is specific to the low-chip-rate mode and its subframe structure.

7.3.2 Channel Coding

The two modes use similar forward error correction.

7.3.3 Interleaving

The interleaving function is carried out in order to spread the burst errors caused by a fading channel. This process enhances the performance of FEC schemes. Similar to the high-chip-rate mode, the span of spreading is 10, 20, 40, and 80 ms.

7.3.4 Radio Frame Segmentation and Rate Matching

The output bits of the first interleaver are divided into one-frame size segments of 10 ms long. Rate matching is carried out by repetition and puncturing to ensure that the total number of bits between different transmission time intervals is equal to the total channel bit rate of the allocated dedicated physical channels. The repletion/puncturing pattern information is contained in a TFCI field, which is transmitted in each frame (Figure 7.11).

7.3.5 TrCH Multiplexing

Bits from two or more streams can be combined and transmitted together over one or more *physical channels* (PhCHs).

7.3.6 PhCH and Subframe Segmentation

This function is used when more than one PhCH is utilized. The bit stream from the TrCH multiplexer is segmented into two or more streams, which are distributed among the different PhCHs to be used.

The output from this stage is further interleaved and then segmented into two subframes, which are then mapped to physical layer channels.

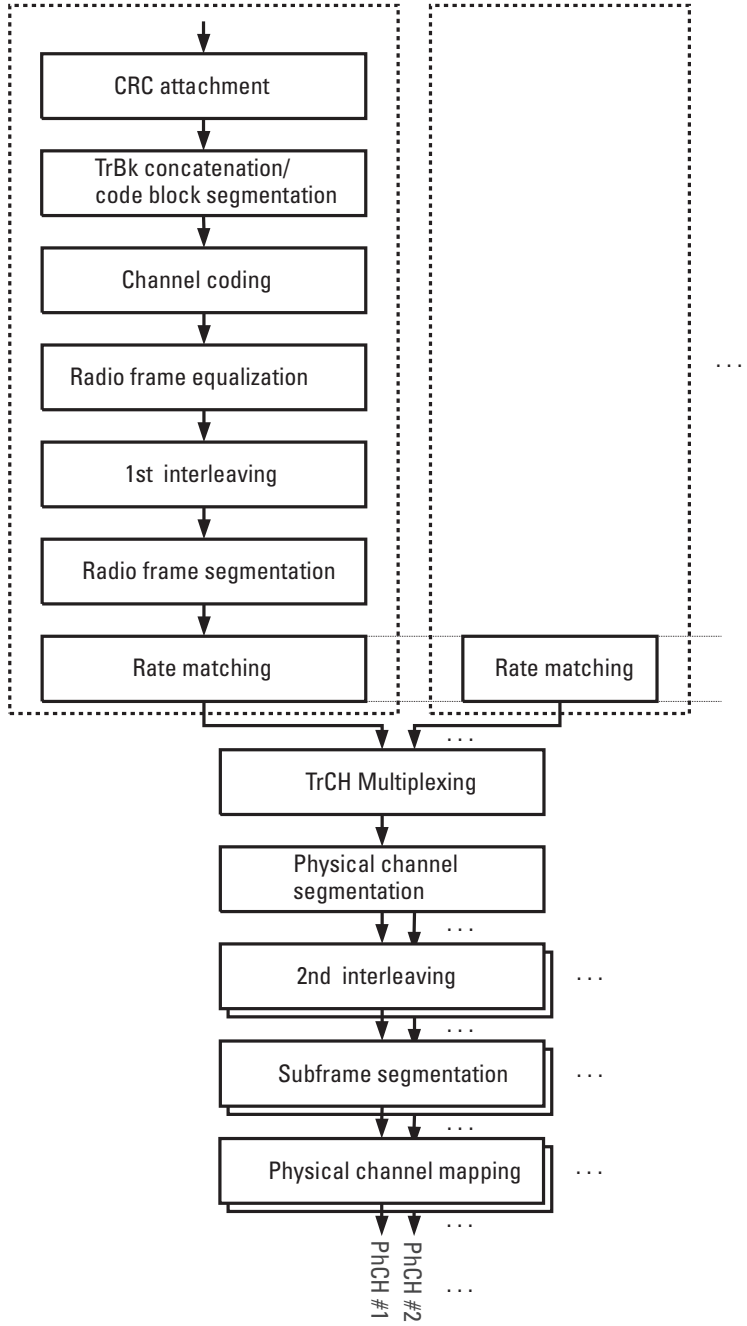

Figure 7.10 Transport channel multiplexing structure for TD-SCDMA. (© 2001 3GPP.)

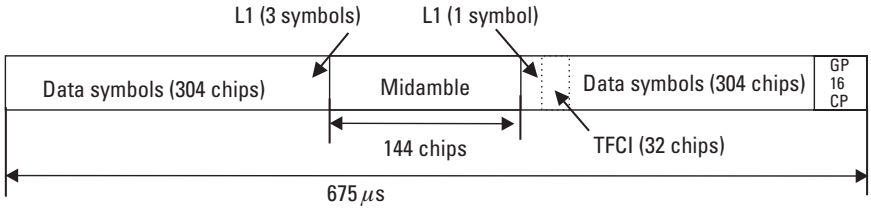

Figure 7.11 Frame structure with TFCI. (© 2001 3GPP.)

7.3.7 Frame and Slot Structure

The frame structure is shown in Figure 7.12. Each frame is 10 ms long, and consists of two equal subframes. Each subframe contains seven slots of 0.675 ms, and three special slots: DwPTS (downlink pilot), G (guard period), and UpPTS (uplink pilot). The special slots divide the frame for downlink and uplink transmissions. The slots before are used for downlink and those after for uplink. The number of slots assigned to the downlink and the uplink is variable and set by the system. Two configurations are illustrated in Figure 7.13.

Each slot will contain two data symbols of length 704 chips, a midamble of length 144 chips, and a guard period of 16 chips (Figure 7.14). The number of symbols depends on the spreading factor as indicated in Table 7.7.

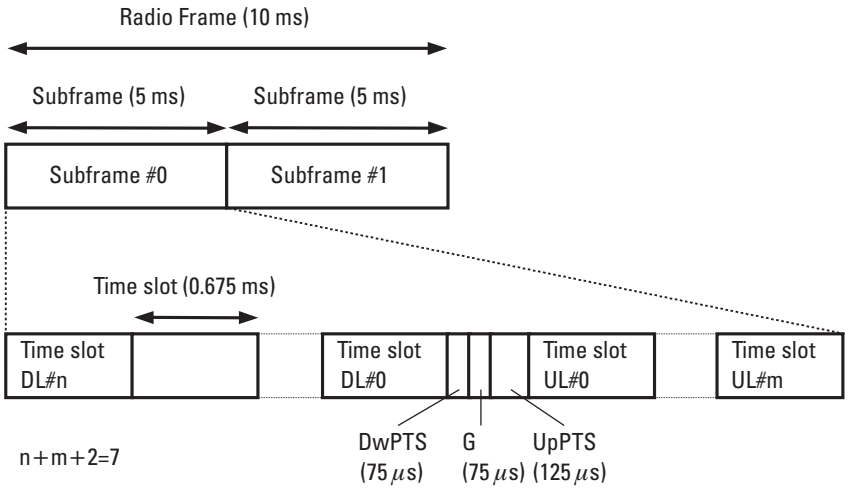

Figure 7.12 Frame structure. (© 2001 3GPP.)

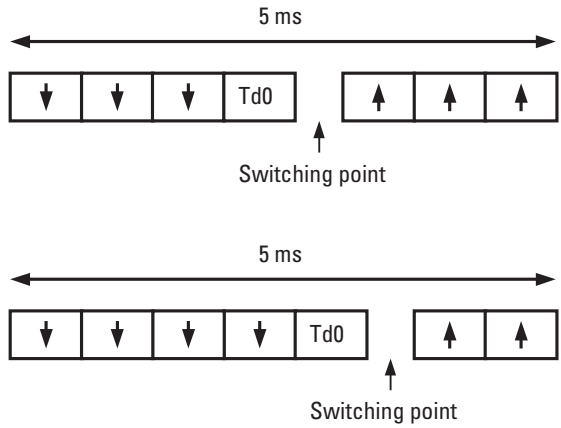

Figure 7.13 Slot configuration. (© 2001 3GPP.)

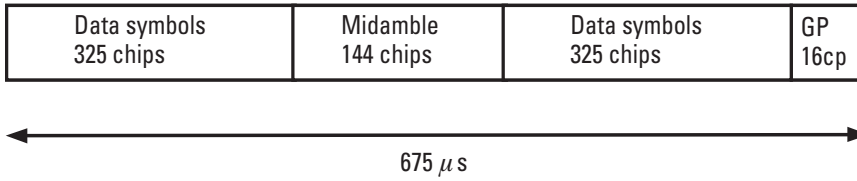

Figure 7.14 Slot structure. (© 2001 3GPP.)

7.3.8 Modulation and Spreading

The TD-SCDMA modulation scheme is similar to TD-CDMA as shown in Figure 7.8. An 8PSK modulation is also specified for higher transmission rates in indoor environments. Spreading and scrambling is also the same as TD-CDMA, and uses the OVSF codes for channelization (Figure 7.9) and a node B-specific scrambling code for reducing intercell interference.

7.4 Summary

The preceding sections gave a general overview of the TDD-based CDMA public mobile communications standards adapted from [10–14]. The techniques introduced in the previous chapters are used for power control, joint transmission, and downlink beam forming by adaptive antenna and uplink quasisynchronous transmission through feedback.

7.5 TD-CDMA Test System

In 1997, the Japanese operator NTT DoCoMo commissioned Matsushita Electric Inc. to develop a TDD-based wideband CDMA test system. The results of the test system have been reported in [15]. The power control function and the selection diversity transmission functions have been tested and verified. However, pre-rake functionality and joint predistortion have not been built and are therefore yet to be realized. Moreover, an uplink synchronous system has been specified in the low-chip-rate version of the standard, but results of a test demonstrating performance have not been reported. The following is a summary of the report of [15].

7.5.1 Elements and Configuration of Experimental Equipment

An experimental TDD-CDMA system was developed with one BS and two mobile stations (one is only for 8 Kbps and the other is for both 8 and 144 Kbps) by Matsushita Communication Industrial Co., Ltd. Major elements of the developed experimental equipment are listed in Table 7.8.

Table 7.8
Major Elements of Experimental Equipment

Item	Element
Access scheme	CDMA/TDD
Carrier frequency	1,990.5 MHz (uplink/downlink)
Frequency bandwidth	5 MHz
Chip rate	4.096 MHz
Symbol rate	32 Kbps
Information transmission rate	8 Kbps/144 Kbps
Spreading code	Short code: 128 cycles + long code: 40,960 cycles
Modulation/demodulation system	Data modulation QPSK, spreading modulation BPSK, with pilot symbol coherent detection
TDD period	1.25 ms
Error correction method	Convolutional coding ($K = 7$, $R = 1/2$), soft decision Viterbi decoding, interleave length:10 ms
Diversity	Path diversity (rake), transmission/reception space diversity at BS
Transmit power control	Open-loop control (control period: 1.25 ms)

The configuration of each BS and mobile station is shown in Figures 7.15. The BS has four antennas branches. On the reception side, the BS estimates the channel condition of each antenna for each user to select a transmission antenna to be used for the downlink signal. For uplink transmission, the mobile station estimates the channel condition from the received signal level, and controls transmission power with open-loop control.

7.5.2 Laboratory Experiments

Laboratory experiments were conducted with a fading simulator using experimental equipment. The propagation path model used was the two-path Rayleigh model (1-μs delay).

7.5.2.1 TPC Characteristic

Figure 7.16 shows the TPC error characteristics (standard deviation of an average received signal power at 0.625 ms per slot on the uplink). The BS has one antenna branch. The period of TPC is 1.25 ms (1 TDD period). With the open-loop TPC, the maximum power to be controlled in a slot to the

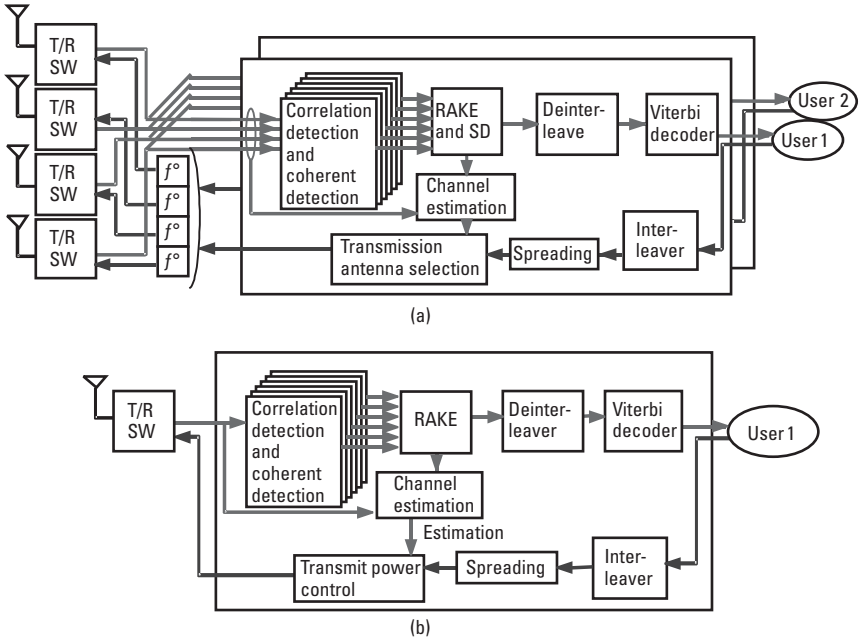

Figure 7.15 (a) BS configuration and (b) mobile station configuration. (*Source:* [15], © 1998 IEICE.)

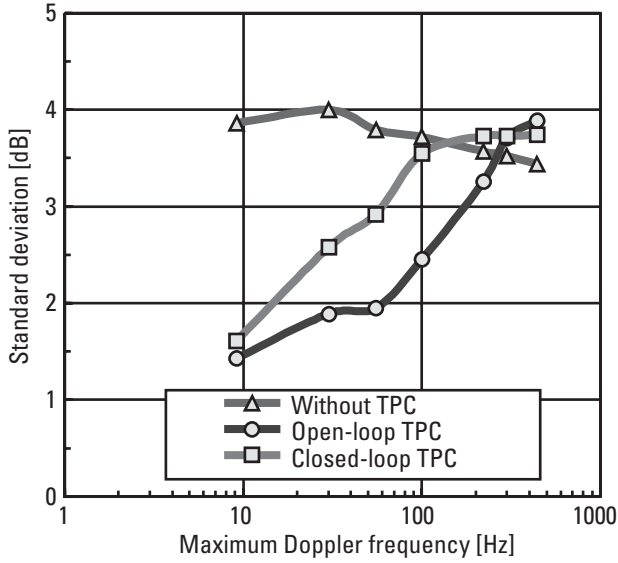

Figure 7.16 TPC error. (*Source:* [15], © 1998 IEICE.)

transmission power from the previous slot is ±10 dB. With the closed-loop TPC, the control step width is ±1 dB. Control delay with the closed-loop TPC is 1.25 ms.

When f_D (the maximum Doppler frequency) is 10 Hz or less, the deviation of the open-loop and closed-loop TPCs is less than 1.5 dB. At higher f_D, the deviation of the closed-loop TPC goes up sharply compared to that of the open-loop TPC. The deviation of the open-loop TPC is below approximately 2.0 dB at f_D = 60 Hz or less. The deviation without TPC goes down as f_D becomes higher, because momentary fading level variations in a slot are accommodated by averages in 0.625-ms slots as the fading level varies faster.

Figure 7.17 shows required E_b/N_0 performance (BER = 10^{-3}) on the uplink Without TPC, the required E_b/N_0 goes down as f_D increases, because errors in propagation are randomized by 10-ms interleaving and BER improvement becomes more effective by fading and FEC. The required E_b/N_0 with each of the open-loop and closed-loop TPCs is approximately 5 dB at f_D =10 Hz.

7.5.2.2 Required E_b/N_0 Performance on the Downlink

Figure 7.18 shows the required E_b/N_0 performance (BER = 10^{-3}) on the downlink. The BS is provided with one or two branches of antennas, while the mobile station has one branch. For the case of two branches,

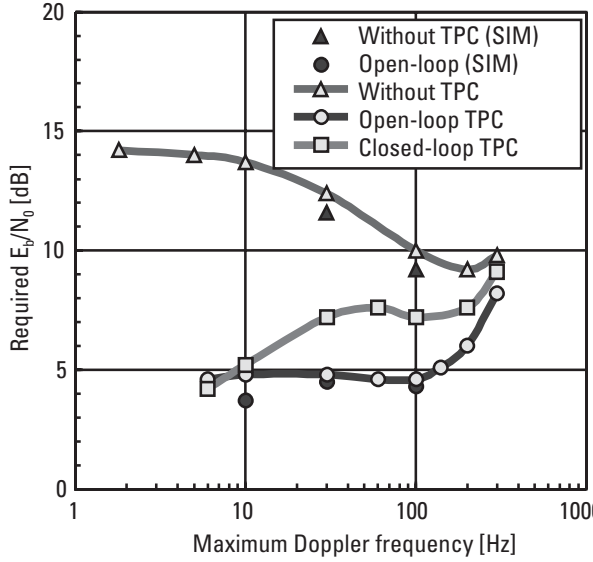

Figure 7.17 Required E_b/N_0 performance on the uplink. (*Source:* [15], © 1998 IEICE.)

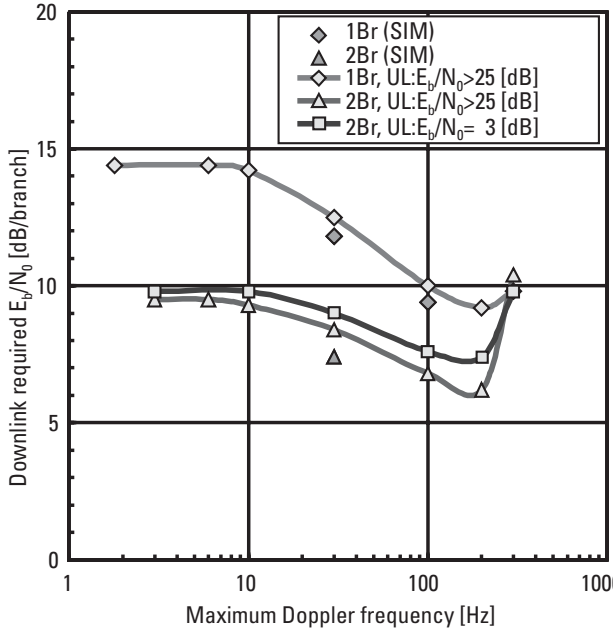

Figure 7.18 Required E_b/N_0 performance on the downlink. (*Source:* [15], © 1998 IEICE.)

transmission diversity allows the required E_b/N_0 to be improved by approximately 3 dB to 4 dB for f_D = 200 Hz or less, compared with the one-branch case. This result shows that antenna selection effectively works at the BS.

7.5.2.3 Required E_b/N_0 Performance on the Uplink

Figure 7.19 shows the required E_b/N_0 performance (BER = 10^{-3}) on the uplink. Just like the downlink case, the BS is provided with one or two branches of antennas, while the mobile station has one branch.

7.5.3 Field Trial

A field trial was conducted in the Saedo area in Yokohama, Japan. Figure 7.20 shows the measurement course of the field trial. The mobile station ran at a speed of 10 to 40 km/hr on the normal road 0.5 to 1.0 km away from the BS. This measurement course passes through houses and factories. The antennas at the BS and mobile station were 20m and 2.2m off the ground, respectively. Figure 7.21 shows an example of the delay profile for this environment.

TEAMFLY

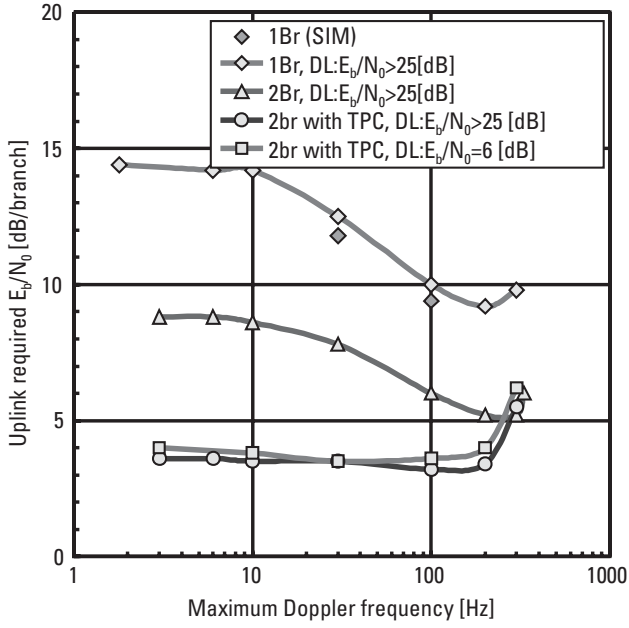

Figure 7.19 Required E_b/N_0 performance on the uplink. (*Source:* [15], © 1998 IEICE.)

Team-Fly®

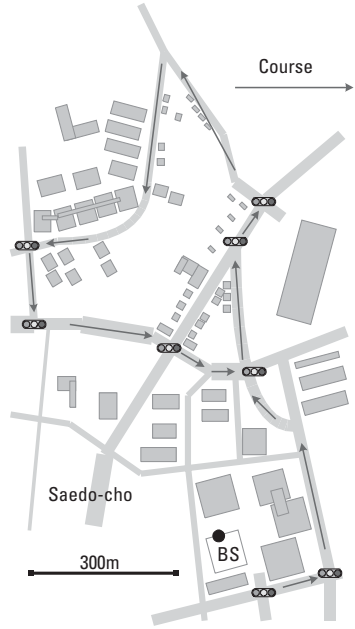

Figure 7.20 Field trial measurement course.

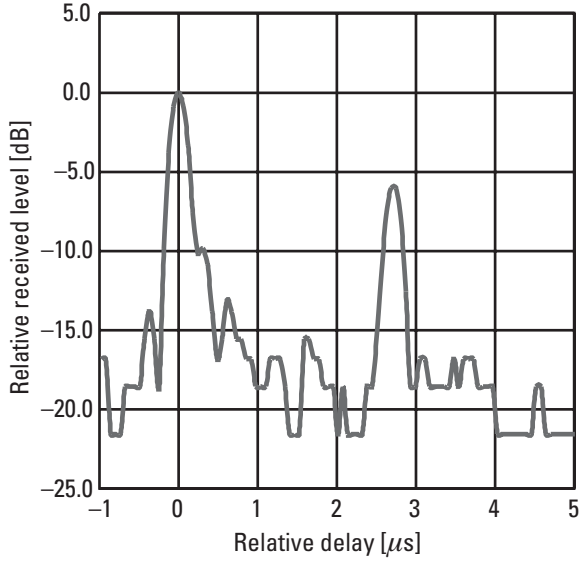

Figure 7.21 Example of delay profile measurement.

7.5.3.1 Average BER Performance on the Downlink

Figure 7.22 shows the average BER performance with transmission space diversity on the downlink. In the figure, Br indicates the number of branches at the BS, and Lab indicates the result of laboratory experiment. The number of antenna branches at the BS is one or two branches, the number of rake fingers is three per branch, and the average speed of the mobile station is approximately 30 km/hr (at f_D = 55 Hz). For the purpose of comparison, the figure also contains the performance under the one-path and equal two-path Rayleigh (1-μs) environment at f_D = 55 Hz.

7.5.3.2 Average BER Performance on the Uplink

Figure 7.23 shows the average BER performance with reception space diversity on the uplink. The figure also contains the performance results of the laboratory trial with the one-path and two-path Rayleigh models.

7.5.4 Summary

The laboratory experiment results indicate that the transmission diversity effect generates a gain of approximately 3 dB to 4 dB at up to f_D = 200 Hz. Further on the uplink, the combination of open-loop TPC with reception

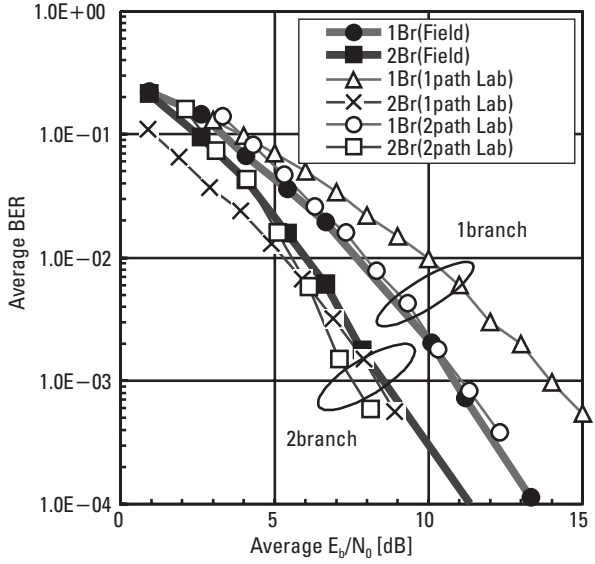

Figure 7.22 Average BER performance (downlink). (*Source:* [15], © 1998 IEICE.)

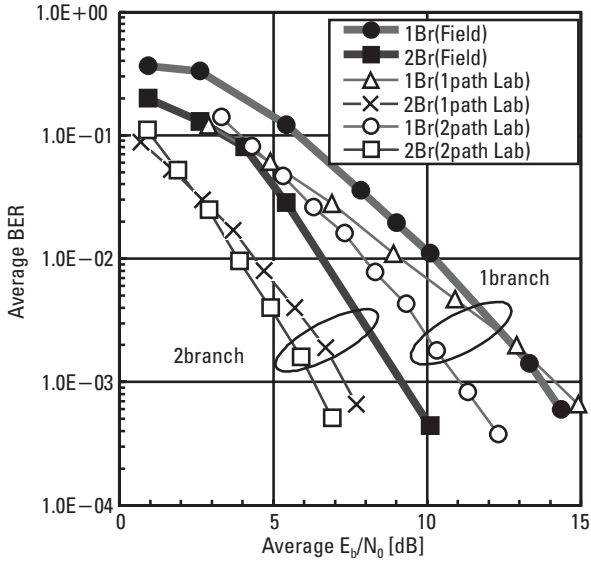

Figure 7.23 Average BER performance (uplink). (*Source:* [15], © 1998 IEICE.)

diversity leads to the average BER = 10^{-3} for the required E_b/N_0 = 3 to 4 dB at up to f_D = 200 Hz. Next, the field trial results indicate the above gain is also achieved under a field environment. Combining the TPC with the reception diversity allows the average BER = 10^{-3} to be realized at the required E_b/N_0 = 5 dB.

References

[1] Povey, G. J. R., "Capacity of a Cellular Time Division Duplex CDMA System," *IEE Proc. Commun.,* Vol. 141, No. 5, October 1994, pp. 351–356.

[2] Esmailzadeh, R., and N. Doi, "A Comparison on the Performance of the FDD and TDD Modes of B-CDMA Communications," *Proc. IEEE ICUPC,* 1995, pp. 339–343.

[3] Acx, A. -G., and P. Mendribil, "Capacity Evaluation of the UTRA FDD and TDD Modes," *Proc. IEEE Vehicular Technology Conference,* 1999, pp. 1999–2003.

[4] Jeong, D. G., and W. S. Jeon, "Capacity of CDMA/TDD Systems for Mobile Multimedia Services," *Proc. IEEE Vehicular Technology Conference,* 1999, pp. 2606–2610.

[5] Tellez-Labao, C., et al., "Capacity Analysis of UTRA/TDD Systems," *Proc. IEEE Vehicular Technology Conference,* 2000, pp. 2893–2898.

[6] Haardt, M., et al., "The TD-CDMA Based UTRA TDD Mode," *IEEE Journal Selected Areas in Communication,* Vol. 18, No. 8, August 2000, pp. 1375–1385.

[7] Geßner, C., et al., "Layer 2 and Layer 3 of UTRA-TDD," *Proc. IEEE Vehicular Technology Conference,* 2000, pp. 1181–1185.

[8] Mohr, W., "The UTRA Concept, Europe's Proposal to IMT-2000," *IEEE Proc. Globecom,* 1999, pp. 2683–2688.

[9] Geßner, C., et al., "UTRA TDD Protocol Operation," *Proc. IEEE PIMRC,* 2000, pp. 1226–1230.

[10] "Physical Layer—General Description," 3GPP Technical Specifications No. 25.201, Ver. 5.0.0, December 2001.

[11] "Physical Channels and Mapping of Transport Channels onto Physical Channels (TDD)," 3GPP Technical Specifications No. 25.221, Ver. 5.0.0, December 2001.

[12] "Multiplexing and Channel Coding (TDD)," 3GPP Technical Specifications No. 25.222, Ver. 5.0.0, December 2001.

[13] "Spreading and Modulation (TDD)," 3GPP Technical Specifications No. 25.223, Ver. 5.0.0, December 2001.

[14] "Physical Layer Procedures (TDD)," 3GPP Technical Specifications No. 25.224, Ver. 5.0.0, December 2001.

[15] Kato, O., et al., "Experimental Performance Results of Coherent Wideband DS-CDMA with TDD Scheme," *IEICE Trans. on Commun.,* Vol. E81-B, No. 7, July 1998, pp. 1337–1344.

8

TDD Spread Spectrum–Based Private Systems

This chapter describes systems where the TDD mode of transmission has been used to transmit and receive spread spectrum signals for private communication systems. In particular, we will discuss the TDD FH-SS Bluetooth systems. We then discuss a typical cordless telephone system based on TDD DS-SS technology. The purpose of this chapter is to review the reasons behind choosing the TDD mode for operation.

8.1 Bluetooth Ad Hoc System

Bluetooth systems were developed initially by Ericsson Mobile Communications AB in 1994 as a low-power, low-cost radio interface between mobile phones and accessories such as headsets and PC cards. The wireless link that connected the devices to the cellular mobile network was known as a *multicommunicator* (MC) link. The technology quickly found applications in WLANs as illustrated in Figure 8.1. By 1998, Ericsson approached other manufacturers about developing further applications for the technology. As a result a *special interest group* (SIG), consisting of five companies—Ericsson, Nokia, IBM, Toshiba, and Intel—was formed to promote Bluetooth and to develop an industry standard for Bluetooth devices. By the end of 2001, more than 1,000 entities had become members of the SIG. Bluetooth is the

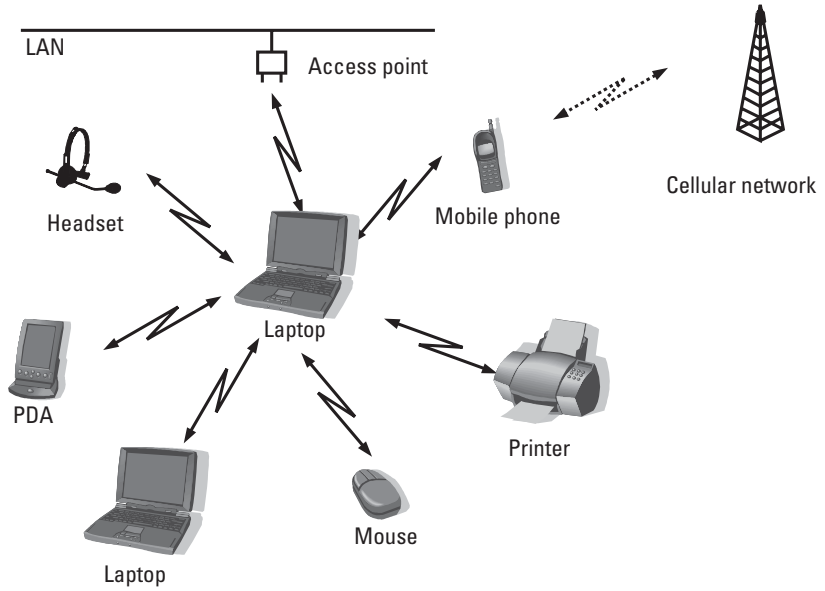

Figure 8.1 WLAN configuration using Bluetooth. (*Source:* [1], © 2000, IEEE. Reprinted with permission.)

title of Danish King Harald, who united Scandinavian people in one country in the tenth century. The name was initially chosen as a temporary name for the project, but it became permanent later on as it became clear a better name was not to be found. In this section, we briefly discuss the physical layer of Bluetooth and its functions. We then describe how Bluetooth devices can form ad hoc networks.

The purpose of this introduction is to review why the TDD mode of operation was chosen. This section has been largely adapted from [1–4]. For detailed information on Bluetooth technology, refer to these references and [5].

8.1.1 Bluetooth Air Interface

Bluetooth operates in the ISM band of 2.4 GHz to 2.483 GHz in Europe and the United States, and 2.471 GHz to 2.497 GHz in Japan. It uses the FH form of spread spectrum, with duplex services using the TDD mode. System parameters are shown in Table 8.1. A block diagram of the transmitter and receiver is shown in Figure 8.2. A TDD switch controls transmission and reception to and from the antenna.

Table 8.1
Bluetooth System Parameters

Frequency band	2.4-GHz ISM band
Carrier separation	1 MHz
RF bandwidth	220 kHz–1 MHz
Peak data rate	1 Mbps
Channels	23 (in Japan)
	79 (in Europe/North America)
Duplex method	TDD
Spreading	FH-SS
Modulation	G-FSK
Chip rate	1.365 Mcps
Output power	< 100 mW

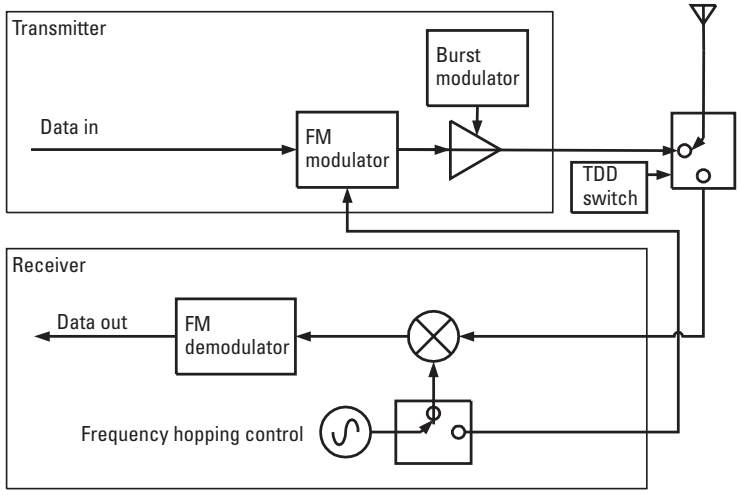

Figure 8.2 Bluetooth transmission and receiving block diagram. (*Source:* [3], © 2001, IEEE. Reprinted with permission.)

8.1.2 Ad Hoc Networking

Bluetooth units within communication range of each other can form ad hoc networks. The communication takes a master/slave topology although, in principle, all units have the same capabilities. Two or more Bluetooth units

that share a channel form a *piconet.* By definition, the unit that starts the piconet, or the one that requests connection to the other unit, becomes the master. A maximum of eight units may share a piconet: one master and seven slaves. Communication among a master and all of its slaves is a one-to-one connection carried out in a TDD fashion as illustrated in Figure 8.3. A piconet is distinguished by the master's identity and follows the master's clock. The frequency-hopping sequence is also set by the master.

Transmission and receptions are carried out in slots that are 625 μs in length. Each slot consists of one packet, with the format shown in Figure 8.4. A packet has three fields: an access code, which is derived from the master identity code; a packet header, which contains control information such as MAC address and flow control bits; and a payload, which can be between 0 and 2,745 bits.

Two types of links are defined in Bluetooth. One is a *synchronous connection-oriented* (SCO) link and the other is an *asynchronous connectionless -oriented* (ACL) link. SCO supports circuit-switched and point-to-point connections such as voice. For these services, two consecutive slots are reserved for transmission at fixed intervals. ACL supports packet-switched and point-to-multipoint connections such as data transmission.

Frequency hopping is carried out at a rate of 1,600 hops per second over a set of 79 carriers in Europe and North America, and 23 carriers in

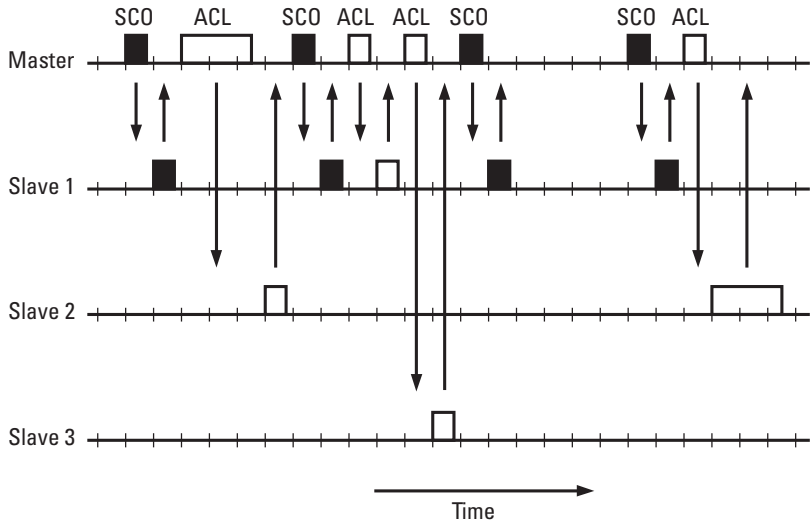

Figure 8.3 Master/slave communication in Bluetooth systems.

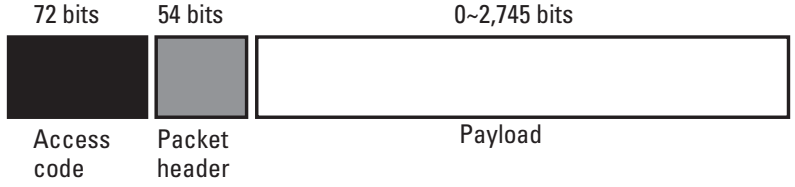

Figure 8.4 Fixed packet format. (*Source:* [1], © 2000, IEEE. Reprinted with permission.)

Japan within the ISM allocated bandwidth. Several piconets may coexist. Because each piconet uses a distinct hopping sequence, mutual interference is kept small.

The TDD mode of operation means that a unit alternately transmits and receives (Figure 8.5). The transmission time is controlled with a master clock, but coexisting piconets may have misaligned slot timing.

A group of colocated piconets is referred to as a *scatternet* (Figure 8.6). Only those units that want to exchange information become members of the piconet. A unit may be a member of more than one piconet. However, a master in one piconet cannot be a master in another. If a master leaves a piconet, then communications within that piconet are suspended until it returns. Alternatively, a new piconet is formed with the remaining units.

8.1.3 Why TDD?

The TDD mode of operation was selected for two reasons. One is superior spectral efficiency in a unpaired band; the second reason is that the

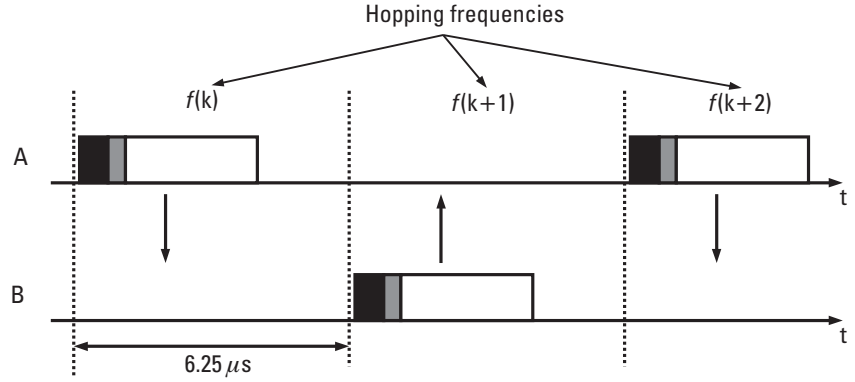

Figure 8.5 TDD/FH-SS operation in Bluetooth. (*Source:* [1], © 2000, IEEE. Reprinted with permission.)

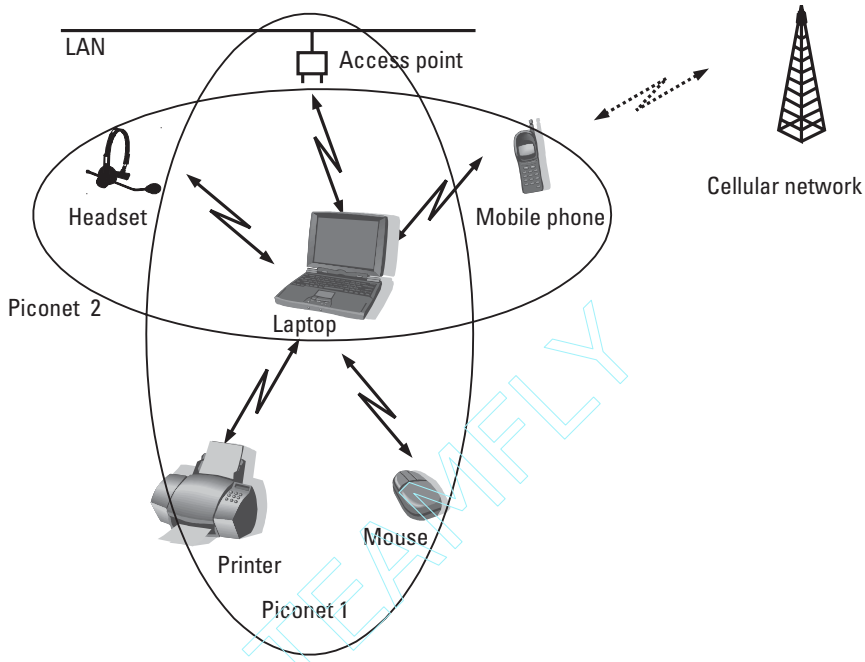

Figure 8.6 Coexisting piconets. (*Source:* [1], © 2000, IEEE. Reprinted with permission.)

separation of transmission and reception in time prevents cross-talk and, hence, simplifies the design of Bluetooth devices. This enables one-chip implementation.

8.2 Spread Spectrum Cordless Telephone

Cordless phones have traditionally used unlicensed bands such as the 2.4-GHz ISM band. One such system has been developed using DS-SS modulation and TDD operation. This section discusses the physical layer aspects of this system and the reasons why the TDD mode of operation has been selected. This section is largely based on a paper by Tanaka [6].

8.2.1 System Configuration

A cordless telephone system can be termed a private network consisting of only a base unit and a handset as depicted in Figure 8.7. Because it operates in an unlicensed band, its transmission power must remain below a specified

Team-Fly®

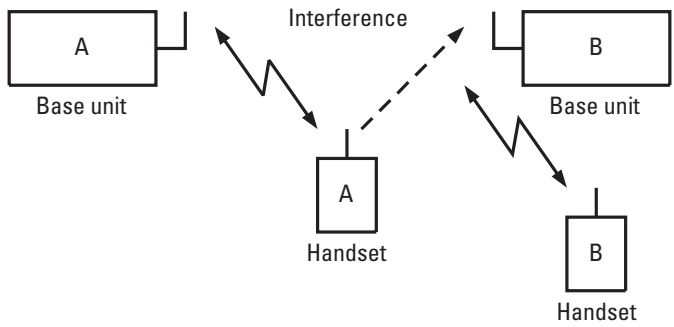

Figure 8.7 Cordless system and interference. (*Source:* [6], © 1994, IEICE.)

level. In the ISM band this level is typically specified as 100 mW or 20 dBm. Because several devices may use the same frequency band, the cordless phone must be designed with a high degree of robustness against interference. This is usually accomplished by the system scanning the available frequencies and measuring the level of interference. It will then select a frequency channel where the required SIR can be obtained. The SIR is continuously monitored and the channel is changed if the SIR is degraded.

The cordless system of this chapter uses the 902–928-MHz ISM band for operation. It uses a DS-SS technique to spread an FSK-modulated 32-Kbps *adaptive differential pulse code modulation* (ADPCM) digitized voice over 23 frequency channels. The system parameters are summarized in Table 8.2.

Table 8.2
System Parameters

Frequency band	902–928 MHz
Carrier separation	1.024 MHz
Channels	23
Duplex method	TDD
Spreading	DS-SS
Process gain	16
Modulation	FSK
Chip rate	1.365 Mcps
Voice coding	32-Kbps ADPCM
Output power	100 mW

8.2.2 TDD Operation

Digitized voice bits are transmitted in 9-ms TDD frames as shown in Figure 8.8. One millisecond of guard time is used for the antenna to switch from receiver to transmitter and vice versa. A system block diagram is shown in Figure 8.9.

Uniden has given two reasons for their choice of TDD. One reason is its operation in the unpaired band, and another reason is good frequency usage efficiency because no frequency guard is required. Further, usage of a TDD system enables the receiver and transmitter to share RF circuitry, resulting in reduced device costs.

It is interesting to note the performance of the system thanks to the use of spread spectrum radio techniques. Uniden reports a communication range of up to 1 mile or 1.6 km under good conditions [6].

8.3 Summary

In this chapter we briefly discussed two TDD spread spectrum-based private communication systems to demonstrate why the TDD mode was selected for

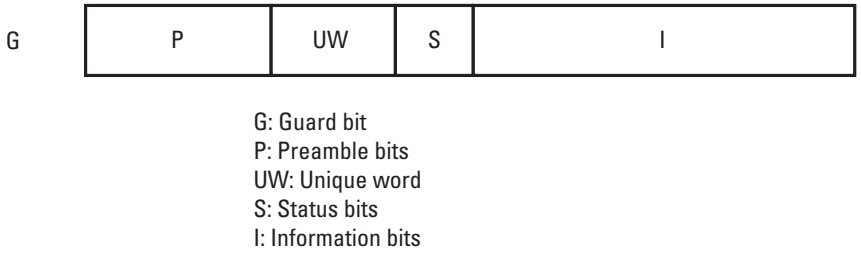

Figure 8.8 TDD burst structure. (*Source:* [6], © 1994, IEICE.)

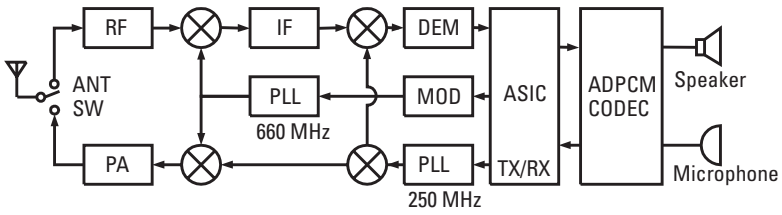

Figure 8.9 System block diagram. (*Source:* [6], © 1994, IEICE.)

certain applications. In both cases examined here, bandwidth usage efficiency and device cost were shown to be the main reasons for choosing the TDD mode.

References

[1] Haartsen, J., "The Bluetooth Radio System," *IEEE Personal Communications Magazine,* February 2000, pp. 28–36.

[2] Arfwedson, H., and R. Sneddon, "Ericsson's Bluetooth Modules," *Ericsson Review,* No. 4, 1999, pp. 198–205.

[3] Bisdikian, C., "An Overview of the Bluetooth Wireless Technology," *IEEE Communications Magazine,* December 2001, pp. 86–94.

[4] Schniederman, R., "Bluetooth's Slow Dawn," *IEEE Spectrum,* November 2000, pp. 61–65.

[5] Miller, B. A., and C. Bisdikian, *Bluetooth Revealed: The Insider's Guide to an Open Specification for Global Wireless Communications,* Upper Saddle River, NJ: Prentice Hall, 2001.

[6] Tanaka, K., "A Spread Spectrum Cordless Telephone," *IEICE Transactions B-II,* Vol. J77-B-II, No. 11, November 1994, pp. 703–710 (in Japanese).

9

TDD and Fourth-Generation Systems

This book has discussed how the TDD mode of operation has been adopted in public and private communication systems. We will now give an overview of where and how TDD systems may be utilized in the future, generally termed the fourth-generation systems.

9.1 Subscriber and Traffic Growth

In recent years, the communications industry has witnessed a tremendous growth in the number of mobile subscribers and the amount of traffic. The rate of growth is expected to continue for the duration of the 2000s. A typical subscriber projection is shown in Figure 9.1 [1]. The total number of world subscribers is expected to reach nearly 1 billion by 2005 and 1.8 billion by 2010. In the more advanced markets, mobile traffic is going to include more data communication, whereas better coverage in the developing markets will bring telephony services to areas where no such services have existed.

We should mention that although the mobile subscriber numbers are fast approaching that of the fixed-line subscribers, the total traffic carried over the mobile links is still comparatively less than a quarter of the fixed lines [2]. Cost and inferior voice quality are the two major reasons why mobile handsets are not used more often, and another reason is because the average length of a conversation is shorter than land-line calls. "True

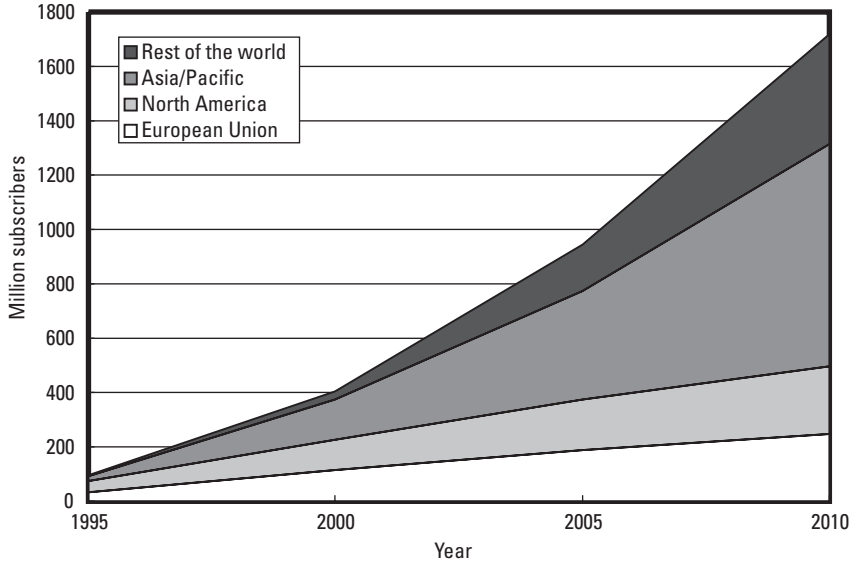

Figure 9.1 World mobile subscribers growth. (*Source:* [1], © 1999, IEEE. Reprinted with permission.)

penetration"[1] of the mobile technology must take into consideration how often and how long mobile subscribers use their mobile handset rather than their fixed-line terminals for their telecommunication needs.

The traffic profile is expected to change dramatically in the coming years. In developed countries, data traffic is expected to become more prolific than voice traffic by 2005. The ratio of downlink to uplink traffic is also expected to rise from slightly over 1 to more than 4 and more by 2007, as illustrated in Figure 9.2. It is predicted that voice communication in fourth-generation systems will use *Voice-over-Internet Protocol* (VoIP) technology for an all-IP mobile system. It is further expected that the fourth-generation systems will provide rich Internet content; interactive music and video content is generally expected. The highest transmission rates for fourth-generation systems are envisioned to be one order of magnitude higher than third-generation, perhaps in the 20-Mbps range. Furthermore, the size of the handsets is expected to decrease to less than 50 cm^3 in size and 50g in weight. Although today's mobile phones are already near the expected sizes, their transmission rate is nowhere near the high rate anticipated from fourth-generation phones.

1. This term was coined by K. Homayoufar of Genista Corporation.

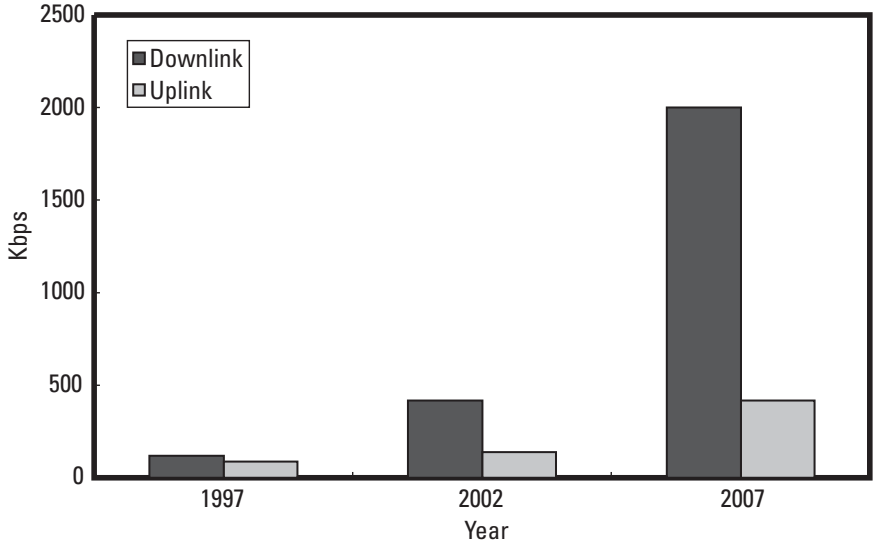

Figure 9.2 Downlink and uplink traffic. (*Source:* [1], © 1999, IEEE. Reprinted with permission.)

9.2 Transmission and Network Technology

What are the technologies that can respond to and provide such high transmission rates? The focus of work has been on a combination of multicarrier CDMA and *orthogonal frequency-division multiplexing* (OFDM). Considering the asymmetry of uplink and downlink traffic, it is likely that the two links will use different modulation techniques. For example, a QPSK scheme in the uplink paired with 64QAM in the downlink. References in this area of research include [3–18].

The system design for 4G also requires novel configurations, because high transmission rates reduce the power a mobile handset can transmit. Reduced power from the mobile terminals requires a different network topology. An asymmetrically distributed transmitting and receiver base station network is one of the proposed options, as illustrated in Figure 9.3 [19].

Several factors make it highly likely that TDD will be chosen as the duplex mode of operation. An important factor is the asymmetry in the uplink and downlink traffic volumes, and the fact that the traffic asymmetry is highly likely to change as new services and systems evolve. This will make it necessary to have flexibility in assigning relative capacity to the uplink and downlink traffic. The frequency bands in which these systems will operate

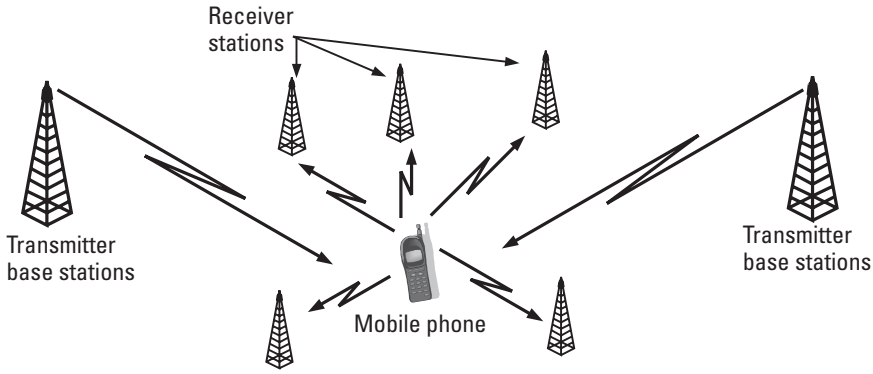

Figure 9.3 Downlink and uplink traffic. (*Source:* [19], © 2001, IEICE.)

are likely to be unpaired and possibly unlicensed. We have already seen that TDD systems are more efficient in bandwidth utilization compared to FDD systems. Furthermore, the size and cost of devices are going to remain a factor. TDD systems are going to be smaller and less power consuming to operate.

The main reason TDD systems had not been utilized thus far had been the synchronous network operation requirement and their limited cell size. However, several FDD systems now operate in a synchronous mode. Also with the increasing amount of mobile traffic, the cell areas have become smaller and smaller. So the reasons for TDD systems being more toward the fringe of usage have gradually diminished.

9.3 Conclusion

In conclusion, TDD systems were not used at all in the first generation of mobile systems. In the second generation, they were partially used, but never became a mainstream part of the standards. In third-generation they are an integral part of the 3GPP standard, and in China the dominant standard. It is likely that they will become the dominant, universal choice for the fourth-generation systems. This is primarily because systems of the future will have to support increasingly asymmetric traffic in mature markets. The services that are envisioned will require very high data rates. The cell size for these systems will not be very large due to limitations on battery power and also due to a distributed transmission and reception network. Therefore, the

disadvantages of the TDD system such as synchronous operation and limited coverage will become largely insignificant. We envision that fourth-generation systems will be based primarily on the TDD mode.

References

[1] Mohr, W., "The UTRA Concept, Europe's Proposal to IMT-2000," *Proc. Globecom,* 1999, pp. 2683–2688.

[2] Telecommunication Information White Paper, Japanese Ministry of Post and Telecommunications, 2001.

[3] Harada, H., and R. Prasad, "A New Multi-Carrier CDMA/TDD Transmission Scheme Based on Cyclic Extended Spread Code for 4th Generation Mobile Communication System," *Proc. ICPWC,* 1997, pp. 319–323.

[4] Takahashi, T., and M. Nakagawa, *Antenna and Multi-Carrier Pre-Diversity System Using Time Division Duplex in Selective Fading Channel*, IEICE Technical Report RCS 95-45, Japan, 1995.

[5] Matsui, Y., S. Sampei, and N. Morinaga, "Study on the Effect of Offset Frequency for Asymmetric Radio Communication Systems Using OFDMA/TDD Technique," *Proc. IEICE National Conference,* 2000, Vol. B-5-14, p. 399.

[6] Watanabe, S., T. Sato, and T. Abe, "Forward Sub-Channel Control Scheme for TDD Multi-Carrier Mobile Communication System," *IEICE Trans. Fundamentals of Elec. Commun.,* Vol. E82-A, No. 7, July 1999, pp. 1172–1178.

[7] Jeong, D. G., and M. J. Kim, "Effects of Channel Estimation Error in MC-CDMA/TDD Systems," *Proc. IEEE Vehicular Technology Conference,* 2000, pp. 1773–1777.

[8] Pu, Z., X. You, and S. Cheng, "Transmission and Reception of TDD Multi-Carrier CDMA Signals in Mobile Communications System," *Proc. IEEE Vehicular Technology Conference,* 1999, pp. 2134–2138.

[9] O'Neill, R., and L. Lopes, "Multi-Carrier TDD Systems Using Channel State Feedback Information," *Proc. IEEE Vehicular Technology Conference,* 1997, pp. 1822–1826.

[10] Ise, M., Y. Matsumoto, and M. Umehiro, *Wireless Multicasting Scheme with OFDM Space Combining Transmission Diversity*, IEICE Technical Report RCS 98-173, Japan, 1998.

[11] Tomisato, S., K. Fukawa, and T. Matsumoto, *Signal Transmission Performance of Temporal and Spatial Pre-Coding for TDD Multimedia Mobile Radio Communication Systems*, IEICE Technical Report RCS 97-178, Japan, 1997.

[12] Matsumoto, Y., N. Mochizuki, and M. Umehira, *OFDM Subchannel Space-Combining Transmission Diversity for TDMA-TDD Broadband Radio Communications System*, IEICE Technical Report RCS 97–209, Japan, 1997.

[13] Umehira, M., et al., "A 5 GHz Band Advanced Wireless Access System for Mobile Multimedia Applications," *Proc. IEEE Vehicular Technology Conference,* 2000, pp. 2300–2304.

[14] Sudo, H., K. Ishikawa, and G. Ohta, "OFDM Transmission Diversity Scheme for MMAC Systems," *Proc. IEEE Vehicular Technology Conference,* 2000, pp. 410–414.

[15] Matsui, Y., S. Sampei, and N. Morinaga, *A Study on Uplink Access Scheme for Asymmetric Radio Communication Systems Using OFDM Technique*, IEICE Technical Report RCS 99-231, Tokyo, Japan.

[16] Matsui, Y., S. Sampei, and N. Morinaga, "OFDMA/TDD Packet Transmission System with an Adaptive Subcarrier Selection Scheme for Asymmetric Wireless Communication Services," *Proc. Int. Conference on Consumer Electronics,* 2001, pp. 54–55.

[17] Stantchev, B., and G. Fettweis, "Burst Synchronization for OFDM-Based Cellular Systems with Separate Signaling Channel," *Proc. IEEE Vehicular Technology Conference,* 1998, pp. 758–762.

[18] Jeong, I., and M. Nakagawa, "A Time Division Duplex CDMA System Using Asymmetric Modulation Scheme in Duplex Channel," *IEICE Trans. on Commun.,* Vol. E82-B, No. 12, December 1999, pp. 1956–1963.

[19] Adachi, F., "Wireless Past and Future—Evolving Mobile Communications Systems," *IEICE Trans. on Fundamentals Elec. Commun.,* Vol. E84-A, No. 1, January 2001, pp. 55–60.

Team-Fly®

About the Authors

Riaz Esmailzadeh has worked with TDD-CDMA since 1991, when he started his Ph.D. studies. He has worked as a research engineer in Telstra, a project manager in Nippon Ericsson, and the chief technology officer at Genista, all in areas related to telecommunications research, development, and management. Presently, he is an associate professor at Keio University, Japan, and a business strategy consultant. Dr. Esmailzadeh has authored or coauthored more than 40 papers in the field, and applied for more than 30 patents, nine of which have been granted so far. His latest research interests are in the fourth-generation mobile communications system and business aspects of the telecommunications industry.

Masao Nakagawa received a B.E., an M.E., and a Ph.D. in electrical engineering from Keio University in Yokohama, Japan, in 1969, 1971, and 1974, respectively. Since 1973, he has been with the Department of Electrical Engineering at Keio University, where he is now a professor. His research interests are in CDMA, consumer communications, mobile communications, intelligent transport systems (ITS), wireless home networks, and visible optical communication. Dr. Nakagawa has received the 1989 IEEE Consumer Electronics Society Paper Award, the 1999-Fall Best Paper Award in the IEEE VTC, the IEICE Achievement Award in 2000, and the IEICE Fellow Award in 2001. He was the executive committee chairman of International Symposium on Spread Spectrum Techniques and Applications in 1992 and the technical program committee chairman of the International Symposium on Information Theory and its Applications (ISITA) in 1994.

Dr. Nakagawa is an editor for *Wireless Personal Communications* and was a guest editor for the special issues on "CDMA Networks I, II, III, and IV" published in the *IEEE Journal on Special Areas in Communications* in 1994 (I and II) and 1996 (III and IV). He currently chairs the Wireless Home Link Subcommittee in the Multimedia Mobile Access Communication Promotion Committee (MMAC).

Index

TEAMFLY

Team-Fly®